ADDIS ABABA UNIVERSITY

SCHOOL OF GRADUATE STUDIES

FACULTY OF TECHNOLOGY

DEPARTMENT OF ELECTRICAL and COMPUTER ENGINEERING

FIELD WEAKENING CONTROL OF PMSM

A thesis submitted to the

School of Graduate Studies of Addis Ababa University

in partial fulfillment of the requirement for the Degree of

Master of Science in Electrical Engineering (Control)

By

Daniel Fita

Advisor

Girma Mullisa (Prof.)

January 2005

ACKNOWLEDGMENT

I would like to express my sincere gratitude to my advisor, Professor Girma Mullisa for his guidance, encouragement, remarkable patience and caring support during my graduate studies. His impressive knowledge, technical skills and creative thinking were the “power supply and control feedback” of this work.

I wish to thank Ato Daniel Gizaw who is a committee member of Danotek Motion Technology Company for his initial idea of my studies, and for his advice and suggestion. I also thank Ato Dawit Mengistie for his support during my graduate studies.

I would like to acknowledge the ECE department staff for establishing a working environment and for constructive discussions.

Finally, I would like to thank my family and friends for their tenacious support.

Table of Contents

LIST OF TABLE

LIST OF FIGURES

FIGURE

LIST OF SYMBOLS

SYMBOL	
B	Damping coefficient
e,V_b	Back emf (induced voltage)
e_α ,e_β	α and β axis back emf
g_{ij}	Observer gain
i_a , i_b ,i_c	Phase a, b, c instantaneous stator current.
i_a ,i_b ,i_c	Phase current
i_d , i_q	d- and q- axis components of stator current
idf	Additional(incremental) d-axis current
idfmin	Voltage regulator output limitation
i_s	Stator current vector
i_{sdref}	d-axis stator reference current)
I_{smax}	Stator current limit (magnitude)
i_{sqref}	q-axis stator reference current
$i_{s\alpha}$, $i_{s\beta}$	α and β axis stator currents, respectively
J	Moment of inertia
K_E	emf constants
K_b ,K_f	Motor constants
K_i ,K_p	Integral and proportional constant
K_{iV}	Voltage integral constant
K_t	Torque constant (motor torque constant)
K_V	Voltage limit constant
L(L_{aa} ,L_{bb}, L_{cc})	Self inductance
L_d , L_q	d- and q- axis stator self inductance
L_S	Average inductance.
L_{Sl}	Leakage component of self inductance
L_{So}	Component of self inductance due to space fundamental air- gap flux

L_x	Inductance fluctuation.
M	Mutual inductance
p	Number of pole pairs.
P_i	Input power
P_o	Output power
R_S	Stator resistance
S	Arbitrary assigned variable
T	Developed (motor) torque
T_1, T2	Switching time
t1, t2	Time vector application in SVPWM
taon ,tbon tcon	PWM commutation instant
T_{fr}	Friction torque
T_L	Load Torque
T_m	Electromagnetic Torque
T_S	Sampling time
v_a ,v_b , v_c	Phase a, b, c instantaneous stator voltage.
V_a ,V_b ,V_c	Phase voltage
v_d ,v_q	d and q- axis components of stator voltage
Vsdref, Vsqref	d and q components of the reference stator voltage
V_{dc}	DC- link voltage
V_{ref}	Reference space vector voltage
V_s	Stator voltage magnitude (steady state)
V_{smax}	Stator voltage limit
$V_{\alpha ref}$,$V_{\beta ref}$	α and β axis reference voltage
w_p	Prevailing speed
X, Y, Z	SVPWM variables
γ	γ current angle between induced voltage E and terminal current I
θ	Electrical rotor angle between the phase a-axis and the north pole
ξ	Saliency ratio
ψ_a ,ψ_b ,ψ_c	Phase stator flux
ψ_d ,ψ_q	d ,q component of stator flux

Ψ_F	Opposing field
Ψ_m	Flux linkage due to permanent magnet.
Ω	Rotational speed at a load-torque slope break point
Φ	Flux in the airgap
ω, ωref	Speed and reference speed of rotation (in electrical rad/Sec.)
ωfb	Estimated (feed back) speed
τ	Time constant

Acronyms

AC	Alternating current
BLAC	Brushless AC machine
BLDC	Brushless DC machine
CCCP	Constant current- constant power
CPSR	Constant power speed region
CVCP	Constant voltage -constant power
DC	Direct current
EKF	Extended Kalman filter
emf	Electromagnetic force
FOC	Field oriented control
FW	Field/Flux weakening
IPM	Interior permanent magnet motor
mmf	Magneto-motive force
MTPC	Maximum torque per unit current (control strategy)
OCV	Optimal current voltage
PI	Proportional integral
PMSM	Permanent magnet synchronous machine
PWM	Pulse width modulation
SVPWM	Space vector PWM
VSI	Voltage source inverter

Subscript

d,q (ds,dq)	synchronous frame quantities(d-axis, q-axis)

α ,β	stationary frame quantities
s	stator reference frame, stator coordinates
b	base (or nominal/rated) parameters
n	normalized quantity(parameters)
r	rotor quantity
ds,qs	q and d axis stator quantity respectively

Superscript

*	reference quantity
^	estimated quantity

Field Weakening Control of brushless PM synchronous motor

Abstract

This master thesis deals with control of PM motor with field weakening capability for electric vehicle (EV) application .A PMSM motor model has been analyzed in a drive able to control the motor both in the constant-torque (constant flux) and in the constant-volt-ampere (flux weakening) regions.

Today's motor for traction in electric vehicle are most often induction motors. In recent years, PM-motors have become attractive due to their high efficiency. This is very important in battery applications.

The first part of the project consists of a literature survey that aims at building knowledge on machine theory for field weakening. An analytical model for PMSM is developed there upon.

An explanation of field weakening and the field orientation concepts implemented in the PMSM are presented. Finally, performance of field weakening control for PM machines with results is presented.

Key words

PMSM, field weakening, electric vehicle

1. Introduction

An important factor in industrial progress during the past five decades has been the increasing sophistication of factory automation which has improved productivity many fold. Manufacturing lines typically involve a variety of variable speed motor drives which serve to power conveyor belts, robot arms, overhead cranes, steel process lines, paper mills, and plastic and fiber processing lines to name only a few. Prior to the 1950s all such applications required the use of a DC motor drive since AC motors were not capable of smoothly varying speed since they inherently operated synchronously or nearly synchronously with the frequency of electrical input. To a large extent, these applications are now serviced by what can be called general-purpose AC drives. In general, such AC drives often feature a cost advantage over their DC counterparts and, in addition, offer lower maintenance, smaller motor size, and improved reliability.

However, the control flexibility available with these drives is limited and their application is, in the main, restricted to fan, pump, and compressor types of applications where the speed need be regulated only roughly and where transient response and low-speed performance are not critical. More demanding drives used in machine tools, spindles, high-speed elevators, dynamometers, mine winders, rolling mills, glass float lines, and the like have much more sophisticated requirements and must afford the flexibility to allow for regulation of a number of variables, such as speed, position, acceleration, and torque. Until recently, such drives were almost exclusively the domain of DC motors combined with various configurations of AC-to-DC converters depending upon the application.

Today's motor for traction in electric vehicles is most often an induction motor. For some applications the characteristics of the induction motor, especially in the field weakening range fits the application demands very well. However, the efficiency is very important in battery applications and therefore a system with a permanent magnet motor is promising.

In these days of soaring fuel prices everyone is concerned about the efficiency of their appliances. The energy consumed by the electric motor represents a large portion of the total energy used in electric appliances such as refrigerators, air-conditioners, and washing machines. Thus, many manufacturers are now using three phase, permanent magnet, inverter driven, variable speed motors to achieve their efficiency goals.

With suitable control, however, PMSM motor drives have been shown to be more than a match for DC drives in high-performance applications. While control of the PMSM machine is considerably more complicated than its DC motor counterpart, with continual advancement of microelectronics, these control complexities have essentially been overcome.

One of the most popular control methods of three-phase motor drive systems, well-developed during the last decade, is field-oriented control, usually realized with a digital PWM controller in rotating, d-q (or dq0 for unbalanced systems) coordinate space.

Permanent magnet (PM) motors became very popular in industry due to their simple structure, efficiency, robustness and high torque/size (or weight) ratio.

In high-speed regions a point is reached where the supply voltage is maximum and the rotor field has to be weakened as an invert to the angular speed. By analogy to dc machines, the term “field weakening” is used to describe a process by which speed increase with falling torque may be obtained above base speed in variable –frequency permanent –magnet machines. A flux-weakening technique is usually applied when an extension of the motor rated speed is desired. The field-oriented control, with its flux/torque decoupling feature, finds no better alternative today in PMSM drive applications in flux-weakening control.

Speed control of a brushless motor is undertaken by the control of the motor's terminal voltage, which is normally achieved by pulse width modulation of the supply voltage. If a brushless motor commutator integrated circuit is used, the pulse width modulation switching waveform can be directly gated with the commutation-switching pattern, in practice only the lower devices need be controlled. The characteristics of the brushless motor are very similar to that of the brushed motor, hence it is possible to control these motors over a wide speed and torque range using a conventional analogue control loop.

Different flux-weakening strategies provide various results in various applications.

Establishing the basic criteria for choosing a flux-weakening strategy based on the analysis of its dynamics and application requirements is the final objective of this work. A comparative analysis of the three most promising flux-weakening control strategies today –

constant power methods in versions with constant voltage and constant current (CVCP and CCCP), and optimum current vector control (OCV) method - served that purpose. The goal of this master thesis is then to analyze PMSM for field weakening operation. Based on analytical models and design the possibilities and limitations of the PMSM are investigated. This master paper explains the design choices that have been made in order to satisfy the typical main requirements for an electrical vehicle, namely, the following:

- Wide flux weakening (FW) region, to minimize the drive power rating in spite of a wide speed range;
- High efficiency performance of the vehicle automation;
- High torque-to-ampere ratios to minimize the inverter cost and low torque ripple.

Chapter 2

General characteristics of PM Synchronous Motor

Motors are electromagnet devices used to convert electrical energy into useful mechanical work. There are two major classifications of ac motors. The first is induction motors that are electrically connected to power source. Through electromagnetic coupling, the rotor and the stator fields interact, creating rotation without any other power source .The second is synchronous motors that have fixed stator windings that are electrically connected to the ac supply with a separate source of excitation connected to field windings when the motor is operating at synchronous speed.

Among the synchronous motor types the permanent magnet synchronous motor (PMSM) is one possible design of three phase synchronous machines. The stator of a PM synchronous motor has conventional three phase windings. In the rotor PM materials have the same function of the field winding in a conventional synchronous machine. Their development was possible by the introduction of new magnetic materials, like the rare earth materials. PM-Synchronous Motors offer a number of advantages in designing modern motion control systems. The use a PM to generate substantial air gap magnetic flux which makes it possible to design highly efficient PM motors.

2.1 Overview of PMSM

Synchronous motors are those which rotate at the speed of the stator revolving field, which is called the synchronous speed. The synchronous speed, ω_S , is determined by the frequency of the stator supply, f_s, and the number of stator pole pairs, p. Unlike the induction motor, the rotor also has p-pole pairs, excited by a separate DC or permanent magnet (PM) source .The stator of a three-phase synchronous motor normally has a sine distributed three-phase winding. When excited with a three-phase balanced supply, a rotating magnetic field develops. The speed of this field (the *Synchronous Speed*) is given by equation 2.1. We will assume that this field is sinusoidally distributed in space in the air gap.

$$N = \frac{120.\ f_S}{P} \quad \text{(rpm)} \tag{2.1}$$

f_S - Frequency of ac supply in HZ , P - Number of poles;

p – pole pairs , N - Synchronous speed

2.1.1 Synchronous motors with dc excitation and with Permanent Magnets

i) Synchronous A.C. motors

The many different types of synchronous motor may be classified into a number of groupings:

- non salient pole (cylindrical or round rotor)
- salient pole
- permanent magnet (surface, inset, buried/interior, imprecated rotor)
- reluctance motor(synchronous reluctance, switched reluctance)
- stepping motor(variable reluctance, permanent magnet, hybrid

General classification of electric machine is shown below in block diagram.

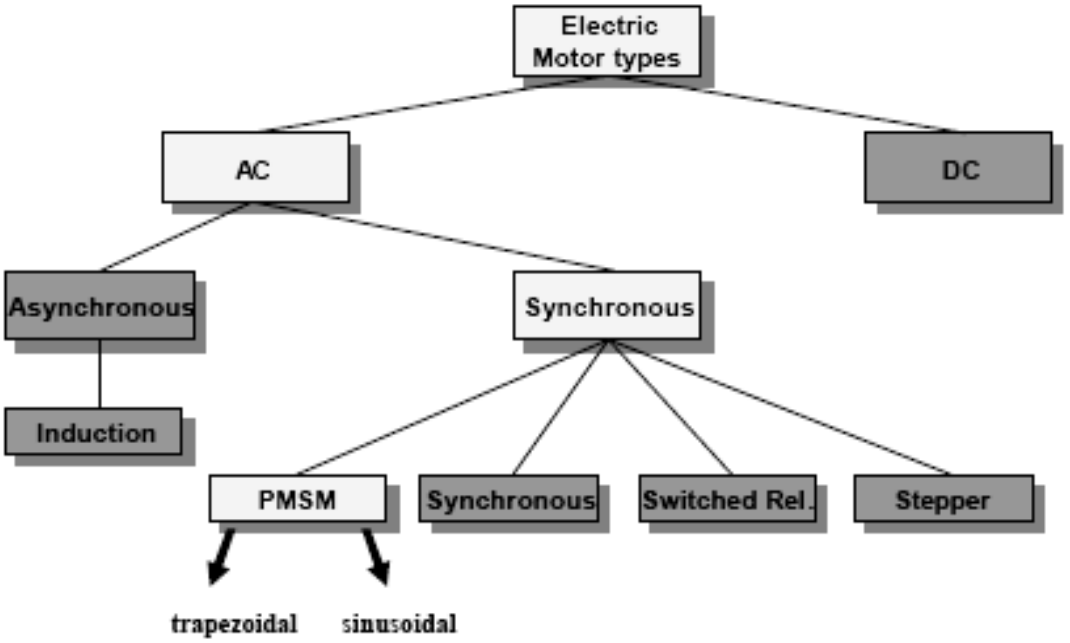

Figure 2.1 Classification of ac motors

All types of synchronous motors have in common that their speed of rotation is precisely related to the frequency of the a.c. supply. With wound-rotor permanent magnet, synchronous reluctance and brushless motors there is a distributed, polyphase armature winding on the stator. Stepper motors and switched reluctance motors are energized by pulse trains applied to appropriate stator windings. Because of the absence of a commutator, synchronous motors are not limited to maximum speed and have lower weight, volume and inertia compared with D.C motors of the same rating. Most types of synchronous motors have a rotor structure that is salient in form.

ii) Synchronous motor with dc excitation

Synchronous motors (with dc excitation), like synchronous generators, consist of a fixed stator and a field that rotates concentric with the stator. The stator contains armature windings that are electrically connected to the ac supply, while the rotor contains a field winding that is electrically connected to a source of excitation when the motor is at synchronous speed .Since the primary purpose of the field winding is to transform the field into the rotating magnet, the field winding is wound around "poles" attached to the rotor in a configuration that produces magnetically north and south poles that are 180^0 electrical degrees apart. Because of this arrangement, the field winding is not effectively coupled with the armature windings in the stator, and no net torque is produced in the field when ac power is connected to the stator winding.

To produce starting torque, a supplementary winding is provided on the rotor that effectively couples electromagnetically with the armature windings. The rotor is typically constructed with a "squirrel cage "arrangement of bars that are electrically shorted at each end so that the ac power connected to the armature is coupled with the squirrel cage winding at time of start up. This results in a net torque that is applied to the rotor when ac power is applied to the stator.

iii) Brushless PM synchronous motors

On the other hand replacing common rotor field windings and pole structure with PM put the motor into the category of brushless motors. It is possible to build brushless permanent magnet synchronous motors with any even number of magnet poles. Motors have been

constructed with one or more magnet pole pairs. A greater number of pole-pairs usually creates a larger torque for the same level of current. The use of magnets enables an efficient use of the radial space and replaces the rotor windings, therefore suppressing the rotor copper losses. Advanced magnets materials such as Samarium Cobalt (Sm_2Co_{17}) or Neodymium-Iron-Boron (Nd-Fe-B) permit a considerable reduction in motor dimensions while maintaining a very high power density. These motors are used in adjustable speed drives which require a range of operating frequencies.

The brushless PM synchronous motors involve adjustment of the armature supply frequency, proportionally as the rotor speed is varied, so that the armature field always moves at the same speed as the rotor. The rotating magnetic fields of the stator (armature) and the rotor (excitation) system are then always in synchronous motion producing a steady torque at all operating speeds. This is analogous to the D.C motor in which the armature and excitation fields are synchronous but stationary for all operating speeds.

Brushless (PM) Synchronous motor requires the very accurate measurement of rotor speed and position and the very precise adjustment of the stator frequency. Rotor position sensing is done by an encoder which forms part of a control loop delivering firing pulses to the electronic switches of an adjustable frequency inverter feeding the armature winding. The combination of an a.c. synchronous motor with permanent magnet rotor, three-phase inverter and rotor position sensor, is often called a ‘‘***brushless dc/ac motor***.’’ The difference between brushless D.C. motors and brushless a.c. motors will be clarified below.

Two common motors are the brushless direct current (BLDC) motor, and brushless alternating current motor (BLAC), which is also known as the permanent magnet synchronous motor (PMSM).In this master thesis the latter type of motor is considered. These motors are more efficient than the induction motors because the magnetic field of the rotor is supplied by the permanent magnet rather than by electromagnet action as in the induction machine.

Their difference is further explained as follows:

- The ***brushless dc motor (BLDC)*** is essentially configured as a PM rotating past a set of current carrying conductors. In order to ensure that the torque is unidirectional, the current in the conductors must reverse polarity every time a magnet pole passes by. The polarity reversal is performed by power transistors being switched corresponding to the rotor position. The phase currents are therefore square-waves and the induced voltages are trapezoidal.

- In contrast, the phases currents of the ***brushless AC motor (PMSM)*** are sine waves. The induced voltage should ideally be sinusoidal too. The sine wave motor operates with a rotating ampere-conductor distribution, similar to the rotating magnetic field in the induction motor or the AC synchronous machine. Therefore it is called a ***brushless synchronous AC motor (PMSM)*** in this thesis. The differences between these two motors are shown in the following table.

TABEL 1 Difference between PMSM and BLDC

	PMSM	BLDC
Flux density (in space)	sinusoidal distribution	square distribution
Back EMF	sinusoidal wave	Trapezoidal
Stator current	sinusoidal wave	square wave
Electromagnetic Torque	constant	almost constant
Energized phases	3 phases on at any time	2 phases on at any time

2.1.2 Types of Permanent Magnet Synchronous Motor (PMSM)

This section is an addition to outline the structure of different motors for various applications and the choice of their names in this master thesis is explained. In the literature one can find various names for the same motor, based on different approaches or points of view. Brushless synchronous AC motors are one type of synchronous motor. Synchronous AC motors are sinusoidal current-driven machines that use a quasi-sinusoidal distributed AC stator winding and inverter. The three main types are shown in Figure 2.2. Figure 2.2a shows the cross-section of a surface-mounted PM-motor (SMPM). Radial or straight-through magnetized permanent magnets are fixed to an iron rotor core. The magnets are normally glued to the rotor surface and bandaged with e.g. glass-fiber to ensure mechanical strength. Due to its isotropic rotor, the d- and q-axis inductances are identical and the saliency ratio ($\xi = L_q/L_d$) is approximately 1.

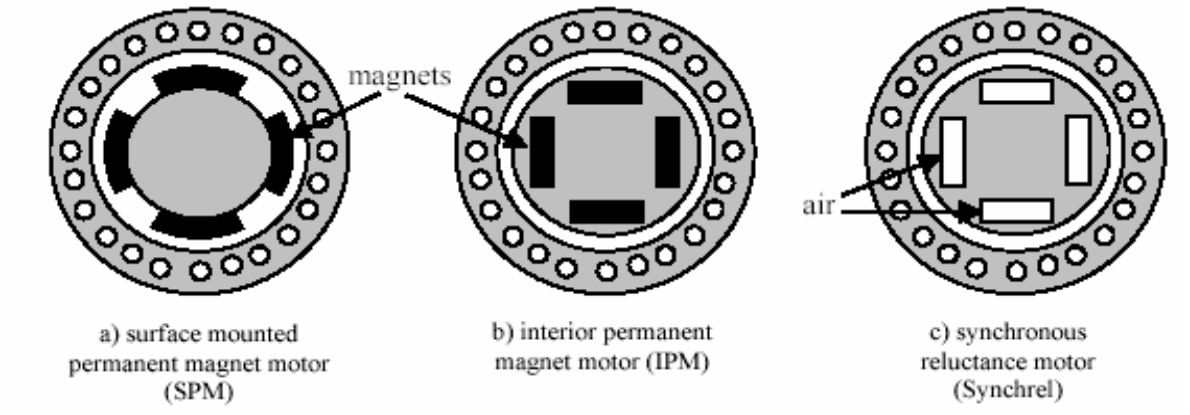

Figure 2.2 Cross section of the three main types of PMSM

Therefore no reluctance torque occurs. In Figure 2.2b, a possible design of an interior permanent magnet motor (IPM) is presented, in which the magnets are buried in the rotor core. Setting the magnets inside the rotor improves the mechanical strength and magnetic protection. By appropriate positioning of the permanent magnets (and additional flux barriers), the saliency ratio ξ of the IPM is varied accordingly. An IPM motor exhibits both

magnetic and reluctance torque. These features allow the PMSM drive to be operated in high-speed mode by incorporating the field –weakening technique. Figure 2.2c, shows the cross-section of a synchronous reluctance motor. Without permanent magnets, the reluctance motor produces only reluctance torque.

TABLE 2 Summary of Rotor Design Types

	surface Mounted	**Inset**	**Buried(Interior)**
Saliency	No	$X_q > X_d$	$X_q > X_d$
Air-gap Flux Density	$B_{gap} < B_{residual}$	$B_{gap} < B_{residual}$	$B_{gap} < B_{residual}$

2.1.3 Starting characteristics of PMSM (General review)

To understand normal operation of the motor, it is important to understand why the field rotates at synchronous speed. Each set of field pole is matched with an equivalent set of stator poles. Since like poles (north and north) repel and unlike poles attract, the poles of the rotating field tend to align themselves with opposite poles produced in the stator by the a.c. power applied to the armature windings of the motor.

Induction motors can be started and accelerated to steady state running condition simply by applying ac power to the fixed stator windings of the motor, but synchronous motors can neither start nor run without special attention because the net torque on the rotor of a synchronous machine (PMSM) is zero unless the rotor winding is rotating at nearly synchronous speed with appropriate excitation applied to the moving winding (in the case of PM machines, we have fixed excitation) for these reason ,various arrangements have been devised for starting synchronous motor and for providing excitation to the field winding at appropriate time in the starting sequence. When the synchronous motor operating at synchronous speed, it is possible to alter the power factor of the ac system supplying power to the motor by varying the excitation supplied to the motor field.

In the case of PMSM motors, the starting from unknown rotor position may be accompanied by a temporary reverse rotation or may cause a starting failure. These eventualities are not tolerable in many applications. Thus, when the initial rotor position information is not available proper starting procedure must be implemented for safe startup. According to the various proposals in literature the possible starting procedures can be grouped with reference to the basic principle as follows:

- starting from predetermined rotor position established by proper feeding;
- open-loop startup (V/f);
- estimation of the rotor position at standstill by means of specific algorithms

The first method refers to the possibility of aligning the magnet axis in the direction of a (fixed) stator current filed .This can be accomplish through closed loop current control (i.e. by the proper setting of the position feedback in a field oriented controller, or in an open-loop scheme, simply imposing a specific inverter gate pattern to align with one of the phase axes. The reliability of this method is affected by the presence of the load torque, whose value can cause a displacement between the imposed alignment position and the actual one.

The open loop startup is intended as the acceleration of the motor following a rotating stator field whose angular position is generated in an open-loop scheme. This method is usually adopted in back-EMF-based sensorless scheme, and the open-loop operation is maintained until a given speed at which the rotor position estimate is sufficiently accurate. The critical point of this method is the choice of the time variation law of the open loop position. It must be carefully selected in order to assure a safe starting with minimum oscillation up to the maximum torque.

Among the specific algorithms for rotor position estimation at standstill, an interesting approach is the use of a field oriented control scheme with incremental encoder. The rotor

position is detected by considering the effect on the measured (incremental) position of a pseudorandom binary sequence test signal added to the direct current reference. In regard to full sensorless applications, other methods must be applied. A wide range of sensorless drives scheme using rotor position estimation techniques are also available, but most of them do not detect the rotor position at standstill.

2.1.4 Why concentrate this study on PMSM?

While the transition from single speed to variable speed systems is in progress, another transition is in effect within the field of variable speed motor drives. Direct current and induction motor drives, which have dominated the field until now, are being replaced by PMSM and BLDC drives for low power applications. Low power is defined here as being less than 10kW. Some of the applications for motors below 10 kW are in home appliances, electric tools and small pumps and fans. PMSM and BLDC have the following advantages over dc motors:

- less audible noise
- longer life
- sparkless (no fire hazard)
- higher speed
- higher power density and smaller size
- better heat transfer

PMSM and BLDC have the following advantages over induction motors:

- higher efficiency
- higher power factor
- higher power density for lower than 10 kW applications, resulting in smaller size
- better heat transfer

The above comparison shows that the PMSM and BLDC are superior to the induction motor for low power applications. The operation of the BLDC and the PMSM is very

similar from a fundamental point of view. Therefore, all the analysis and control strategies developed for the PMSM readily applies to the BLDC. The above discussion justifies the choice made in this thesis. The same techniques developed in this thesis can be applied to all high performance motor drives.

2.1.5 Applications

Among many applications of PM synchronous motor here we mention some:

Robotics and factory automaton (servo drives)

- pick and place robots (Motion control)
- positioning tables
- automatic guided vehicle
- Power supply inverters

Computer and office equipment

- copier and microfilm machines
- printers/plotters
- tape drivers

Appliances

- washers
- blowers
- compressors

Automotive control

- Power steering
- Anti-lock brakes
- Suspension controls

HVAC

- heating
- ventilation and air conditioning

etc...

2.2 Derivation of a PM Synchronous Motor Model

In a rotating machine there is always a rotating member and a stationery one. Because of this, a situation always arises wherein the self and mutual inductances, which are responsible for various voltages induced in the coils, become time varying. These time varying inductances cause difficulties in using the routine procedures for the analysis. In a permanent magnet synchronous motor where inductances vary as a function of rotor angle, the two phase (d-q) equivalent circuit model is commonly used for simplicity and intuition. In this section, a two phase model for a PM synchronous motor is derived and the properties of the circuits and variables are discussed in relation to the physical 3 phase entities. Due to the lack of developed procedures in the past, obtaining model parameters were very difficult and uncertain, because some model parameters are not directly measurable and vary depending on the operating conditions. Formulation is mainly for interior permanent magnet synchronous motors but can also be applied to surface permanent magnet motors.

Conventionally, a 2-phase equivalent circuit model (d-q model) has been used to analyze reluctance synchronous machines. The theory is now applied in analysis of other types of motors including PM synchronous motors, induction motors etc. In subsequent Section, an equivalent 2-phase circuit model of a 3-phase IPM machines is derived in order to clarify the concept of the transformation and the relation between 3-phase quantities and their equivalent 2-phase quantities.

Throughout the paper, the following assumptions are made:

(1) Stator windings produce sinusoidal mmf distribution. Space harmonics in the air-gaps are neglected.

(2) Air-gap reluctance has a constant component as well as a sinusoidally varying component.

(3) Balanced 3 phase supply voltage is considered.

(4) Although magnetic saturation is considered, eddy current and hysteresis effects are neglected.

(5) The constants of the machine do not vary with temperature

2.2.1 Mathematical Description of PMSM

When permanent magnets are buried inside the rotor core rather than bonded on the rotor surface, the motor not only provides mechanical ruggedness but also opens a possibility of increasing its torque capability. By designing a rotor magnetic circuit such that the inductance varies as a function of rotor angle, the reluctance torque can be produced in addition to the mutual reaction torque of synchronous motors. This class of Interior PM (IPM) synchronous motors can be considered as the reluctance synchronous motor and the PM synchronous motor combined in one unit. It is now very popular in industrial and military applications by providing high power density and high efficiency compared to other types of motors.

Fig.2.3 illustrates a conceptual cross-sectional view of a 3-phase, 2-pole IPM synchronous motor along with two reference frames. To illustrate the inductance difference ($L_q > L_d$), rotor is drawn with saliency although actual rotor structure is more likely a cylinder. The stator reference axis for the a-phase is chosen to the direction of maximum mmf when a positive a-phase current is supplied at its maximum level. Reference axis for b- and c-stator frame are chosen 120° and 240° (electrical angle) ahead of the a-axis, respectively. Following the convention of choosing the rotor reference frame, the direction of permanent magnet flux is chosen as the d-axis, while the q-axis is 90 degrees ahead of the d-axis. The angle of the rotor q-axis with respect to the stator a-axis is defined as θ. Note that as the machine turns, the d-q reference frame is rotating at a speed of $\omega = d\theta/dt$, while the stator a-b-c- axes are fixed in space. We will find out later that the choice of this rotating frame greatly simplifies the dynamic equations of the model.

The electrical dynamic equation in terms of phase variables can be written as

$$v_a = R_s i_a + \frac{d\psi_a}{dt} \tag{2.2}$$

$$v_b = R_s i_b + \frac{d\psi_b}{dt} \tag{2.3}$$

$$v_c = R_s i_c + \frac{d\psi_c}{dt} \tag{2.4}$$

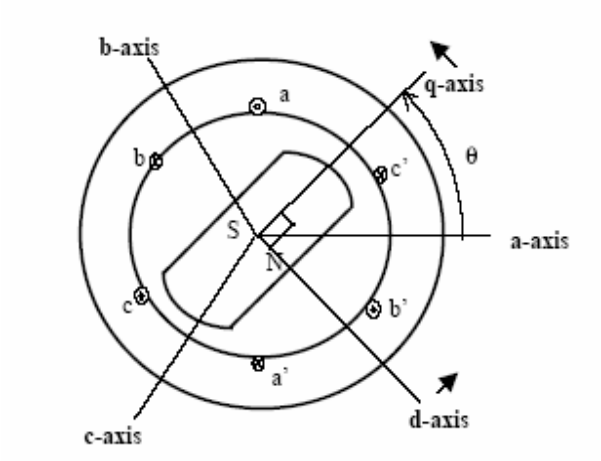

Figure 2.3 Three - Phase PMSM motor with one pole pair permanent magnet

While the flux linkage equations are

$$\begin{aligned}\psi_a &= L_{aa}\, i_a + L_{ab}\, i_b + L_{ac}\, i_c + \psi_{am}\\ \psi_b &= L_{ab}\, i_a + L_{bb}\, i_b + L_{bc}\, i_c + \psi_{bm}\\ \psi_c &= L_{ac}\, i_a + L_{bc}\, i_b + L_{cc}\, i_c + \psi_{cm}\end{aligned} \tag{2.5}$$

or in the matrix notation

$$\begin{bmatrix}\psi_a\\ \psi_b\\ \psi_c\end{bmatrix} = \begin{bmatrix}L_{aa} & L_{ab} & L_{ac}\\ L_{ab} & L_{bb} & L_{bc}\\ L_{ac} & L_{bc} & L_{cc}\end{bmatrix}\begin{bmatrix}i_a\\ i_b\\ i_c\end{bmatrix} + \begin{bmatrix}\psi_{am}\\ \psi_{bm}\\ \psi_{cm}\end{bmatrix} \tag{2.6}$$

considering symmetry of mutual inductances such as $L_{ab} = L_{ba}$. Note that in the above equations, inductances are functions of the angle θ. Since stator self inductances are maximum when the rotor q-axis is aligned with the phase, while mutual inductances are maximum when the rotor q-axis is in the midway between two phases. Also, note that the effects of saliency appeared in stator self and mutual inductances are indicated by the term 2θ.

For the stator self-inductances

$$L_{aa} = L_{so} + L_{s1} + L_x \cos(2\theta) \tag{2.7}$$

$$L_{bb} = L_{so} + L_{s1} + L_x \cos(2\theta + 120^0) \tag{2.8}$$

$$L_{cc} = L_{s0} + L_{s1} + L_x \cos(2\theta - 120^0) \tag{2.9}$$

where $L_s = (1/2)(L_q + L_d)$ and $L_x = (1/2)(L_q - L_d)$.

It has its maximum value when the axis of the field and axis of the phase (under consideration) are in one line.

For the stator mutual inductances

$$L_{ab} = -(1/2)L_{so} + L_x \cos(2\theta - 120^0) \tag{2.10}$$

$$L_{bc} = -(1/2)\, L_{so} + L_x \cos(2\theta) \tag{2.11}$$

$$L_{ac} = -(1/2)L_{so} + L_x \cos(2\theta + 120^0) \tag{2.12}$$

For mutual inductances in the above equations, the coefficient -(1/2) comes due to the fact that stator phases are displaced by 120°, and cos(±120) = - (1/2). Meanwhile, flux-linkages at the stator windings due to the permanent magnet are

$$\psi_{am} = \psi_m \cos(\theta) \tag{2.13}$$

$$\psi_{bm} = \psi_m \cos(\theta - 120^0) \tag{2.14}$$

$$\psi_{cm} = \psi_m \cos(\theta + 120^0) \tag{2.15}$$

For this model, input power P_i can be represented as

$$P_i = v_a i_a + v_b i_b + v_c i_c$$

7sî□4¡Ä×ƒ[ÑÔGSŸò0ÎßFl□□ÛÛÑ„SÞ□ø;^½“ØFÐ˜øÆ”7!¾1w□Û□îf¿□åÍ^¿□š£¹—
ø□*.<Ë‰g9À□oÙð-;¾eÇ·œàÆ»Üx—□ïòâ]-pá_NüË□v<Ì†‡Ùñ0‰□sãc□/ó£□/óàe.¼Ì

üÌ□ŸÙð3;~&qâin<MâÅ×¼øš□_sákNpàmv¼Í†·Ùñ Thursday, October 2, 2008ÞæÆÛ¼x
??

›□oóàm.pâo

¼□□

È-™x

åQÄG□□□±ÄÇ□Gy□â»□×□º□Û□â)□'>□z□Ÿ□Ih’ÐøÆF’66¶ø□

y¾'ÚdêL¦□□êìÅ¶[7X)·R_-

èK}¯ A?êì‡&•sýÑô'îu4□Ø¦©??ñI7>)ñâ•^¼ÒƒWºðJ'8ðK ~iÃ/íø¥Ä‰ºgºñL‰□ßôâ›-|Ó…o
??

òNÍ□Ä□Dó!ÛQ*NüÓ□□zñO/þéÁ?]àÄC□ø§

µ©Û1Ä□IùXâÇ□;-¾"~□ñ□(ŸHü7Ä}

rû-ñßQ>‰øï‰ý□&□?™ø-

)ŸBü□b¦□;□íOð3å?□?□f□?□f¡™…f6çæ ™C\:š¹lçÁ|Êç□¿@Å‹—zñR□^êÂK□àÀOíø©

?µã§□'□êÆS%^|Õ‹¯ zðU□¾ê□□ÞjÇ[mx«□o•8ñW7þ*ñâ±^<ÖÃ8(□□¹Ú˜°ië□¯ öÜ¥<¿□í

VêÜN}Û@nwPçNÊ³©o□uí†□êÛCü-Ê÷□¿Ÿ¸}

·□^?Hy.ñyÄæÃ!â□□o£ÜN¼□□□±N¶.pSî&Þ□^â□Ã□4GÐ□åÜ14Çˆ+@SÈö8□Q^Dü
8Iü)(FS™ÿ©7ú3`üë*ëó7”JþOQ□,"+ð÷]EûŒ‘Š<c°L«÷Y□®”~>›ÿ3□¾sµÎóŒ□lV,YDŠx‘
(º‹."AÄÒWr›,R(Oàg²hDY·ÓÏ!T×¶A□!~Ÿ□§?Ö.ûí□ýÙ?çêûOäkB□Ö÷þŸ•åû|¬
¿ÏÇz3èb|>ÖŸû¹XêÇý‰Ÿ‹¥ÿ|,ÙÅú×À□0

†hÏ□oÑ=g3L+»ê<¯ □8õ5□H□¢E□-
□=ÉU”¸‹Ò†ºÿ#

Ñ□ãs□ñ

□?Œ□ó.ís□□œoÂ´¿sÈûË`ÿ:]_ûÎ…□§¯G©ÏI&«¯^xz9Eëó□¢□û=Ø†□•‹□-ÌÊÏ□Ô§□ÏäF?ï

T?Ç¼□|□9¨¬¼□éâ.×¶ÕÊ™ÛŒøŒ+YO=□,ç˜Óu'B$_{??}$Ê$‰âb~ÆUYŸe¥oSÕ2Ú□r□v]èg

Yù®ûG□–

Õ`íº¾g©|Ç□<ß□¢õÝ…>ßåë{ÿ6%□Ø¦Á□´é¯ÖO!º6…\¢¹û«öS½Kl<ýýº»øãéb¯…î×Þ□□¹
□šÒê•Ú§µÿ‡ó_
ùÎ□—óY□VÖ9=ù¾\·æ(ïý«¯ □‡hÏ è□/ö³¹aZ®åšå>m[E-
kÄq#q¡ã°¾V×¥ôÞ_□…¶□□¿QZ½-Õ1$D»2Æ_KMs®ñ'Çp

ëðîê*¼§¶â¶Rf>ýÞ>¨Œõsˆß°Ø·*V*

t¼^Œg´lc´µ6F[Ÿ-£-9n□Đ□m}□Ñç

-£□µzŸÐÆç

eŒÑ'*ð?0Vm~

þ□ÇYe□çð□³ Ú8ëtzœuâ¸S@ã¬Ó%8Îº□<ÎÆiõ¾¬ým¤{□ãL□»ºœß□ù¼8üw³bÃßùs°ßüx

N

¾9ò□□¯•Ÿ□£´ñ□uz¼Fq□□Ðx□ª`n□□—

Wkÿ/ÕÞ/þïÏh/ýŒöò>Ÿ]öÛÿ□]c§µ□□□□D□d□□□□□□□□□□□38 38□□□□□□□□

38

Đ

□□é□□□□□□□□□□□□□□□□□□□□□□□□□□□□□□□□□□□□ð??□□□²□
□ð□□□□D□□□□□□□□08 40 9:16:51 AMð3□□□□A(□□□ÿ□□□□□□□□□ð

40 40□??□□□"□□ð□□□□□□□ùˆÓ□ÿÉĸ ±S?ÏTè□ƒÿ□ö□
□□□□□□;ä□□□□□□

@=□ðî□□□ù^Ó□ÿÉK□±S?ÏTè□*f*□e□□□□□□□□□□□1□41□i□□□ðcQ□^R4□¼□□

□□þx íœ

Ú

lÔd¾†¿´ƒÅ#«î-□Ë-×µ□.¨à*"r□¨UTPpÅ;ºb3Ó{)´□¤ha) r□□□-□□□ï(è9$_{Q}$T(wäZî—

RhË¥´Ì7-…A.-vŸ¤I□r†vJ,úóØþ□&“ÉûåKþß¼oÒ Q„□ã BÔ~5□"F□u_Y□

¦

□ÕIˆÈÛï¾C□E^□â/.!Îâ½ó

□î,Èp!z¡□B{@X¾v¹DÖGáânq‹x@ôàç-"RÜ!’D,xB¤‹8cµßC3h□gÃù □œcym}ÿ□†Vëú}

î,Èp!z¡□B{@X¾v¹DÖGáânq‹x@ôàç-"RÜ!’D,xB¤‹8cµßC3h□gÃù □œcym}ÿ□†Vëú}□¦

çÔ□ú_S#Ü¢Ø•þ3ÒÝl9ÆÎ«[2ë’□cú¾¿è□óuÓ¢uçE&¯Öçsš-

âç@ú□™#Ü¿+x-ï3´Ÿ□8*Î«□Ø□ê^□cú¾¿è□óuÓ¢uçE&¯Öçsš-

Þ Ji{°âÒ——□lÇüú´‰o□‰oí,,□?«vZ2`Y†6mÓL¡_□{ë□-'Vëí¯¥a-□f□}àHF□~\

gŒa}m□m

‘□vNó□/0úÓó"íˆ¹D,z•6-úØAz©Äe□ÇÞœÿ□M´9EM

ý„5i□äØ7¦&=ú°□±î0□™öºþš¬>□5yø·šüâjòˆ□5ùmþôç»C□\-å–Q□Åàü□ê×

«Åúú□æ;³r˜¶0¼{í{úÇ□²ôŸBäæ□ý;—

mEE±¬Æxc<L†™ÚJ□□…PÁöYál^„«!□z,□iZÛ0-&ÃLÈ…<(„□-ý□ä□È

‘ç!ÏE>□ùdää‘g!OC®"ï‰<□ùÕÈ#‘Ÿ¯É□r□\ □È□r□\ □5Ú¾¥□Á‰\

□È□r□\ß½□coòŒ½›ìì-¶×YÆ1×ê □»

Ff□«□Ë³Z3m¡□bóø×Ô„□~-´å□A[í³□ÚúUJí¹„K_□¥ä°´JÑˆRL□ç,Yæ¼Ö-h~t□µšNÆ¶:□
Œ□åÄöOr□³
—±í□ÆxÒ¾V-ZuR_µå□□ûoík“ }Õ^Ÿª¿m□¶Û&àX□-»□íf]hŒks»

□‡ð□□ƒõë²

}Ðö©£±]m?[□ç}□□¼Ö†Á©ú□Ê¾hÇ®!}}}Òô□}ŠRìõÉlÃNŸ~iÇÉ□3fŸÌ×¿¶Úýœ ÇI
ñ³*k*·□□•“û×Ù□cVŸŸ„Ò§+,Çì□›cë3èYÏqjqb>ìOÆ¼æÕÍO,çZ³□--.´5[;çULÿ‹¼UÃlO[ÖÃ
â‡5ÆWOÃï#B¨¯ßf}ý–úú□¨¯ßf}ý–
úú□¨ï~‡ê«□mi5ü1H}Í÷Âë©¯ ÖÎ5TØ¬qDˆµîh3'4}`-Í×v□kGÅ^-5}`-Í×vúÔVq®ÖZ[]Œãn-
µù^Cµn□□µÎ°Yë

K-3□¨u†ÍZgXj□á@-û:Xë¾F=‡□©uß□k}íiÔz□ÍZï Ôz□□µ□c³Ös,µ□ã@-g:Xë™F=□□

±

©õÌ□kÝá4jíÄ¹~$_g$Ë9lg□®?ìÔºÊRë*□j]é`-+□zj□k°Öº2ÄZ_WO-□ŠóðÙâäk□óõÏyÝyÄr=u

Ä□ë©wáv□êÞËh«□mÍ`ÚÕRwó½°□ÎÃÛ±·®□?ÛZ□[Ú¬qKK□[:Pã–6kÜÒRã–

Ô¸□ƒ5¾Ð¨ñ□AjlaH5îÐ¨□GØ¬q„¥Æ□

Ô8Âf□#,5□p ÆÍ□¬±ö□T-Æç□©q□□¥Æí□Uc¯ °Wc¯ 8¹Æ^a¿ÆvútD9¹Oæκ;}úPÔþíÝ‰

ß™hmí6j|Pœ\có=§~g’cü□ÁN}ó,õÍs ¾y ë›g©o□□õÝè`}—

??

□õÝ□¤¾ËB¨oûFÔ7Çf}s,õÍq ¾96ë›c©o□□õýÊÁúN7êûu□úN□¡¾□□Qßl›õÍ¶Ô7Û□úfÛ ¬o¶¥¾Ù

Ôw’ƒõ□oÔ÷í õ□B};6¢¾™6ë›i©o¦□õÍ´YßLK}3□¨o–ƒõ□`ÔwD□ú

□¡¾□□Qßh›õ□¶Ô7Ú□úFÛ¬o¥¾vû4□b…3çÐS□û□´úÆ[êk¾×Ð9´ö7‹^FÔ¸‹Í□w±Ô¸‹□
5îb³Æ],5îâ@□»9Xã□Œ□ß□¤Æ7„Tãö□ªqk›5nm©qk□jÜÚf□[[jÜÚ□51 u°Æ□□5¾*H□/

©Æ□~²□ÿv□Ïÿ¯ {x□ºGÒl£š□·(ÿ÷uà}i!ßWV□Ú}eZÆý9ìÄùG{#£³ô~E‹Yð□Ì†/á+˜□_Ã7

ð-Ì…y□

óa□„„E°□–ÀRX□ßÁrX□+a□¬†5□□ka□¬‡

°□6ÁfØ□[aAM Ãv(□□°□□¡□Ša□ì†=°□J`-
ä

”B□ì□/HðA9TÀ□¨„ƒp□üp□¾‡#p□□Áq¨,jø□~„□íÈ)ÑB□0□□□4□³ □šÂÙðp

4ƒßÁ¹p-œ□¿‡?À□Â□ð_Ð□þ□-àOðßp!ü□.,¿ÀÅ□—À¥Ð□ZÁeðWh
màr¸□®„¶Ð

®,¿ÁÕp

´□sl˜câó□±¡½□-t□ë #\Thursday□à□à□á□è

7ÂMp3DÁ-p+t□Ûàv¸□ºB7¸□î,îÐ□î†¿Ã=Ð□î…ûà~x□-„‡´þB/x□-…□ÀcÐ□-‡hPÁ
-^□X^ƒxH□DH,dè□)Ð□úA*¤A□H‡□0□□□A□□ƒáIx□2a□

…□Â0È,á0□FÂÓð

<9:16:51 AM£`4Œ□±ð□Œƒçá□□□□àEx??^†‰ð□¼□Ùð□¼

oÀ›0Þ,·a2L□©ð

Lƒwá=x>□□á#ø□¦Ã'ð)Ì□™ð□|nŒ□nÊ‰1a^+t×ÇI´ø□äÀ,ø□fÃ—
ð□Ì□¯á□ø□æÂ<È…ù°□□Â″X

K`),$f_i$`9¬□•°□VÃ□Èfµ°

ÖÃ□Ø□›`3l□-°

òa;□À

Ø…P□Å°

vÃ-Ø

%°□J¡

öƒ□$ø □*à□TÂA8□~8

ßÃ□8□Çà8TiŸÍ□îKn”ç‹Æ{~©áùåu□ïÅó÷ãùex~□□_Šç—âù¥x~)□_Šç—

âù¥x~□□_†ç—áùûñüýxþ~<ß‹ç{ñl‰çK<ß‡çûðl□ïÃó}x¾ ThursdayÏ÷áùåx~9□_□ç—

ãùåx~9□ïÃó}x¾□Ï÷áù><ß‡çûð|□ïÃó%□/ñ|‰çK<_âù□Ï—x¾Äó%□/é©¤‡'□Iz%õo-

”C□□□J8□‡À□‡á{8□Gá□□‡??¨†àG¨□¡H<_âù□Ï—x¾Äó October □/ñl‰çK<_âù□Ï—

x¾Äó%□/ñl‰çK<_âù□Ï—x¾Äó%□/ñl‰çK<_âù□Ï—x¾Äó%□/ñl‰çK<_âù□Ï—
x¾Äó%□/ñl‰çK<_âù□Ï—x¾Äó%□/ñl‰ç{ñlÉ8□'y¾×ðlYçù□Ï—
x¾Äó%□/ñl‰çK<ß‹ç{ñl/□/ñl‰çK<_âù□Ï—x¾□Ï÷âù^<ß‹çK<_â#□Ï—
x¾Äó½x¾□Ï÷âù^<ß‹çK<_âù□Ï—x¾Äó½x¾□Ï÷âù^<ß‹çK<_âù□Ï—x>
□*¸Á□1□Ë{q□□□È²$H†>□□}¡¤ò~□ôg>□□À@x□□A□

†'Yç)Èd~□

…□Â0È,á0□F²ÎÓLŸ□ga□Œ†10□□ƒqð<¼□ãa□¼□/ÁË0□^□W!□^ƒ×á

x□&Á[ð6L†)0□Þ□ið.¼□ïÃ□ð!|□-

Ãtø□>…□0□>ƒÏµc□àùÞ□¿¿Õz¾□Ï÷âùø□|□³áKø□æÀ×ð

|

sa-äÂ|X□

a□,†%°□–Áw°□VÀJX□«a

äÁZX□ëa□l„M°□¶ÀVØ□ù°□□`□ì„B(‚bØ□»a□ì…□Ø□¥P□ûÁ
□|P

…cp□ªÀIÏ¯ □5□öüþp‘Q»□□OÍ6.yÂ÷÷AÞ¿□ïß
??

Åø□!þ¿□¶“□ÛÈ□-°™□ØH

¬‡µdÁ□²` □¬ □–“□Ë`

ß‹È„□0□%ßÂ7dÃ□Öø□f³ö,ò!□þ…ús2â3˜AkŸ'□ŸÀtZÿ˜¬ø□ kï"□ï±åwÉ‹iôb□½y‡¼˜J

VL¦w“õévñ6¼EnL¢ço’□o°□o□□¯³G¯ ‘□ÙìÝ«ìå+0‘ìx™½~‰½□‘£0□£1□£2□£ó□^ø<
Ù1□ìx□ì□KnŒ&?FëÓƒb□ù1Šüx–üx†üx†ì□I†ŒÔ§ÇÄ□2d8ı6 œ

??

É"C²È□,*8Œ,

#?†’#Cõi¸2„□É$G2É‘Lr$“□yŠ□yŠ□y’□□L□d□#□äÈ rd□92ˆ□□D□

"G□

G□'#□É'□äÈ□r$□□I'GÒÉ'tr$□qÐ¿nlhcB»7l'R;F²ôqÒŸœéOÎ¤'3iäL*9"JÎ¤'3©äL*9"JÎ ô#gú'3}É™¾äL□9"BÎ¤□3)äL□9"BÎ¤□#}È'>äH29'L□$"#ÉäH29'L□$"#ÉäH□9'D□$'# ‰äH"9'H□$'#‰äH"9'H□$□#xS<9□O□$□# äH□9'@□$□#ñäH<9□G□Ä'#qäH□9□G□Ä"#ñäH□9□G□Ä#±äH,9□K□Ä'#±äH□9□ G□Ä'#±äH

9□C□Ä□#1äH

9??$_{K}$□Ä'#±ä*H*

9□C□Ä□#-rÄC□xÈ‘□r$†□‰!GbÈ‘□rÄC□xÈ□□9â!G<äˆ‡□ñ□#-rÄC□xÈ□□9â&GÜä
ˆ›□q“#-rÄC□xÈ□□9â!GÜäˆ›□q“#nrÄM□¸É□79â!G<äˆ›□q“#*9¢’#*9â&GÜäˆ›qàÖÇ†6-

&□œç»…9NÜäŒ›œq“*3*⁎9£’3*9£’3*9ã&gÜäŒ›œq“3nrF%gTrF%gTrF%gÜäŒ›œq“#nrD %GTrD%GTrD%GTrD%GÜäˆ›□QÉ□5àÚA%GTrD%GTrD%GTrD%GTËµƒJ□¨äˆJ□¨äˆ J□¨äˆj¹vPÉ□•□QÉ□•□QÉ□5ÈµƒJ□¨äˆJ□¨äˆJ□¨§¸vPÉ□•□QÉ??µ□k□•□QÉ□•□QÏøµC □8½ß$_{09}$i÷DiÿŸp"G´ß□¥‘%Ãqô

0□wŸA□Ì…□¸ý□rDË“□Ü¿Š□8Kù□×š‹«ÍÃ-æáb¹¸Úl□n>

·□ù…,[^›-Â½□ãF‹q□%¸ÌR??e)[_†□-Ãe¾Ã¥–

ã|ËqÊ□ìÚJÜv%î»□7^-s,,,9N□Ô□KYË6×áÊëpÝõ¸÷□œ□□I±‘Ÿ›Xc□ŠÍ(¶°Æ□æ¶’-Ûèû6
R

Ÿö¶“□Ûqþ□t□ï` □□¤ÒNÖ/¤□"^□±¼˜„*ÙE,ìb□»Ùþ-Ü}□ú½ô£„Ä(á½}¼Sƒ²□ ´é~TûYÃ«_±Tê*

W!>ö©œ}+§Ï□´q□„©½vÙ□…´¾ƒÖ□`'□´‹-

*ifr*Ö:Ì□W*f*K9Êü1¶{Œµ□³µ*zXÅ^T³W?èl"“□YCë□g□Ê!□Îq□WÂ□?[ý□*ii-
ÙT□Û©à6ÆAAÝØÐÆD>ó□iÿ;lŒ
íý¦¬ßT)1®…üPM•]J3å0•®¡Ò□É²R(&ÏThu, Oct 2, 2008..z>#c□yV

%TÖÇ(ðC5#Å¥4G×□Ýéc9:16:51 AM¥

Š□!□□OÆå“q; ˜œ+!Çlàgô T3J\ÊÅh#Ñ^Â6/a›—²^K´-

Ñµ,Ë˜¿Œþþ□mký:ÊO¾U“o.år´W ½??í•hÛ¢mÇúíÐ]¥S@Þ□1:KÀ$_G$æùÉ¼jp)×¢í□¶□ÚëÐ

vDÛ‘õ¯G×I§□

,&□KÀG

úÉÁjp)7¢½íMhoF□ÅzQ¬□

º[u□ÈÅ"(!□}d£ªÉG—

Ò□mW´ÝÐÞ‰öN´w±~wt=˜Þ□înt□Gw□°{ÐõDw/º{ÑÝ‡î~t÷£{□õ-

D÷□Vst□£ë…®□ºGĐ=ŠîQtÿ@÷□ºÇĐ™cã1cl-06´÷{Óîã´÷8íFƒÊ¼JÛnÚöĐ¶‡¶ch;–
¶ci;□¶ãi;-m□ÚDÖOD—□ÉÌ'£íƒ¶□Ú□´}ÑöEÛ□m*ÚT´ihû£íÏúéè□è□ËEärøÈf?Ù\
.e0Ú'Ñ>‰ö)´™h3Y□□º¡:□du□Y]□>òÚ□Õd¶K□□v□Ú‘hŸFû4ÚgXÿYt£˜□F7□Ý□tcÑ

□E÷□ºqèÆ¡{-Ý

è^@7□õ' {'éKè^B÷2º‰è&¢{Ý+è^E—

□.□Ýkè^gý×Ñ½□o2ÿ&ÚIhßBû□Ú·ÑNF;□í□´SÑNEû

Úi¬?

Ý»ð-óï¡}í□h?@û!Ú□Ð~„öc´£□□ö□´Ÿ°þ§èfè□□õEd}ø□□~}ll5®+ó□s

ml¤êãÄÏù@5¸”□Ú□EÛ³hû

Ú□MÛ³iïKÚýJ§□ó*f*"Î□JÀÇ9,Ÿs„jp)sÑÎE;□m.Ú\´óY□□º…L□¡[„n*1‰*è–

[Šn□ºeè¾C·□Ýrt+X□%ºULW£[□n

º<tyèÖ¢[‡n□ºõèÖ£Û□n#ëoD·63¿□í□´[ÑnE»

m>Ú|´ÛÑ□ -@»□íNÖß‰®□Š˜/B[Œv□Ú]hw£Ý*f*v□Ú½hKÐ– Ý‡vë—¢+Ó)àü£ˆó□□ðq

âç□¤□\J9Ú□´□h□ -D[Éú□Ñ□Ò)àœ¤ˆs'□ðq^âç¼,,\A{□í1´ÇÐ-G[…¶1ÿ«íôsE□Û□ö\□¥‘ÿ«¢Ý3ï

áï†ŠñìŠPþv½Øh÷□□¯Ô>ó+ðo×æ{□Ôó·ë□ú}HnÑ—*s*®□‘*$ú*‰□□•6□ □¼-

?□^¶,ëS÷÷ísŒi¸□¹Ü□äµuÞ□0ïôódNuì³□ç Ø9ö□Ï_2Ÿ¹□-ðÌ¥§ÃÏÄ3—~Þg-
é□Ôù□Ÿµd}æ'v^-Ÿ□)0□ÆÀkF□□?□c□eçÖó□HÔ?□iÔ)NÄòiO§R±âo,‹£j—
Ÿôÿi□AÆ±u¬›¯O×Cœ□÷²v¼:ê9-Œßçë□U2î÷□<Þæ{-ê9Þ□™□Óý%
ßq3Õ□{$Ç=•ùT¦'□õ^□ñÆ²

~Þ¨ß1w¢BVï9ç□ÞãªÇ‡,Õ6Ü²ÞÙÆ´i□þÖPMnã`]äpMRŒvµöã•Úû•□kb¾×¤□šh÷Ai

¥□ùö§8.¡ŒÃÆ<'*Bÿ-

™□□□□□□□□□□□□Ϗ□□□

□□□

□□□□□□□□□□÷□□□□□□□□□□□□□□□□□□□□□□□□□□□□□□□□□□□□ □□□ □□□□□ŝ□□□ □□□□□□□□□□□□□□□□□□□□□tion.

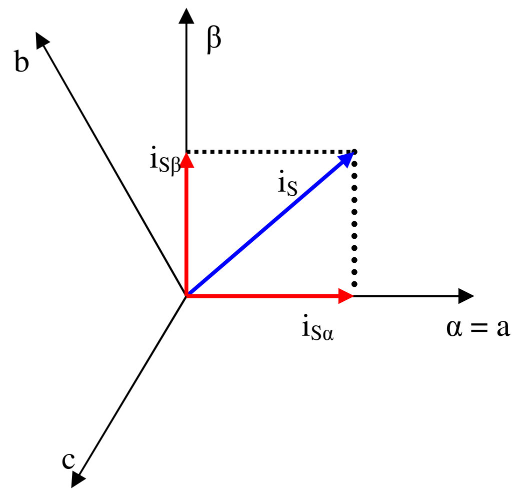

Figure 2.5 Transformation of stator quantities to stationary (α, β) coordinate axis

The Clarke transformation in matrix notation is

$$\begin{bmatrix} S_\alpha \\ S_\beta \\ S_0 \end{bmatrix} = \frac{2}{3} \begin{bmatrix} 1 & cos(120^0) & cos(120^0) \\ 0 & sin(120^0) & sin(240^0) \\ 0.5 & 0.5 & 0.5 \end{bmatrix} \begin{bmatrix} S_a \\ S_b \\ S_c \end{bmatrix}$$ Clarke transformation. (2.36)

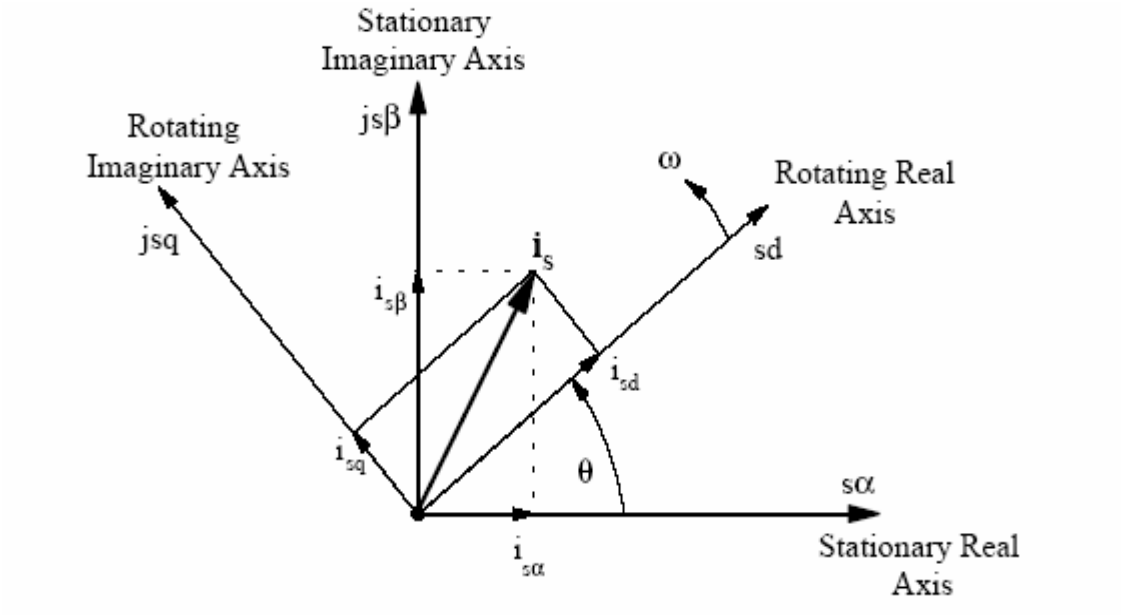

Figure 2.6 Transformation from the static α, β -frame to the rotating d, q-frame (Park transformation.

As before, the variable *S* represents voltage, current or flux linkage and the zero sequence components S_0 is always zero for a balanced 3 phase system. The second (Park transformation) simply converts from stationary α-β frame to the rotating d-q frame as

$$\begin{bmatrix} S_d \\ S_q \end{bmatrix} = \begin{bmatrix} \cos\theta & \sin\theta \\ -\sin\theta & \cos\theta \end{bmatrix} \begin{bmatrix} S_\alpha \\ S_\beta \end{bmatrix} \qquad \text{(Park transformation)} \qquad (2.37)$$

The voltages at the terminals of various windings in the two–axis model (in α-β frame) are obtained by applying phase transformation to the three-phase voltages. They are

$$v_\alpha = Ri_\alpha + \frac{d\psi_\alpha}{dt} \qquad (2.38)$$

$$v_\beta = Ri_\beta + \frac{d\psi_\beta}{dt} \tag{2.39}$$

Sometimes it is advantageous and preferable to have the equations in state variable form given by

$$\dot{x} = Ax + Bu$$

Equations can be rearranged and can be written in the following form.

$$\frac{di_\alpha}{dt} = -\frac{R}{L} i_\alpha + \frac{\psi}{L}\omega\sin(\theta) + \frac{v_\alpha}{L} \tag{2.40}$$

$$\frac{di_\beta}{dt} = -\frac{R}{L} i_\beta - \frac{\psi}{L}\omega\cos(\theta) + \frac{v_\beta}{L} \tag{2.41}$$

or in the matrix notation, in a synchronously rotating rotor d-q reference frame:

$$\begin{bmatrix} \frac{di_d}{dt} \\ \frac{di_q}{dt} \end{bmatrix} = \begin{bmatrix} \frac{-R_a}{L_d} & \frac{L_q\omega}{L_d} \\ \frac{-L_d\omega}{L_q} & \frac{-R_a}{L_q} \end{bmatrix} \begin{bmatrix} i_d \\ i_q \end{bmatrix} + \begin{bmatrix} \frac{v_d}{L_d} \\ \frac{-\psi_f\omega}{L_q} + \frac{v_q}{L_q} \end{bmatrix} \tag{2.42}$$

Since the d-q frame itself is rotating at a synchronous frequency, all sinusoidally modulated terms vanish after the transformation into this d-q frame. Notice that since the transformation of Eqs. 2.22 (and Eqs. 2.36) is not orthogonal (square matrix is orthogonal if its inverse is the same as its transpose), the power and torque of the 2-phase equivalent system is different from those of the original 3-phase system.

To calculate power and torque from the two phase equivalent circuit, (3/2) factor has to be included as shown in Eqs. 2.33-2.35. The reason that this non-orthogonal transformation of Eqs. 2.22 is popular is because the magnitude of voltages, currents and flux linkages are the same in both frames. In this two phase equivalent circuit, inductances are roughly (3/2) times those of the actual three phase value (refer to Eqs. 2.28-29). These "synchronous inductances" L_q and L_d are the effective inductances seen by a phase winding during balanced operation. In addition to the self-flux linkage of one phase, additional flux linkages are produced from the other two phase currents.

For some applications, it is useful to define voltage vector v_S and current vector i_S whose magnitudes are

$$|v_S| = v_S = \sqrt{v_d^2 + v_q^2} \quad , \tag{2.43}$$

$$|i_S| = i_S = \sqrt{i_d^2 + i_q^2} \quad , \tag{2.44}$$

Assume that current vector i_S is φ degrees ahead of the q-axis. Then, the relation between the stator current magnitudes i_S, and i_d and i_q are

$$i_d = -i_S \sin\varphi \tag{2.45}$$

$$i_q = i_S \cos\varphi \tag{2.46}$$

and Eqs. 2.35 can be expressed in terms of φ as

$$T = (3/2)\,p(\psi_m i_S \cos\varphi + 0.5(L_q - L_d) i_S^2 \sin(2\varphi) \tag{2.47}$$

For surface PM motors whose $L_q = L_d$, the reluctance torque term of the above equation vanishes and the above equation is reduced to

$$T = (3/2)\,p\,\psi_m i_S \cos\varphi \tag{2.48}$$

Here, the maximum torque is produced when $\varphi = 0°$, or the angle between the stator flux linkage vector and the PM flux linkage vector on the rotor is 90 degrees which is analogous to the characteristics of a separately excited DC motor. For interior PM synchronous motors, the reluctance torque is not negligible and higher torque can be produced by appropriately adjusting the angle φ.

Chapter 3

Control of PMSM drives

This document describes the most efficient form of vector control scheme: the Field Orientated Control. It is based on three major points: the machine current and voltage space vectors, the transformation of a three phase speed and time dependent system into a two co-ordinate time invariant system and effective Pulse Width Modulation pattern generation. Thanks to these factors, the control of AC machine acquires every advantage of DC machine control and frees itself from the mechanical commutation drawbacks. Furthermore, this control structure, by achieving a very accurate steady state and transient control, leads to high dynamic performance in terms of response times and power conversion.

Usually, high-performance motor drives require fast and accurate response, quick recovery from any disturbances, and insensitivity to parameter variations. The dynamic behavior of an ac motor can be significantly improved using vector control theory where motor variables are transformed into an orthogonal set of d-q axes such that speed and torque can be controlled separately. This gives the PMSM machine the highly desirable dynamic performance capability of the separately excited dc machine, while retaining the general advantages of the ac over dc motors.

3.1 Field Oriented Control (FOC)

The field orientated control is an efficient method to control a synchronous motor in adjustable speed drive applications with quickly changing load in a wide range of speeds including high speeds where field weakening is required.

The Field Orientated Control (FOC) consists of controlling the stator currents represented by a vector. This control is based on projections which transform a three phase time and speed dependent system into a two co-ordinate (d and q co-ordinates) time invariant system. These projections lead to a structure similar to that of a DC machine control. Field orientated controlled machines need two constants as input references: the torque component (aligned with the q co-ordinate) and the flux component (aligned with d co-ordinate). As Field Orientated Control is simply based on projections the control structure handles instantaneous electrical quantities. This makes the control accurate in every working operation (steady state and transient) and independent of the limited bandwidth mathematical model.

Field oriented control can be considered as:

- a commercial reality in high performance drives
- vector control involves control of the spatial orientation of the air gap flux
- the purpose is to decouple that portion of the stator current involved in producing air gap flux from that portion involved in the direct production of torque, there by providing independent control of torque and flux

3.1.1 The basic scheme for the FOC

The following diagram (Fig 3.1) summarizes the basic scheme of speed control with FOC. The field –oriented controller is based on a current-controlled voltage source inverter (VSI) structure. The current control loops are arranged in the two-phase synchronously rotating reference frame dq aligned with the rotor flux, while the rotor position and speed detection (observer) operates in the two phases stationary frame αβ.

The currents i_a and i_b are measured with two current sensors. The Clarke transformation is applied to them to determine the stator current projection in the two co-ordinates α, ß non-rotating frame. The Park transformation is then applied in order to obtain this projection in the d, q-rotating frame. The speed controller calculates a reference torque, which is proportional to the quadrature-axis stator current component i_{Sqref}. The direct-axis stator current component i_{Sdref} is set to zero if there is no field weakening. The stator current

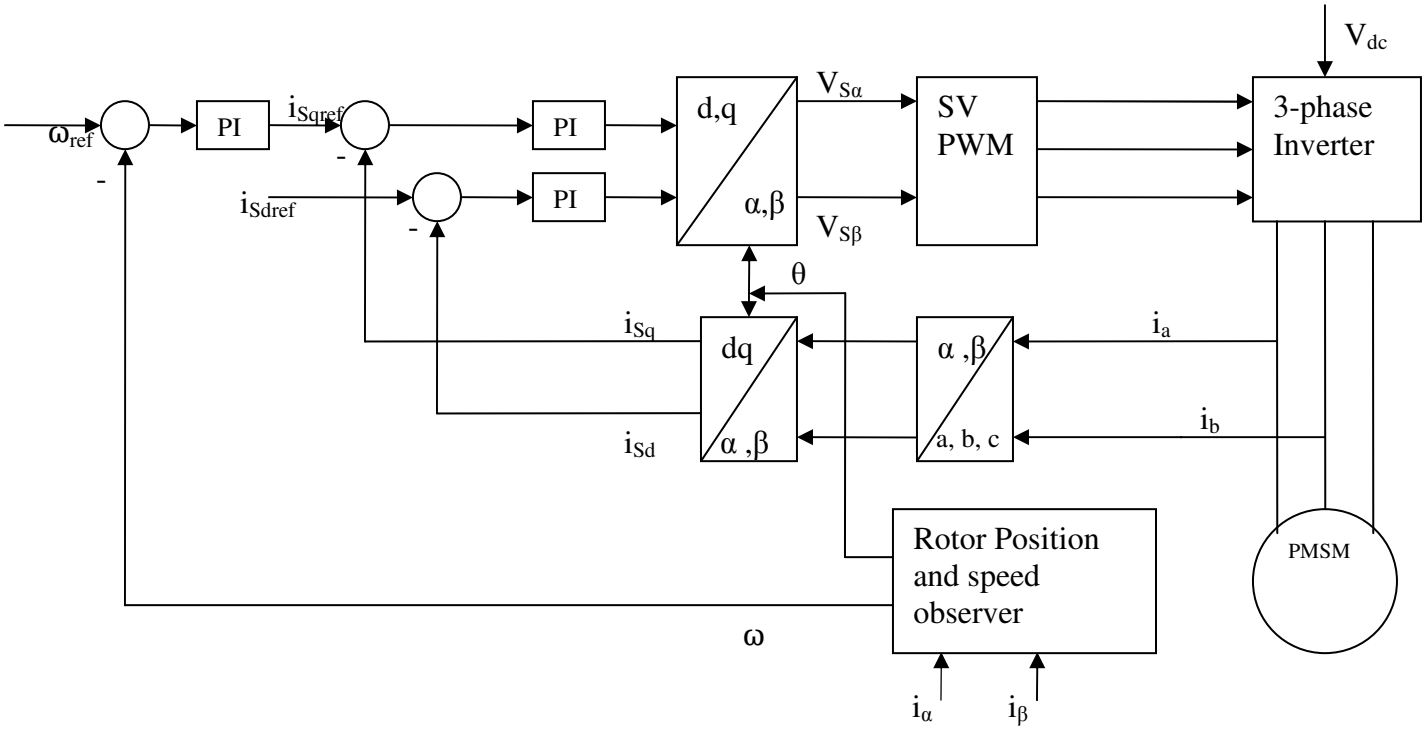

Figure 3.1 Basic scheme of FOC for PMSM-motor

components i_a ,i_b are used inside the observer, while the rotor current components i_q, i_d are needed for the current regulators. Standard PI controllers, with limitation and correction of the integral component, are used for all regulators.

The d, q projections of the stator phase currents are then compared to their reference values i_{sqref} and i_{Sdref} and corrected by mean of PI current controllers. The outputs of the current controllers are passed through the inverse Park transform and a new stator voltage vector is impressed to the motor using the Space Vector Modulation technique. The information about the phase currents can be obtained by two current sensors e.g. by phase shunts or current transducers. The information about the rotor position can be obtained by position sensors (e.g. incremental encoder, absolute encoder, resolver etc.) or indirect (with mathematical methods: like reduced order observer, Luenberger observer, etc).

3.1.2 Current sensing

In most of the inverter systems, information on the phase currents is required. The first method of obtaining those currents is to directly sense them but this requires, depending on the load schematic, at least two sensors applied directly on the motor phases. These types of sensors are usually expensive due to their sophisticated design and their need to operate in isolation. The other method is to sense only the line current, and estimate the 3 phase currents. This second method requires a simple cheap SHUNT as a sensor. As we directly control the inverters switching state, it is possible to know the exact electrical route taken by the input current through the inverter to the phase. We can then directly link the phase currents to the line current. The information we measure to obtain the phase currents is a result of a real sense on the current and not the result of a simulation requiring a model of the output circuit. The measurement process is totally independent from the input and output hardware of the inverter.

3.1. 3 Starting the Motor

Another major task is starting the motor. This was discussed briefly in section 2.1.3. A disadvantage of sensorless control is the fact that the motor needs to be running before a BEMF signal can be generated. Therefore, a mechanism is required to start the motor rotating until a reliable back EMF signal is captured. For this application a software state machine is used to initially align the rotor to a known position and then run the motor up to a minimum speed using a predefined commutation sequence to enable a back emf signal to be generated. Once a reliable signal is received the motor is commutated normally using the back emf signals.

When the rotor is not moving, there is no way to determine the rotor position without sensors. Therefore, this sensorless algorithm requires the rotor to be placed into a known initial position. This can be done physically by moving the rotor, or by energizing two phases. Energizing two phases will cause the rotor to move and then come to rest in a known position.

Generally, when two phases are energized for a long period, the rotor can come to rest in one of two possible positions. One of these two positions (equilibrium points) is stable and the other is not. If the motor is constructed properly, the unstable position will never be achieved. However, in some motors, cogging can give some stability to the unstable rotor position. In designs where this is possible, the rotor can be "kicked" out of this state by briefly energizing another combination of phases.

Once the rotor position is initialized, the commutation can be advanced by two states and maximum torque will be produced. Generally the PWM of the first commutation can be set to control the motor's acceleration. If the PWM is large enough, and if the load allows it, the motor can reach a high enough speed so that the sensorless algorithm can immediately take over.

To compensate for the low back-emf and high acceleration that results from the first commutation, it is useful if the second commutation occurs when the back-emf reaches some fixed value that is just beyond the zero crossing occurs (no delay). After the second commutation, the sensorless algorithm can operate normally.

3.2 Space vector pulse width modulation (SVPWM)

Control methods that generate the necessary PWM patterns have been discussed extensively in the literature. Pulse Width Modulation technique is used to generate the required voltage or current to feed the motor or phase signals. This method is increasingly used for AC drives with the condition that the harmonic current is as small as possible and the maximum output voltage is as large as possible. Generally, the PWM schemes generate the switching position patterns by comparing three-phase sinusoidal waveforms with a triangular carrier.

In recent years, the space vector theory has demonstrated some improvement for both the output crest voltage and the harmonic copper loss. The maximum output voltage based on the space vector theory is $2/\sqrt{3}$ times as large as the conventional sinusoidal modulation. It enables to feed the motor with a higher voltage than the easier sinusoidal modulation method. This modulator allows to have a higher torque at high speeds, and a higher efficiency.

The structure of a typical three-phase voltage source power inverter is shown in Figure 3.2. V_a, V_b and V_c are the output voltages applied to the windings of a motor. Q1 through Q6 are the six power transistors that shape the output, which are controlled by a, a', b, b', c and c'. For AC motor control, when an upper transistor is switched on, i.e., when a, b or c is 1, the corresponding lower transistor is switched off, i.e., the corresponding a', b' or c' is 0. That means, tuning the upper line switch on requires turning off the lower line switch and vice versa. The on and off states of the upper transistors Q1, Q3 and Q5, or equivalently, the state of a, b and c, are sufficient to evaluate the output voltage.

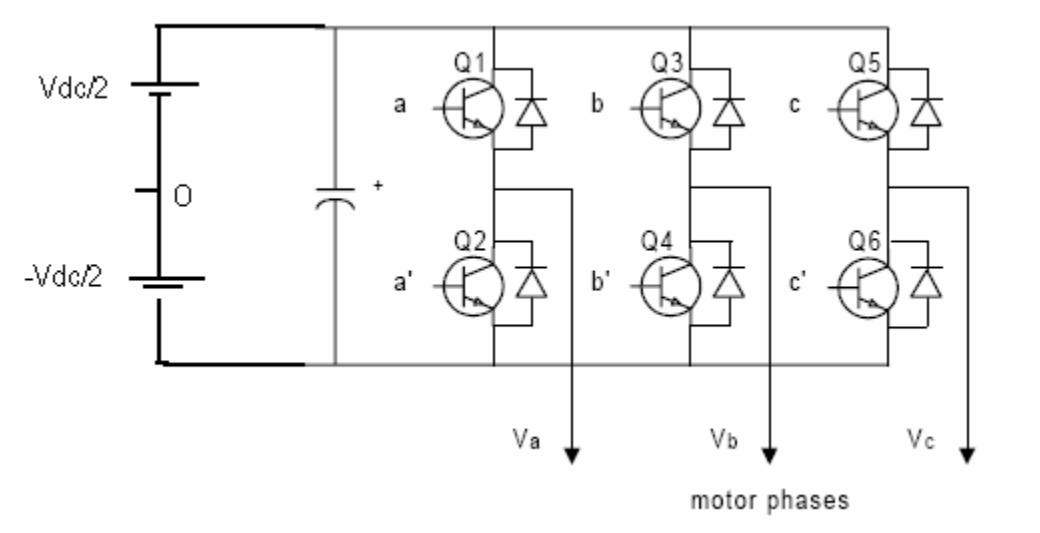

Figure 3.2 Power circuit Topology for a three-phase Voltage Source inverter(VSI)

The most popular power devices for motor control applications are Power MOSFETs and IGBTs. A Power MOSFET is a voltage-controlled transistor. It is designed for high-frequency operation and has a low voltage drop; thus, it has low power losses. However, the saturation temperature sensitivity limits the MOSFET application in high-power applications. An insulated-gate bipolar transistor (IGBT) is a bipolar transistor controlled by a control signal voltage (gate-emitter voltage) on its base. The IGBT requires low drive current, has fast switching time, and is suitable for high switching frequencies. The disadvantage is the higher voltage drop of a bipolar transistor, causing higher conduction losses.

Switching Patterns and the Basic Space Vectors

As shown in Figure 3.3, there are eight possible combinations of on and off patterns for the three upper power transistors that feed the three phase power inverter. Notice that the on and off states of the lower power transistors are opposite to the upper ones and so are completely determined once the states of the upper power transistors are known. It has been shown to generate less harmonic distortion in the output voltages and or currents applied to the phases of an AC motor and provide more efficient use of supply voltage in comparison with direct sinusoidal modulation technique.

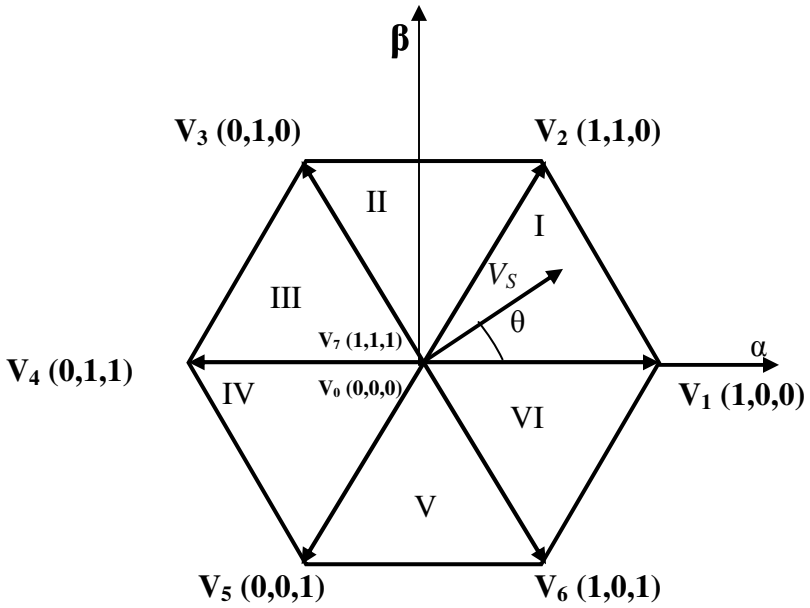

Figure 3.3 Inverter voltage space vector

Due to the fact that all three Line-to-Neutral voltages must sum to zero, a space vector V_S is easily calculated by the formula

$$V_a = V\cos(\omega t) \tag{3.1}$$

$$V_b = V\cos(\omega t + \frac{2\pi}{3}) \tag{3.2}$$

$$V_C = V\cos(\omega t + \frac{4\pi}{3}) \tag{3.3}$$

$$V_S = V_{an}.e^{j0} + V_{bn}.e^{2\pi/3} + V_{cn}.e^{-j2\pi/3} \tag{3.4}$$

where V_{an} , V_{bn} and V_{cn} are the phase voltages of the inverter output.

The phase to neutral voltage of the inverter output for the three phases is given by

$$\begin{aligned} V_{an} &= (1/3)(2*V_{ao} - V_{bo} - V_{co}) \\ V_{bn} &= (1/3)(2*V_{bo} - V_{ao} - V_{co}) \\ V_{cn} &= (1/3)(2*V_{co} - V_{ao} - V_{bo}) \end{aligned} \tag{3.5}$$

The expression of the 3 phase voltages in the (α, β) frame are given by the general Clarke transform equation:

$$\begin{bmatrix} V_{S\alpha} \\ V_{S\beta} \end{bmatrix} = \frac{2}{3}\begin{bmatrix} 1 & -\frac{1}{2} & -\frac{1}{2} \\ 0 & \frac{\sqrt{3}}{2} & -\frac{\sqrt{3}}{2} \end{bmatrix}\begin{bmatrix} V_{an} \\ V_{bn} \\ V_{cn} \end{bmatrix} \tag{3.6}$$

The eight combinations and the derived output phase voltages and the 3 phase voltage in terms of DC supply voltage V_{dc} in the (α, β) frame, according to equations (3.4) and (3.5), are shown in Table 3.

Table 3. Switching patterns and output voltages of a 3-phase power inverter

a	**b**	**c**	$\mathbf{V_{AO}}$	$\mathbf{V_{BO}}$	$\mathbf{V_{CO}}$	$\mathbf{V_{AN}}$	$\mathbf{V_{BN}}$	$\mathbf{V_{CN}}$	$\mathbf{V_{S\alpha}}$	$\mathbf{V_{S\beta}}$	
0	0	0	-1/2	-1/2	-1/2	0	0	0	0	0	V_0
0	0	1	-1/2	-1/2	1/2	-1/3	-1/3	2/3	-1/3	$-1/\sqrt{3}$	V_1
0	1	0	-1/2	1/2	-1/2	-1/3	2/3	-1/3	-1/3	$1/\sqrt{3}$	V_2
0	1	1	-1/2	1/2	1/2	-2/3	1/3	1/3	-2/3	0	V_3
1	0	0	1/2	-1/2	-1/2	2/3	-1/3	-1/3	2/3	0	V_4
1	0	1	1/2	-1/2	1/2	1/3	-2/3	1/3	1/3	$-1/\sqrt{3}$	V_5
1	1	0	1/2	1/2	-1/2	1/3	1/3	-2/3	1/3	$1/\sqrt{3}$	V_6
1	1	1	1/2	1/2	1/2	0	0	0	0	0	V_7

The nonzero vectors form the axes of a hexagon as shown in Figure3-3. The angle between any adjacent two non-zero vectors is 60 degrees. The zero vectors are at the origin and apply zero voltage to a motor. The eight vectors are called the basic space vectors and are denoted by V_1 , V_2 , V_3 ,V_4,V_5 ,V_6 ,V_0 and V_7.The same transformation can be applied to the desired output voltage to get the desired reference voltage vector V_S in the d-q plane. The objective of space vector PWM technique is to approximate the reference voltage vector V_S by a combination of the eight switching patterns. One simple means of approximation is to require the average output of the inverter (in a small period, T) to be the same as the average of V_S in the same period.

Approximation of Output with Basic Space Vectors

Eight space vectors can be represented as a complex –vector expression

$$V_k = \begin{cases} \frac{2}{3} V_{dc} \exp j(k-1)\pi/3, & k = 1,2,...,6 \\ 0, & k = 0,7. \end{cases} \qquad (3.7)$$

If for example, a voltage reference vector V is located in sector 1of Fig.3, the integral for V over a single space-vector modulation cycle gives

$$\int_0^{T_S} V dt = \int_0^{T_1} V_1 dt + \int_{T_1}^{T_2+T_2} V_2 dt + \int_{T_1+T_2}^{T_3} V_0 dt \qquad (3.8)$$

where the T_1 and T_2 are the switching time duration spent on the output voltage vectors V_1 and V_2 , respectively. Also, the T_S is the sampling time. The remainder T_0 of T_S is the time duration spent on the V_0 or V_7.For sufficiently high switching frequency the reference space vector V_{ref} is assumed constant during one switching cycle.

Taking into account that the states V_1 and V_2 are constant and $V_7 = 0$, one finds

$$V_1.T_1 + V_2.T_2 = V_{ref}.T_S \qquad (3.9)$$

If the space vectors in the equation are described in d-q coordinates, it follows

$$T_1.\frac{2}{3}V_d.\begin{bmatrix}1\\0\end{bmatrix} + T_2.(\frac{2}{3}).V_d.\begin{bmatrix}\cos 60^0\\ \sin 60^0\end{bmatrix} = T_S.(\frac{2}{3})V_d.m.\begin{bmatrix}\cos\theta\\ \sin\theta\end{bmatrix} \qquad (3.10)$$

where $0 \leq \theta \leq 60^0$, $m = \dfrac{|V_{ref}|}{2V_{dc}/3}$

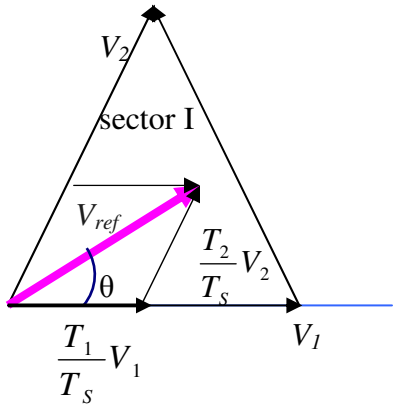

Figure 3.4 Determination of switching times

The time durations T_1, T_2 and T_0 are solved by Eqs.3.8 , and can be arranged as follows:

$$T_1 = T_s.m.\frac{\sin(\pi/3-\theta)}{\sin(\pi/3)} \tag{3.11}$$

$$T_2 = T_s.m.\frac{\sin\theta}{\sin(\pi/3)} \tag{3.12}$$

$$T_0 = T_7 = T_S - (T_1 + T_2) \tag{3.13}$$

For the sectors II-VI the same rules apply. A voltage reference vector V_{ref} can be approximated by two adjacent switching space vectors and two zero vectors using PWM

technique. It is necessary to arrange the switching sequence so that the switching frequency of each inverter leg can be minimized.

Fig.3.3 shows the switching sequence to minimize the ripple content of output current. The three-phase inverter legs are switched at the beginning from the zero state, at the ending of the other zero state during the sampling time T_S . This rule applies normally to the three-phase inverters as the switching sequence, for example,''..V_0 –V_1-V_2 - V_7 - V_7- V_2- V_1 - V_0 - .'' in sector I. Therefore , the switching cycle of the output voltage is double the sampling time, and two output voltage waveforms become symmetrical during 2*Ts. This operation is called the "three-phase symmetrical modulation.''

Space vector algorithm (Implementation)

The first step is to determine in which sector the voltage vector defined by $V_{\alpha\, ref}$, $V_{\beta\, ref}$ is found. The following few code lines give the sector as output:

sector determination

$$\begin{aligned} &If\ V_a > 0 \quad Then \quad A=1 \quad else \quad A=0 \\ &If\ V_b > 0 \quad Then \quad B=1 \quad else \quad B=0 \\ &If\ V_c > 0 \quad Then \quad C=1 \quad else \quad C=0 \end{aligned}$$

$$sector = A+2B+4C \tag{3.14}$$

The second step is to calculate the duration of the two sector boundary vectors .This can be obtained as follows.

The magnitude of all the space vectors is $2V_{dc}/\sqrt{3}$ .When this is normalized by the maximum phase voltage (line to neutral), $V_{dc}/\sqrt{3}$ the magnitude of the space vectors become $2/\sqrt{3}$ i.e., the normalized magnitude are $2/\sqrt{3}$.Therefore, from the last two equations the time durations are calculated in (α ,β) coordinate as follows:

$$T_1 = \frac{T_S}{2}(\sqrt{3}V_{\alpha ref} - V_{\beta ref}) \tag{3.15}$$

$$T_2 = T_S V_{\beta ref} \tag{3.16}$$

where V_a and V_b also represent the normalized (α ,β) components of V_{ref} with respect to the maximum phase voltage . The rest of the period, T_0 is spent in applying the null vector V_0 or V_7 .The durations, as fraction of the total T_S , are given by

$$t_1 = \frac{T_1}{T_S} = \frac{1}{2}\left(\sqrt{3}V_{\alpha ref} - V_{\beta ref}\right) \tag{3.17}$$

$$t_2 = \frac{T_2}{T_S} = V_{\beta ref} \tag{3.18}$$

We can calculate in the same manner the relative time durations, t_1 and t_2 for each sector of the Fig. 3.3 space vectors. By making the calculus of the times (as shown in equation 3.8) in all of the sectors one can find that they have only three different forms in six sections as follows:

$$\begin{aligned} X &= V_{\beta rtef} \\ Y &= \frac{1}{2}\left(\sqrt{3}V_{\alpha ref} + V_{\beta ref}\right) \\ Z &= \frac{1}{2}\left(-\sqrt{3}V_{\alpha ref} + V_{\beta ref}\right) \end{aligned} \tag{3.19}$$

then for the example above, when V_{ref} is in sector contained by V_1 and V_2 , t_1 =-z and t_2 =x. For different sectors, the expressions of t_1 and t_2 are listed below.

Case sector of

1	$t_1 = Z$,	$t_2 = Y$
2	$t_1 = Y$,	$t_2 = -X$
3	$t_1 = -Z$,	$t_2 = X$
4	$t_1 = -X$,	$t_2 = Z$
5	$t_1 = X$,	$t_2 = -Y$
6	$t_1 = -Y$,	$t_2 = -Z$

end times calculation

The third step is to compute the three necessary duty cycles. This is shown below:

$$t_{aon} = T_S - t_1 - t_2 \quad (3.20)$$

$$t_{bon} = t_{aon} + t_1 \quad (3.21)$$

$$t_{con} = t_{bon} + t_2 \quad (3.22)$$

The last step is to assign the right duty cycle (txon) to the right motor phase according to the sector.

Comparison SV-sinusoidal PWM

The SVPWM generates minimum harmonic distortion of the currents in the winding of 3-phase AC motor. SV Modulation also provides a more efficient use of the supply voltage in comparison with sinusoidal modulation methods. In fact, with conventional sinusoidal modulation in which the sinusoidal signals are compared with a triangular carrier,we know hat the locus of the reference vector is the inside of a circle with a radius of $1/2V_{dc}$ .In the

SV modulation it can be shown that the length of each of the six vectors is $2/3V_{dc}$ .In steady state the reference vector magnitude might be constant. This fact makes the SV modulation reference vector locus smaller than the hexagon described above. This locus narrows itself to the circle inscribed within the hexagon, thus having a radius of $1/\sqrt{3}V_{dc}$ .In Fig.3.5 below the different reference vector loci are presented.

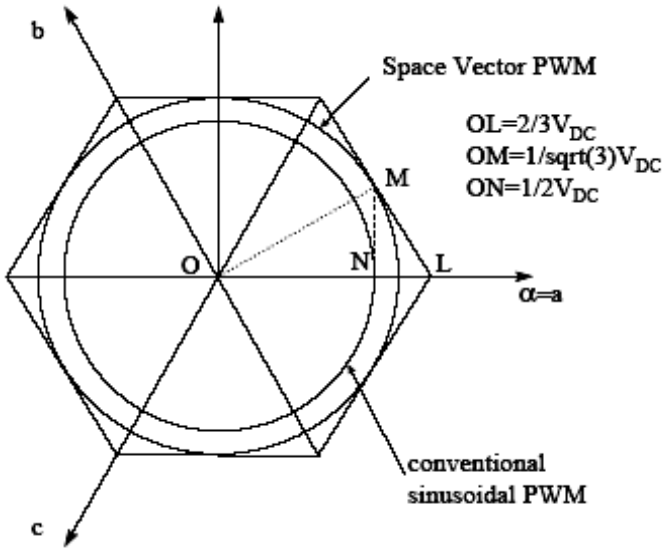

Figure 3.5 Locus comparison SVPWM with sinusoidal-PWM

Therefore, the maximum output voltage based on the Space Vector theory $\frac{2}{\sqrt{3}}$ (=OM/ON) times as large as that of the conventional sinusoidal modulation. This explains why, with SVPWM, we have a more efficient use of the supply voltage than with the sinusoidal PWM method.

3.3 Estimation of rotor speed and position

Controlling PMSM motors is not an easy task. Achieving the peak efficiency requires that the magnetic field that is created by the stator currents be kept in very precise alignment with the permanent magnets on the moving rotor. In the past, various types of sensors were mounted on the rotor to keep track of the position and velocity. These included Hall effect sensors, resolvers, and optical encoders. Today the use of such sensors is not acceptable. It adds too much to the system cost and reduces the reliability of the product. The expected benefits of these indirect techniques are: elimination of the electrical connections of sensors, reduced size, no maintenance, nonsusceptible to environmental factors, increased reliability, and above all these, operating at zero, low and higher speed.

Sensorless controllers rely on software estimators to take the place of these hardware sensors. The task of an estimator is to provide the same high quality rotor position and velocity information that the hardware sensors previously supplied. There are many types of estimators in use today ranging from ad-hoc solutions, to simple mathematical observers, to advanced, optimal algorithms such as the Kalman filter. Precise control of the pulse width modulated (PWM) inverter, and accurate measurement of the motor currents is required for these estimators to work correctly. In all cases, removing the hardware sensors places an additional computational burden on the controller.

Different approaches to estimate the state variables can be found in the literature. In some literature, nonlinear full-order observers are employed for speed estimation. The rotor position is obtained, integrating the speed estimate in open loop. In some others, an algorithm to estimate flux and current by the integration of differential equations was proposed. An alternative approach is to use reduced-order observers to decrease the computational load. Among them, reduced –ordered Luenberger observers can be found in their linear and nonlinear versions. In these approaches, the EMF is estimated first and then the rotor position and speed are reconstructed using the relationship between EMF and rotor variables.

In order to obtain good estimates, the EMF, must be estimated with low error since the EMF estimation error is propagated to the rotor variables. In some others, the

implementation of an extended Kalman filter (EKF) is proposed for speed and rotor position estimation. Among these proposals, the sliding-mode observer represents an attractive choice for its being robust to disturbances, parameter deviations, and system noise. In this paper, rotor position estimation is presented, based on a sliding mode observer.

Configuration of the observers (sliding mode type)

The classical solutions rely on the dependency of the rotor position from the back electromotive force induced in the stator windings. These approaches are quite simple and they use the motor voltage equations to calculate the induced EMF (or its integral) from current and voltage measurements (the stator resistance and inductance must be known parameters).

State observers require a relative accuracy in the modeling of the system, the measurements of motor currents (system input).The instantaneous error between the estimated and the measured motor currents is used as feedback to adjust the estimation of the unknown variables. The observer detects the rotor back emf components in the two phase stationary reference frame, using the motor voltage equations. The motor speed is then obtained by a further relation.

IPM Motor model

The motor model is described in a stationary two-axes reference frame. Thus, the model voltages and currents are related to the actual physical quantities by a simple linear transformation

$$i_\alpha = \frac{2}{3}(i_a - \frac{i_b}{2} - \frac{i_c}{2}) \tag{3.23}$$

$$i_\beta = \frac{i_b - i_c}{\sqrt{3}} \tag{3.24}$$

$$v_\alpha = \frac{2}{3}(v_a - \frac{v_b}{2} - \frac{v_c}{2}) \tag{3.25}$$

$$v_\beta = \frac{v_b - v_c}{\sqrt{3}} \tag{3.26}$$

The dynamic model for *p* pole -pair machine can be written as

$$\frac{d\theta}{dt} = \omega \tag{3.27}$$

$$\frac{d\omega}{dt} = \frac{-3}{2}\frac{p\psi}{J} i_\alpha \sin(\theta) + \frac{3}{2}\frac{p\psi}{J} i_\beta \cos(\theta) - \frac{B}{J}\omega \tag{3.28}$$

$$\frac{di_\alpha}{dt} = -\frac{R}{L} i_\alpha + \frac{p\psi}{L}\omega\sin(p\theta) + \frac{v_\alpha}{L} \tag{3.29}$$

$$\frac{di_\beta}{dt} = -\frac{R}{L} i_\beta - \frac{p\psi}{L}\omega\cos(p\theta) + \frac{v_\beta}{L} \tag{3.30}$$

where i_α ,i_β ,v_α ,v_β ,R ,L, and Ψ are currents, voltages, resistance, inductance, and permanent magnet flux linkage, respectively, and θ ,ω ,B and J are rotor position, angular velocity, viscosity, and inertia, respectively.

The above expression can be rewritten as:

$$\frac{d\theta}{dt} = \omega \tag{3.27}$$

$$\frac{d\omega}{dt} = \frac{K_T}{J}(i_\alpha \sin(\theta) + i_\beta \cos(\theta)) - \frac{B}{J}\omega \tag{3.28}$$

$$\frac{di_\alpha}{dt} = -\frac{R}{L} i_\alpha + \frac{K_E}{L}\omega\sin(\theta) + \frac{v_\alpha}{L} \tag{3.29}$$

$$\frac{di_\beta}{dt} = -\frac{R}{L} i_\beta - \frac{K_E}{L}\omega\cos(\theta) + \frac{v_\beta}{L} \tag{3.30}$$

where K_T and K_E are torque constant and EMF constant respectively.

In back-EMF based sensorless schemes for sinusoidal machines, the information on the rotor position is extracted from the estimated waveforms by means of inverse trigonometric functions.

Taking into account the motor constant the motor electrical equations (3.29) and (3.30), it is clear that the rotor position and speed information is contained in the back-EMF terms, given by

$$e_\alpha = -K_E \omega_e \sin(\theta) \tag{3.31}$$

$$e_\beta = K_E \omega_e \cos(\theta) \tag{3.32}$$

The non linear observer obtains the dynamic equations for the EMF calculating the time derivatives of (3.31) and (3.32), and adding the correction terms

$$\dot{\hat{e}}_\alpha = -K_E[\dot{\hat{\omega}}_e \sin(\hat{\theta}) + \hat{\omega}_e^2 \cos(\hat{\theta})] + Lg_{11}(\dot{\hat{i}}_\alpha - \dot{i}_\alpha) + Lg_{12}(\dot{\hat{i}}_\beta - \dot{i}_\beta) \tag{3.33}$$

$$\dot{\hat{e}}_\beta = K_E[\dot{\hat{\omega}}_e \cos(\hat{\theta}) - \hat{\omega}_e^2 \sin(\hat{\theta})] + Lg_{21}(\dot{\hat{i}}_\alpha - \dot{i}_\alpha) + Lg_{22}(\dot{\hat{i}}_\beta - \dot{i}_\beta) \tag{3.34}$$

where $\dot{\hat{\omega}}_e$, $\dot{\hat{i}}_\alpha$, and $\dot{\hat{i}}_\beta$ are calculated with (3.28)-(3.30) evaluated on the estimated values. The gains g_{ij} are selected to set the convergence speed in a way similar to pole assignment in linear systems.

The rotor position and speed can be reconstructed from EMF estimated values as follows:

$$\hat{\theta} = \tan^{-1}\left(\frac{-\hat{e}_\alpha}{\hat{e}_\beta}\right) \tag{3.35}$$

$$\hat{\omega}_e = \frac{1}{K_E}\sqrt{\hat{e}_\alpha^2 + \hat{e}_\beta^2} \tag{3.36}$$

The nonlinear observer is an asymptotic state estimator of the EMF. Therefore, assuming the parameters are perfectly known, position and speed estimated as in (3.35) and (3.36) converges to the actual values. The nonlinear observer presents small errors due to uncertainties in K_E , B and J.

To avoid taking derivatives of the measurements, the following equations are actually implemented for the above nonlinear observer, where the actual rotor position and speed are calculated instead of those in electrical degrees:

$$\dot{u}_1 = \frac{p^2 K_E \hat{e}_\alpha}{J K_E \hat{\omega}^2}(i_\alpha \hat{e}_\alpha + i_\beta \hat{e}_\beta) - \frac{B}{J}\hat{e}_\alpha - \frac{\hat{e}_\beta \hat{\omega}}{p} + g(-Ri_\alpha - \hat{e}_\alpha + v_\alpha) \tag{3.37}$$

$$\dot{u}_2 = \frac{p^2 K_T \hat{e}_\beta}{J K_E \hat{\omega}^2}(i_\alpha \hat{e}_\beta + i_\beta) - \frac{B}{J}\hat{e}_\beta + \frac{\hat{e}_\alpha \hat{\omega}}{p} + g(-Ri_\beta - \hat{e}_\beta + v_\beta) \tag{3.38}$$

$$\hat{e}_\alpha = u_1 - Lgi_\alpha \tag{3.39}$$

$$\hat{e}_\beta = u_2 - Lgi_\beta \tag{3.40}$$

$$\omega = \frac{\sqrt{\hat{e}_\alpha^2 + \hat{e}_\beta^2}}{pK_E} \tag{3.41}$$

$$\hat{\theta} = \frac{1}{p}\tan^{-1}\left(\frac{-\hat{e}_\alpha}{\hat{e}_\beta}\right) \tag{3.42}$$

where p is the number of pole pairs of the motor.

Nevertheless, it must be remarked that only a part of the nonlinear terms is considered and that the observer correction term is calculated via Popov's hyperstability theory assuming constant speed. The Sliding Mode Observer for back –emf estimation is shown in Fig.3.6, where K is a gain matrix.

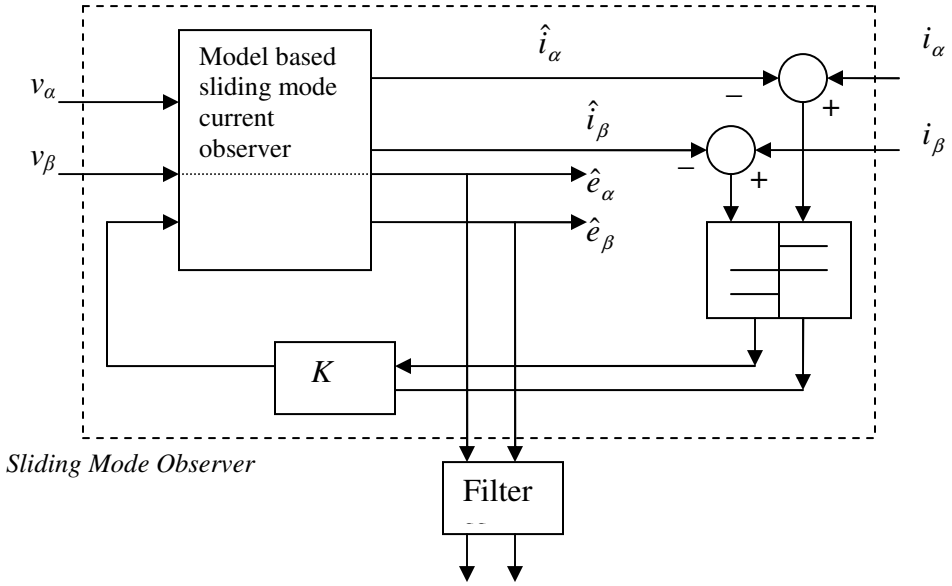

Figure 3.6 Sliding Mode Observer

3.4 PI regulator

The PI controller is an effective means of regulating torque and voltage magnitudes to the desired values. It also improves the steady state error and the error sensibility. This is achieved by providing a gain for the error term with an integral component correction.
K_p is the proportional gain and K_i is the integral gain of the feedback loop.

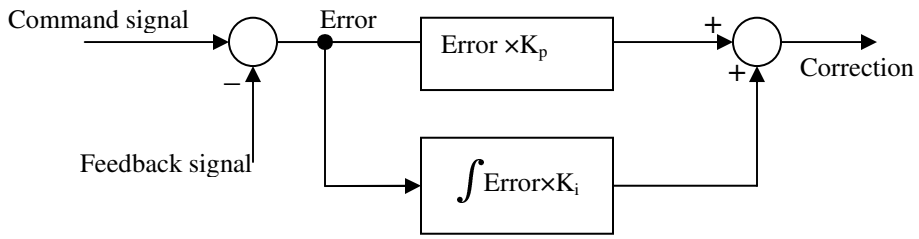

Figure 3.7 PI regulator

There are four PI controllers used in this thesis. The first PI controller is called the voltage controller as it calculates the FW current i_{df} required for field weakening operation. The other three are used in the current controller section of the design from the speed error signal. These PI controllers regulate the voltage into the PM machine by making sure that the PMSM machine is not drawing too much or too little current.
Synchronous frame proportional plus integral (PI) current regulators are the most common option in field–weakening applications, but very few papers have studied their saturation capability, i.e., the capability to use the available voltage. Much attention has been paid in recent years to the design of current regulators for ac drives. A bandwidth high enough to provide the required dynamic response to the drive is commonly the major design goal. Any regulator intended to work in field weakening operation should, therefore, address two important issues: maximum dc-bus voltage utilization and the necessary bandwidth.
Assuming that a proper flux reference is available, dynamic field weakening relies on the dynamic response of both the flux and current regulators. At high speeds, the available voltage will mostly be used to counteract the back EMF. Small transient errors in flux regulation could result in insufficient voltage margin to create the desired torque-

producing current, dramatically affecting the drive performance. The synchronous frame PI current regulator has become the standard for current regulation of multiphase ac machines due to its capability of regulating ac signals over a wide frequency range with zero steady-state error. Nevertheless, it is known that its transient response deteriorates as the synchronous frequency increases due to the excitation frequency cross coupling added to the machine model by the synchronous frame transformation.

The Field Oriented Control of a PMSM needs three PI Controller. One for each current in rotating frame (I_d and I_q) and one for the angular speed. (See Figure 3.1)
The structure of a PI controller is shown in Figure 3-8.

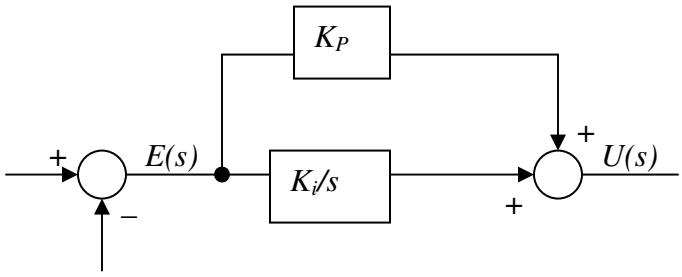

Figure 3.8 Structure of PI regulator

The Laplace transformed equation of a PI Controller is given by:

$$U(s) = \left[K_P + \frac{K_i}{s} \right] E(s) \tag{3.43}$$

For a discrete implementation as a digital PI Controller (Fig. 3.9) we have the following equation:

$$U(k+1) = K_p.e(k) + K_i\ e(k) + \sum_{n=0}^{k-1} e(n) \tag{3.44}$$

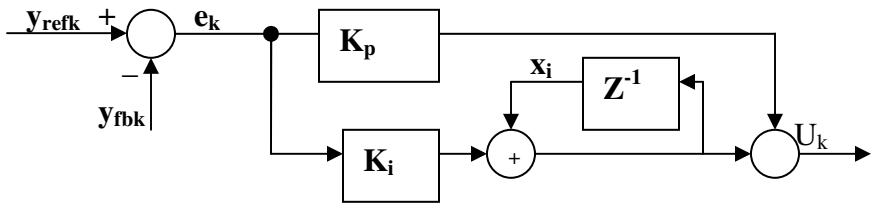

Figure 3.9 Numerical PI regulator (classical)

Closed-loop current regulators are responsibility for controlling the applied PWM voltage excitation so that the instantaneously phase currents follow their commanded value within narrow limits determined by the regulator gains. Tight regulation of the stator phase currents force the stator current components i_d and i_q in the rotor reference frame to likewise closely match their commanded values i_d^* and i_q^* .The stator current regulators might adopt one of many alternate implementations such as the familiar hysteresis or ramp-comparison configurations. Saturation of the current regulators occurs at elevated speed when the motor terminal voltage increases sufficiently to approach the maximum voltage that the drive inverter can apply.

Chapter 4

Review of Field/Flux weakening (FW) operation

In this chapter, the field-weakening operation is introduced. The principal of field weakening operation is exemplified by the separately excited DC commutator motor drive, which shows an ideal field-weakening characteristic. Thereafter the main types of brushless synchronous AC motors are introduced and their coherence to the separately excited DC commutator motor drive is outlined. In section 4.2 the field-weakening operation of permanent magnet motors in general is investigated. The chapter closes with some comments on practical aspects and limitations.

4.1 Principal of field-weakening operation

The separately excited DC commutator motor drive shows an ideal field-weakening characteristic. Therefore it is appropriate to consider the principal of field-weakening operation using this familiar motor characteristic. This is shown schematically in Figure4.1. There are two circuits, called the field circuit and armature circuit. Let $i_f(t)$ and $i_a(t)$ be the field current and armature current, respectively. Then the torque generated by the motor is given by

$$T_m(t) = K_m i_f(t) i_a(t) = J\frac{d\omega}{dt} + T_d + B\omega \qquad (4.1)$$

where K_m is a motor constant. The generated torque T_m is used to drive a load through the shaft. Assume that the total equivalent moment inertia and the friction coefficient of the load, the shaft, the gears, the rotor of the motor, etc, are J and B, respectively. Let ω be the angular speed of the motor and T_d (t) the load (or disturbance) torque. Frequently the control of motor voltage is combined with field-current control in order to achieve the widest possible speed range. With such dual control, base speed can be defined as the normal-armature-voltage, full-field speed of the motor. Speeds above base speed are obtained by reducing the field current; speeds below base speed are obtained by armature – voltage control.

Now we shall consider two different cases.

Field-Controlled DC Motors

For a field-controlled DC motor, we assume $i_a(t)$ = constant. In this case, $V_f(t)$ becomes the control signal. Let

$$K_f = K_m i_a \tag{4.2}$$

then

$$T_m(t) = K_f i_f(t) \tag{4.3}$$

The field current satisfies the following equation

$$V_f = R_f i_f + L_f \frac{di_f}{dt} \tag{4.4}$$

$$T_m(t) = K_m i_f(t) i_a(t) \tag{4.5}$$

$$V_b = K_b \Phi_f \omega \tag{4.6}$$

$$\phi_f = f(i_f) \tag{4 .7}$$

where the voltage V_b is the voltage generated in the armature coil because of the motion of the coil in the motor's magnetic field and is usually called the back emf (electromotive force) voltage. V_b is proportional to the angular speed of the motor where K_b is a constant and ϕ_f is the flux in the air gap which is related to the field current by $\phi_f = f(i_f)$.

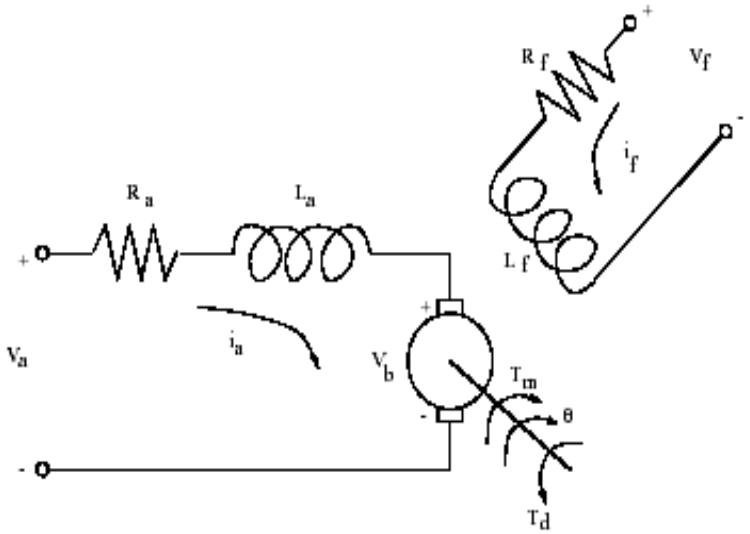

Figure 4.1 separately excited DC commutator motor drive

For increasing speeds above rated value, armature voltage may be held constant at rated level and field current may be reduced (weakened) so as to regulate armature current to rated value. Hence in this region, torque will be directly proportional to field current and speed will be inversely proportional to field current if there is no saturation. The output power will hence be constant. The torque is inversely proportional to the speed increase. As the power is constant beyond the rated speed ($P_{out} = P_b$), this is called ***constant-power region or field weakening region***. These terms are normally used interchangeably in the literature though one should be careful with the latter as it is usually possible to keep increasing the speed at a reduced power. Figure 4.2 shows the ideal field-weakening characteristics for a drive with a limited inverter volt-ampere rating capability.

Armature-Controlled DC Motors

In this case, we assume $i_f(t)$ = constant and $V_a(t)$ becomes the control signal.

Let

$$K_a := K_m i_f \tag{4.8}$$

Then

$$T_m(t) = K_a i_a(t) \tag{4.9}$$

The armature current satisfies the following equation

$$V_a = R_a i_a + L_a \frac{di_a}{dt} + V_b \tag{4.10}$$

Hence for increasing speed of DC motor, up to rated level, field current may be held constant and applied voltage increased from zero to rated value so as to hold armature current at rated value. Thus at low speed, the rated armature current i_a and the rated excitation-flux linkage ψ_b are used to obtain the rated torque T_b. The voltage V_a and output power P_{out} both rise linearly with speed. Hence in this region, torque will be constant and output power will be proportional to speed. This operating range is referred to as ***constant-torque or constant-flux region.***

Figure 4.2 shows a plot of maximum power and maximum torque versus speed for a synchronous motor under variable-frequency operation.

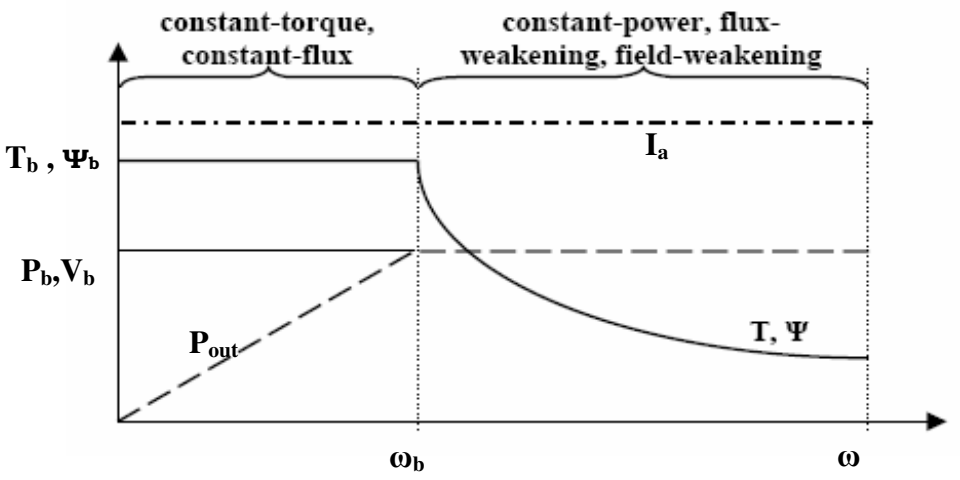

Figure 4.2 Ideal field-weakening drive characteristics

Real motors do not have flat output power against speed characteristics above rated speed ω_b. In Figure 4.3 the dashed line is the ideal field-weakening characteristic and the solid line is the actual characteristic. Rated power is the output power at rated speed ω_b with rated torque T_b. The inverter utilization is the ratio of rated power to the ideal output power. This is less than unity as the motor does not have unity power factor and 100% efficiency under rated operating conditions. The constant-power speed range (CPSR) is the speed range over which rated power can be maintained.

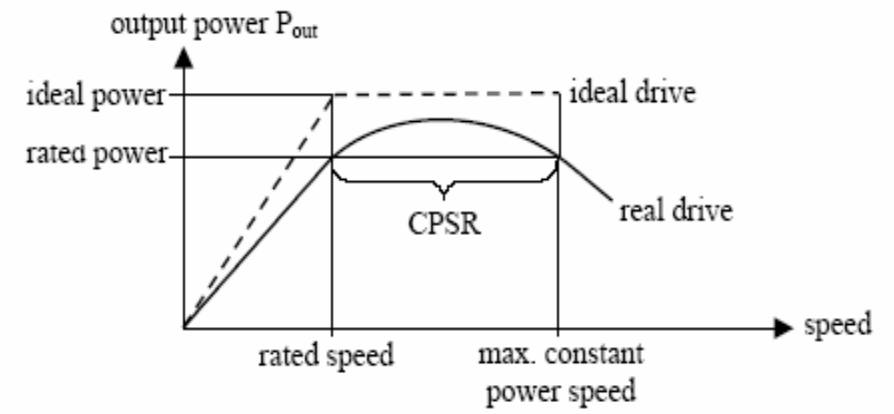

Figure 4.3 Definition of field-weakening parameters

4.2 Field-weakening operation of Permanent Magnet Motors

The separately excited DC machine has separate windings for the excitation and torque producing currents (as seen in section 4.1). Permanent magnet synchronous motors have a single stator winding which generates a current phasor *I*. This current phasor can be split into the two components in d- and q-axis, I_d and I_q.

$$I^2 = I_d^2 + I_q^2 \tag{4.11}$$

In permanent magnet machines the flux is produced by magnets. Hence the magnetic (excitation) field or flux can not be controlled by varying the field current. The permanent magnets can be pictured as "fixed excitation flux" sources Ψ_m. However, flux control (or field-weakening) is achieved by introducing an opposing field Ψ_F against the fixed excitation from the magnets. It is achieved by injecting a negative d-current I_d (or field current I_F), as shown in Figure 4.4.

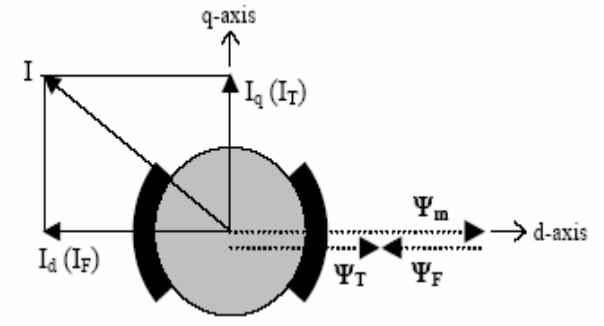

Figure 4.4 Flux-weakening of permanent magnet motor

The concept of using an imposing field can be further explained with a simple vector diagram. Figure 4.5a shows the voltage phasor diagram when the motor is running at a low speed well below the rated speed. When the motor is operated at rated conditions, as shown in Figure 4.5b , it can be noted that the voltage vector is on the voltage limit contour (maximum possible voltage V_b).

It is virtually impossible to increase the speed with keeping a current I in the q-axis once the induced voltage E equals the rated voltage. In order to increase the speed beyond this limit, the current phasor can be rotated towards the negative d-axis (introduction of a negative d-axis current I_d). Figure 4.5c shows that the voltage vector V is kept within the voltage limit.

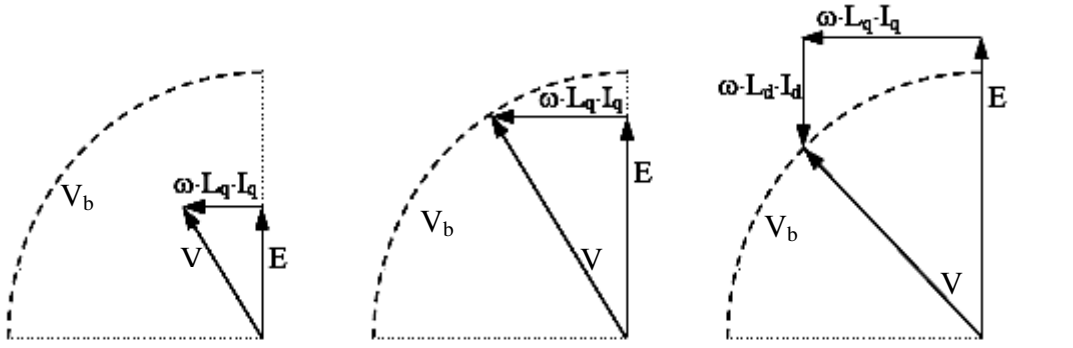

a) at low speed **b) at rated speed** **c) beyond rate speed**

Figure 4.5 Voltage phasor diagram of the PM motor at ideal conditions

The voltage limit V_b of the PM motor can be expressed as

$$V_b^2 \geq \omega^2[(\psi^2 + L_d I_d)^2 + (L_q.I_q)^2 \quad (4.12)$$

where ω is the electrical operating speed, Ψ_m is the magnet flux, L_d and L_q are the d-axis and q-axis synchronous inductances. The torque equation of a PM motor can generally be expressed as

$$T = (3/2).p.[\psi_m I_q + (L_d - L_q).I_q.I_d] \quad (4.13)$$

One can notice that the generated torque comprises two parts, the magnet torque and the reluctance torque. The total torque varies according to machine parameters as the saliency ratio ξ or the magnet thickness (defining the magnet flux Ψ_m).

The output power is from the shaft torque T and the electrical speed

$$P_{out} = T.\omega \quad (4.14)$$

.

4.2 Practical limitations

Under normal load the mechanical power increases as a linear function of speed up to the nominal power (reached when speed is equal to its nominal speed).Knowing that mechanical speed is proportional to the torque T times the speed ω and that its nominal speed has been reached when the speed is equal to nominal value (in most cases it assumed as 3000rpm), the torque production must be reduced if the desired speed is to be greater than nominal speed.

The drive constraints for the extended speed range are first the phase voltages and second the phase currents. Knowing that the phase voltage references increase with speed and as their value can not exceed the nominal value, the flux component must then be reduced down to a value that allows the nominal phase voltage to be maintained and the desired speed to be reached. Knowing that phase currents increase with load, the maximum resistive torque put on the drive during the extended speed range operation must be set to a

value that keeps the phase currents not greater than their nominal value. The maximum resistive torque decreases then as a function of speed (see figure.4.6)

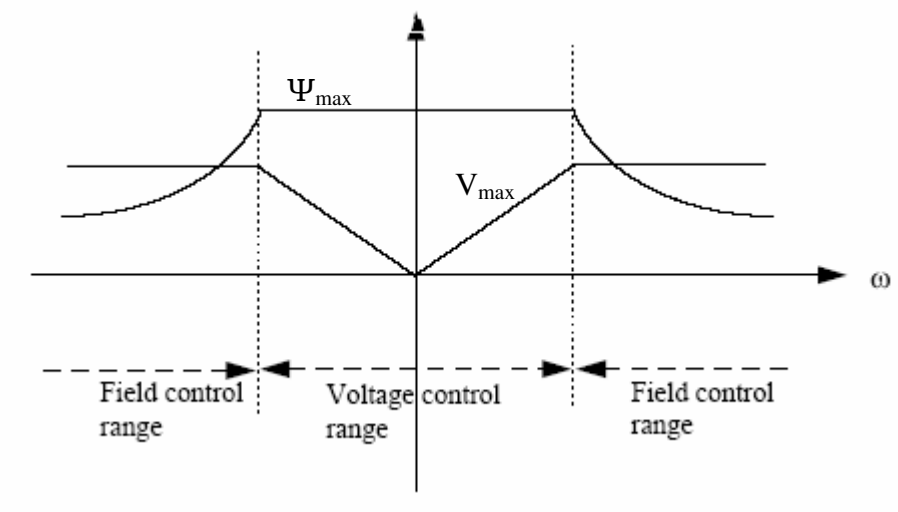

Figure 4.6 Control Range of a PMSM in Steady State

In order to achieve high speeds, the stator current frequency is increased. The back-EMF condition of the motor flux is kept constant. Then a maximum stator speed is attained when V is directly proportional to the motor flux Ψ and the angular speed ω . In normal conditions this reaches the limit output voltage of the power converter. To reach a higher speed, the flux is reduced as an invert of the angular speed in order to keep the back-EMF constant and equal to its maximum ($V \approx \omega\psi$).

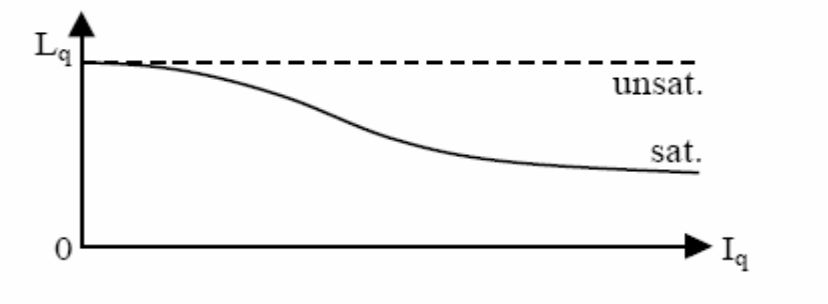

Figure 4 .7 Effects of magnetic saturation on q-axis inductance

Up to this point it has been assumed that the inductances are constant. In general, this is far from the case and the inductances are functions of the currents in both axes. Saturation describes the effect of a current in an axis on the inductance in that axis. Figure 4.7 shows a possible dependency of the q-axis induction L_q on the q-axis current I_q for unsaturated (dashed line) and saturated (straight line) conditions. Furthermore, cross-coupling is the effect of a current in an axis on the inductance in the other axis. When designing a motor it can be important to take these practical factors into account.

Chapter 5

Field Weakening control of PMSM

This chapter deals with different aspects of the PM- synchronous motor in regard to flux weakening. At first, a common normalization is introduced. The maximum field-weakening control and FW control scheme for SMPM drives is then explained. Some final design considerations about the SMPM characteristics conclude this chapter. In this chapter, a sort of recent flux weakening control scheme is described. The approach followed in this section is based on the machine equation written in steady-state operating conditions because, in general, during field-weakening operation, the electrical transient can be neglected compared to the mechanical transient, as in traction drives or in spindle drives.

5.1 Normalization

It is often convenient to express the quantities of an AC system, such as a motor, in a dimensionless form, in so-called per unit values. This way motors of different dimensions can easily be compared with each other.

The parameter normalization is based on the definition of three "base'' quantities T_b, ω_b, and V_b ,which are respectively ,the amplitudes of the torque T, the electrical speed ω ,and the speed-voltage vector V at full load operation and at the maximum speed of the constant-torque region. The base quantities are assumed as follows:

- The base torque T_b is the limit torque of the constant torque region, which is the rated torque.

- The base angular frequency ω_b is the maximum electrical speed of the constant torque region (base or rated speed)

- The base voltage V_b is the voltage amplitude (of the space vector) under base torque (T=T_b) and base angular frequency ($\omega = \omega_b$). The base voltage is also referred to as rated voltage.

The normalized quantities (subscript n indicates normalized parameters) are therefore

expressed by the following equations according to Bianchi and Bolognani [24].

$$T_n = T/T_b \quad , \tag{5.1}$$

$$\omega_n = \omega/\omega_b \ , \tag{5.2}$$

$$V_n = V/V_b \ , \tag{5.3}$$

$$I_n = I/I_b \quad , \quad I_b = \frac{2.T_b.\omega_b}{3.p.V_b} \tag{5.4}$$

$$L_n = L/L_b \ , \qquad L_b = \frac{3.p\,V_b^2}{2.T_b.\omega_b^2} \tag{5.5}$$

$$\psi_{mn} = \psi_m/\psi_b \quad , \ \psi_b = L_b.I_b = V_b/\omega_b \tag{5.6}$$

where p is the number of pole pairs of the motor. As far as the current and the motor parameters (Equation 5.4 to Equation 5.6) are concerned, their base values are derived from the power balance (presuming ideal conditions without losses or leakage)

$$T_b.\frac{\omega_b}{p} = \frac{3}{2}.V_b.I_b \tag{5.7}$$

With this normalization and the choice of the magnet flux on the d-axis, the motor equations become

$$V_n^2 = \omega_n^2.((\psi_{mn} + L_n.I_{dn})^2 + (L_N.I_{qn})^2) \tag{5.8}$$

$$T_n = \psi_{mn}.I_{qn} \tag{5.9}$$

5.1.1 Operation at rated speed

This subsection illustrates the operation at rated (or base) speed. This operation point is characterized by:

• Normalized rated torque $T_n = 1$

• Normalized electrical base speed $\omega_n = 1$

• Normalized rated voltage $V_n = 1$

• The q-axis current is set to $I_{qn} = I_n$ and the d-axis current is set to $I_{dn} = 0$ to receive the maximum torque-to-current ratio (see section 5.2 about the maximum field-weakening). Solving the voltage (Equation 5.8) and torque equation (Equation 5.9) of the SMPM drive, the motor inductance and the drive current can be analytically obtained as a function of the normalized magnet flux Ψ_{mn}.

$$L_n = \psi_{fn} \cdot \sqrt{1 - \psi_{fn}^2} \left(= L_{dn} = L_{qn}\right) \tag{5.10}$$

$$I_n = 1/\psi_{fn} \tag{5.11}$$

5.1.2 Confusion in the Definition of Base Speed

The base speed of a machine is defined here as the speed after which generation of maximum torque requires application of maximum voltage (i.e., the speed beyond which the applied phase voltage must remain constant) .In some literature, base speed is defined as the speed at which the back emf reaches the maximum possible value along the maximum torque vs. speed curve .It is common among traditional high performance control techniques to use the ***rated speed*** as the ***base speed***. Using the rated speed as the transition point to the flux weakening range is proper for all PMSM machine running in a nominal environment at rated voltage. It is assumed that the base speed is a function of motor parameters, maximum voltage available to the phase, and the control strategies used in the lower and higher than base speed operating ranges.

5.2 Maximum torque field-weakening control

In this section, the particular field-weakening control strategy to obtain maximum torque (and hence power) at any speed within the inverter volt-ampere rating of the SMPM drive is presented. This section is based on the studies of Soong [27] and Morimoto [26]. The circle diagram is a well known graphical technique for determining the maximum torque field-weakening control strategy for synchronous motor drives. These drives are usually current controlled and so it is convenient to define an operating point in terms of its location in the (I_d ,I_q)-plane. The current limit constraint is I_{qn} in this plane. From Equation 5.8 it can be shown that the voltage limit constraint $V_n \leq 1$ defines a circle whose centre is offset from the origin (Fig. 5.1).The size of this circle is inversely proportional to speed. Its centre is termed the infinite-speed operation point as the operating point must converge towards it at high speed. A given operating point will not exceed the voltage- or current-limit constraint if it lies within the intersection of the voltage- and the current-limit circle. From Equation 5.9 it can be shown that lines of constant torque form straight lines parallel to the d-axis (Fig. 5.1).

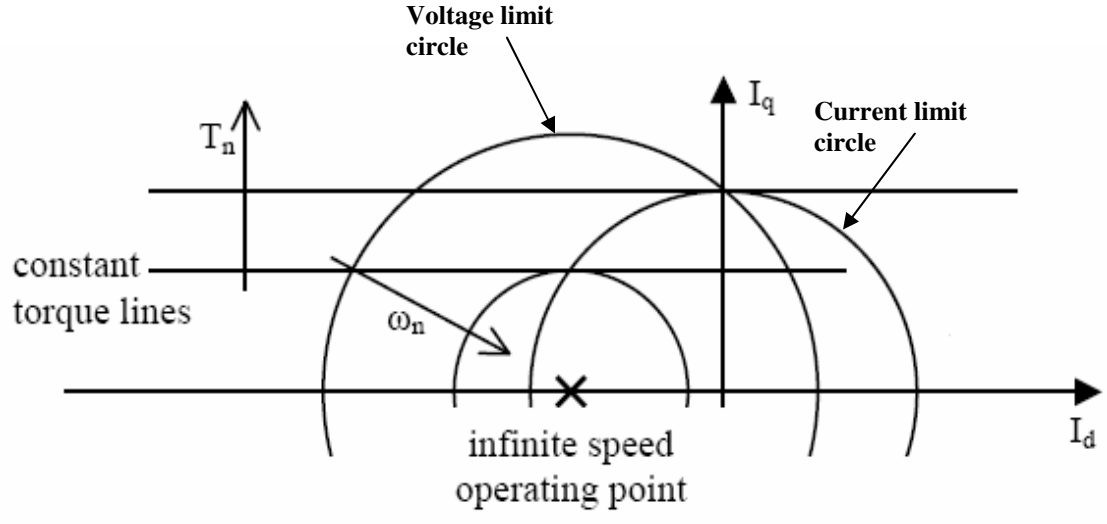

Figure.5-1 Circle diagram for surface mounted PM motor (SMPM)

5.3 Flux Weakening control analysis and design

This section concentrates on the control analysis of an IPM machine. Specific parameter coherences are shown and general design reflections are outlined. An adequate analytical model is derived and used in the design process. Buried magnets(like IPM) create a rotor anisotropy($L_d \neq L_q$) ,which in turn yields several advantages, as extended flux weakening range, high torque -to- ampere ratio. Since IPM motor behaves like a salient-pole machine, stator inductances are functions of rotor position. Buried magnets yield different paths for d and q axes .In particular, the quadrature path runs mostly in the stator and rotor iron and, thus the quadrature inductance L_q is higher than L_d , and it is also more subjected to saturation than L_d. Additional considerations on the flux weakening and control strategy of the machine are also discussed.

5.3.1General description of the flux/field weakening control

The examination of the output (Torque versus Speed) characteristics of the PMSM is necessary to get a view for the motor operating limitations, and consequently, to determine base speed values (rated speed) for the beginnings of the flux weakening in both operating modes. The motor is represented here by the steady-state part of its state-space voltage Eq.s (5.12)-(5.16). For the sake of simplicity, we set $i_d = 0$.

$$v_d = -pL_q \omega i_q \tag{5.12}$$

$$v_q = R\, i + k_t \omega \tag{5.13}$$

$$T_e = T_L + J_m \frac{d\omega_e}{dt} + B.\omega_e = \frac{3p}{2}(\psi_m i_q) = \frac{3}{2} k_t i_q \ , \quad k_t = p\psi_f \tag{5.14}$$

$$v_S = \sqrt{v_d^2 + v_q^2} = V_{ph} \quad ; v_{S\max} = mV_{dc} \quad , \text{m=2/3} \tag{5.15}$$

$$i_S = \sqrt{i_d^2 + v_q^2} = I_{ph} \tag{5.16}$$

A motor speed at the moment when the voltage v_S reaches its limit (nominal value), v_{Smax}, under maximum operating current (nominal value), i_{smax}, is called the rated (base) speed, ω_b. During the motor start-up (at zero speed), the transient current is allowed to be approximately twice its nominal value, but it will not be considered here for the sake of simplicity. The base speed is used to be the starting point of a flux-weakening region.

5.3.1.1 PMSM Characteristics with FW in the d-q Coordinates

Current and voltage polar plots in d-q coordinate space are useful characteristics for the PMSM drive design in order to understand the interactions between the motor nature and current and voltage limitations. They are applied especially for flux-weakening control design, discussed in Section 5.3.2.

An interior permanent magnet (IPM) motor current and voltage limits can be explained through their polar diagrams, given in Figure 5.2 and Figure 5.3, respectively. The circles on the diagrams represent current and voltage limits due to their maximum vector magnitudes. The families of ellipses are derived from the motor voltage d-q state-space Eq.s (2.42), with neglected stator resistance and current dynamics in the vicinity of operating points ($\frac{di_q}{dt}, \frac{di_d}{dt} \approx 0$), which is a generally applied approximation in flux-weakening designs . Each ellipse represents current and voltage limits due to the motor voltage state-space d-q model, Eq.s (2.42), at some interesting operating point (base (rated) speed, ω_b, critical speed, ω_{cr}, and maximum speed ω_{max}), which will be more closely defined in Section 5.3.2.

Hence, the ellipses represent PMSM d-q current and voltage state-space limits in steady-state. The derivation of their analytical forms from Eq.s (2.42) is given in Eq.s (5.17) and Eq.s (5.18) for current and voltage characteristics, respectively. It should be noticed from Eq.s (5.17) that the current ellipse axes, a and b, decrease with speed and that the center location is on the negative d-semi axis and it is constant, i.e. the current state-space limits are concentric ellipses, with speed as a parameter. On the other hand, it can be seen from Eq.s (5.18) that the voltage ellipse axes, a and b, increase with speed, as well as that their centers, which are equal to the motor back emf at a given speed, located on the positive q-semi axis, move further from the origin.

These phenomena are easy to explain from voltage d-q state-space Eq.s 2.42. In order to increase speed while keeping voltage constant, the current must decrease and, inversely, if the current should be constant, the voltage must increase with speed. This explains the current and voltage ellipse axes relationships with speed in Eq.s (5.17) and Eq.s (5.18). However, the behavior of the ellipse centers releases an interesting phenomenon. The only reason for the ellipse eccentricity in the d-q plane, in both cases, is the existence of motor back emf, $k_t\ \omega$. At zero speed the back emf is also zero and the center of the hypothetical voltage ellipse, which has collapsed to a single point, is at the origin, which is expected.

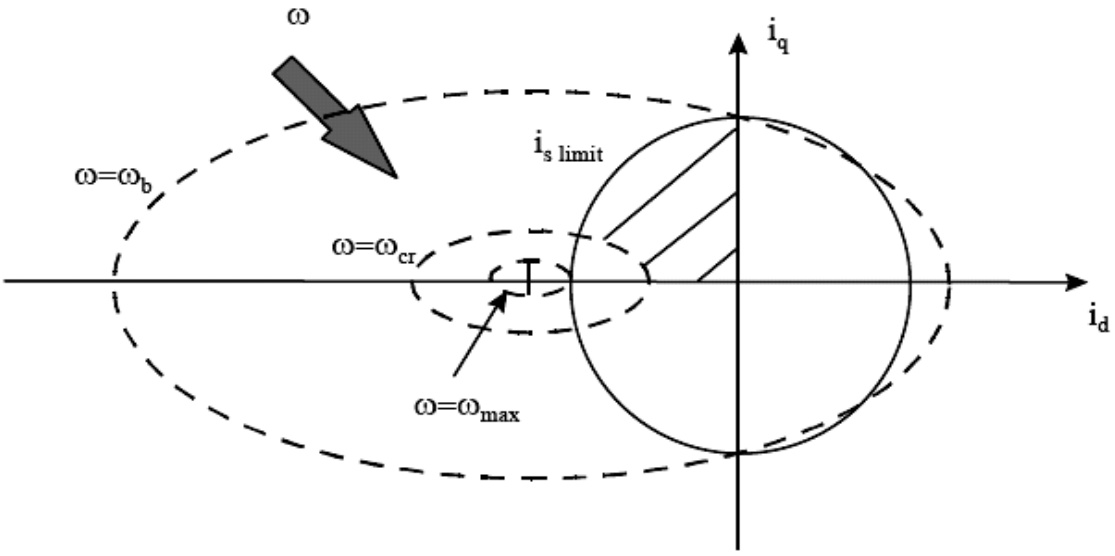

Figure 5.2 PMSM current limit d-q polar diagram

However, the center of the current ellipse depends only on motor parameters - back emf constant, k_t , number of pole pairs, p, and d-axis inductance, L_d - but not speed, so that whatever back emf is developed, the center stays the same for the same motor. Moreover, since the current ellipses collapse with increasing speed, it converges to that point.

The following discussion will show that it helps a lot in flux-weakening control design. On the other hand, the voltage limit diagram, Figure 5.3, helps in the design of a constant

$$\frac{v_d^2}{\omega^2} = \left(pL_q\right)^2; \qquad \frac{v_q^2}{\omega^2} = \left(pL_q i_d + k_t\right)$$

$$\frac{v_s^2}{\omega^2} = \left(pL_q\right)^2 i_q^2 + \left(pL_d\right)^2 \left(i_d + \frac{k_t}{pL_d}\right)^2$$

$$a = \frac{v_s}{pL_q\omega}; \quad b = \frac{v_s}{pL_d\omega}; \quad c = \frac{k_t}{pL_d}$$

$$\frac{i_q^2}{a^2} + \frac{(i_d + c)^2}{b^2} = 1 \tag{5.17}$$

$$i_d = \frac{v_q - k_t\omega}{pL_d\omega}; \qquad i_q = -\frac{v_d}{pL_q\omega}$$

$$I_s^2 = \frac{(v_q - k_t\omega)^2}{(pL_d\omega)^2} + \frac{v_d^2}{(pL_q\omega)^2}$$

$$a = \frac{pL_d\omega}{I_s}; \quad b = \frac{pL_q\omega}{I_s}; \quad c = k_t\omega$$
$$\frac{(v_q - c)^2}{a^2} + \frac{v_d^2}{b^2} = 1 \tag{5.18}$$

current flux-weakening control strategy. It should be noted that there are two distinguished speed regions: one where the relative speed increase is higher than the relative i_q current (motor torque) decrease, which includes an increasing or constant current (motor torque) region, causing a v_d voltage increase, and the other, where the torque decreases faster than the speed increases, so that the v_d voltage decreases, so that the phase voltage vector moves toward a positive q-semi axis. The passing point between the two regions, speed ω_p, can be calculated from Eq.s (2.42), which will be explained in Section 5.3.2. A PMSM voltage d-q

vector diagram, developed from Eq.s (2.42), is shown in Figure (5.4) for the maximum torque operating region (for the sake of simplicity, it was approximated with i_d =0 condition), Figure 5.4a, and the flux-weakening region, Figure 5.4b. The current and voltage vectors cannot exceed the limits from Figures 5.2 and 5.3.

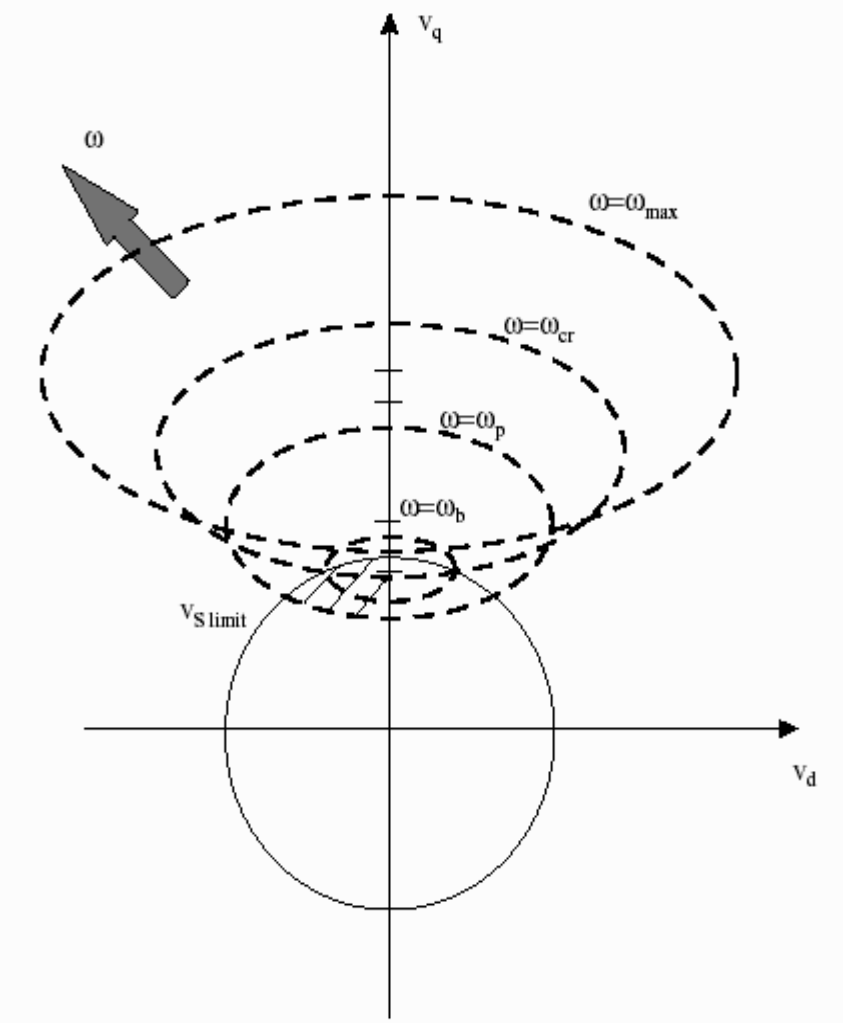

Figure 5.3 PMSM voltage limit d-q polar diagram

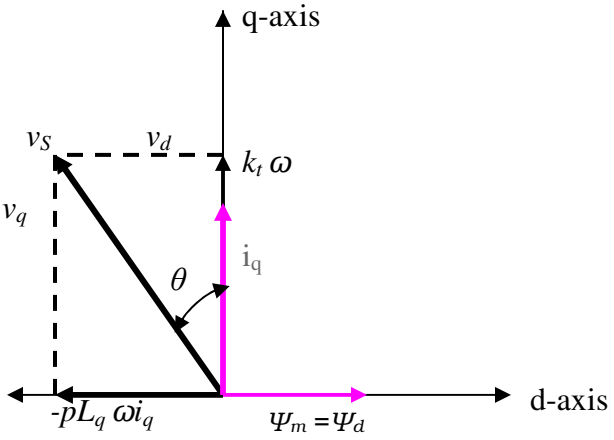

a) i_d=0

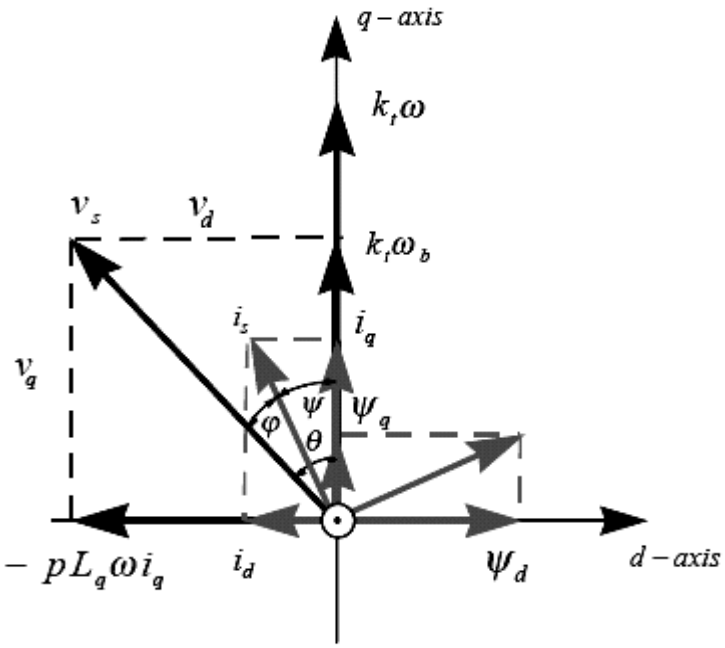

b) $i_d \neq 0$

Figure 5.4 PMSM voltage d-q vector diagram for a) i_d=0, and b) $i_d \neq 0$

5.3.1.2 Reference Motor torque profile

In order to minimize energy consumption, the motor torque should keep its maximum value until the rated speed is reached, except during the relatively short time periods when it rises from zero to the maximum value with a certain maximum slope, determined by mechanical limitations of the motor drive system . The validation for that suggestion lies in the minimum energy (noted as E) Eq. (5.19), derived as:

$$min\ E = min \int_{t_1}^{t_2} P_m dt = J\ min \int_{\omega_1}^{\omega_2} \frac{\omega}{1 - \left(\frac{T_L + T_{fr}}{T_m} \right)} d\omega$$

$$\omega_1 = \frac{1}{J}\left(T_{mb} - T_{frb} - T_{Lb}\right).t_1 = \omega_b \quad , x_b \text{-}base\ value\ of\ x \tag{5.19}$$

$$\omega_2 = \frac{1}{J}\left(T_{m\ final} - T_{fr\ final} - T_{L\ final}\right).t_2 = \omega_{final} (= \omega_{max}) \ , x_{final} \text{–}final\ value\ of\ x$$

where P_m is the motor power, J motor inertia, ω motor speed, ω_1 and ω_2 motor speed values at time moments t_1 and t_2 , T_m , T_L and T_{fr} motor, load and friction torque, respectively, and x a common variable for ω, T_m ,T_L and T_{fr} .The base and final values are related to base and final motor speed. It can be noticed from Eq.s (5.19) that when $T_L \geq 0$, the energy consumption is lowest with the maximum motor torque. If $T_L < 0$, a trade-off must be made between minimum energy consumption and starting time period. If the reluctance torque component in Eq.s (2.42) is negligible, the maximum torque at a base speed usually means a maximum i_q current. It allows the largest flux-weakening region, Figure 5.4b, which will be explained in Section 5.3.2.

Hence, under a lower i_q current, the voltage-to-current phase shift is smaller in the out of flux weakening region and it decreases more rapidly within the flux-weakening region than in the maximum i_q current case. So, it reaches its limit, determined by the VSI limitations, under a lower speed than in the maximum i_q current case, if the flux-weakening begins at the same speed. All the above mentioned facts provide a good reason to continue with maximum torque (or maximum i_q current) reference out of the flux-weakening region, as long as the speed profile is not important. Short time periods for the torque ramping from

zero to its maximum value with a certain maximum slope, are necessary restrictions due to mechanical limitations on the motor shaft.

5.3.2 Common Flux-Weakening strategies

In order to produce the maximum torque, which main component is proportional to q-axis component of the armature current , it is convenient to control the inverter-fed PMSM by keeping the direct, *d-axis*, current component to be i_d =0 as long as the inverter output voltage doesn't reach its limit. At that point, the motor reaches its maximum speed, so-called ***rated speed*** (called also ***base speed*** when talking about flux-weakening). Beyond that limit, the motor torque decreases rapidly toward its minimum value, which depends on a load torque profile.

To expand the speed above the rated value, the motor torque must be reduced. A common method in the control of synchronous motors is to reduce the magnetizing current, which produces the magnetizing flux. This method is known as ***field-weakening***. With PM synchronous motors it is not possible, but, instead, the air gap flux is weakened by producing a negative d-axis current component, i_d. Because nothing has happened to the excitation magnetic field and the air gap flux is still reduced, so is the motor torque, this control method is called *flux-weakening*. As a basis for this analysis, the PMSM current and voltage d-q vector diagrams from the previous section, Figure 5.4, are used.

During flux-weakening, because the demagnetizing (negative) i_d current increases, a phase current vector i_s rotates toward the *negative d-semi axis*. The rotation of the phase voltage vector is determined by a chosen flux weakening strategy, but at the end of flux-weakening it always rotates toward the *positive q-semi axis* because of i_q current, i.e. v_d voltage magnitude decrease. A big concern of flux-weakening control is a danger of permanent demagnetization of magnets. However, large coercitivity of materials such as Samarium-Cobalt allows significant i_d current which can extend the motor rated speed up to two times.

Three commonly used flux-weakening control strategies are:

I) constant-voltage-constant-power (CVCP) control;

II) constant-current-constant-power (CCCP) control; and

III) optimum-current-vector (OCV or CCCV - constant-current-constant-voltage) control.

I. Constant Voltage Constant Power (CVCP) Control

This strategy is very popular in industry because of its simplicity. It is based on keeping the voltage steady-state d and q components constant:

$$\begin{aligned} P_m &= T_m\omega = \frac{3}{2}(v_d i_d + v_q i_q) = const. \\ v_d &\approx -pL_q\omega i_q = -pL_q\Omega_b I_{qb} = const. \\ v_q &\approx k_t\omega + pL_d\omega i_d = k_t\Omega_b = const. \\ v_s &= V_{s\max} = V_{qb} = const. \end{aligned} \tag{5.20}$$

Values v_{qb} , i_{qb} and ω_b are base voltage, base current and base (rated) speed in the beginning of flux-weakening, respectively. Usually, $I_{qb} = I_{s\,max}$.

Reference i_d and i_q currents are derived from Eq.s (5.20):

$$\begin{aligned} i_d &= -\frac{k_t}{pL_d}\left(1 - \frac{\Omega_b}{\omega}\right) \\ i_q &= I_{qb}\frac{\Omega_b}{\omega} \end{aligned} \tag{5.21}$$

Regarding the complexity, this is the easiest flux-weakening control, due to i_d / i_q linearity which is obvious from Eq.s (5.21).By this strategy, the voltage vector V_s on the PMSM voltage vector diagram, Figure 5.4b, is supposed to keep a constant position, while the vertex of the current vector, i_s , moves from point (0, I_{qb}) down the slope i_q/i_d, derived from Eq.s (5.21) toward the *negative d-semiaxis*. The current and voltage d-q vector tendencies in CVCP flux-weakening control strategy are shown in Figure 5.5. However, when the phase current limit, Figure 5.2, is reached, i.e. after passing the critical speed, ω_{cr}, the strategy fails and vector I_s follows the limitation circle, while vector V_s naturally rotates toward the v_q -axis. The critical speed, where the current reaches its limit is:

$$\omega_{cr} = \frac{I_p^{\,2} + I_{qb}^2}{I_p^2 \quad I_{qb}^2}\Omega_b = \frac{V_{qb}^2 + V_d^{'2}}{V_{qb}^2 + V_d^{'2}}\Omega_b \qquad (5.22)$$

where

$$I_p = \frac{k_t}{pL_d}; \qquad V_d^{'} = \frac{L_d}{L_q}V_d$$

If we want to be precise, the phase voltage vector v_s doesn't stay constant at $\omega \leq \omega_{cr}$. Vector v_s rotates toward the *negative d-semi axis*, in the same direction as the current vector, but much slower.This rotation of v_s occurs because of transients $di_d/dt < 0$ and $di_q/dt < 0$ in Eq.s (2.42).

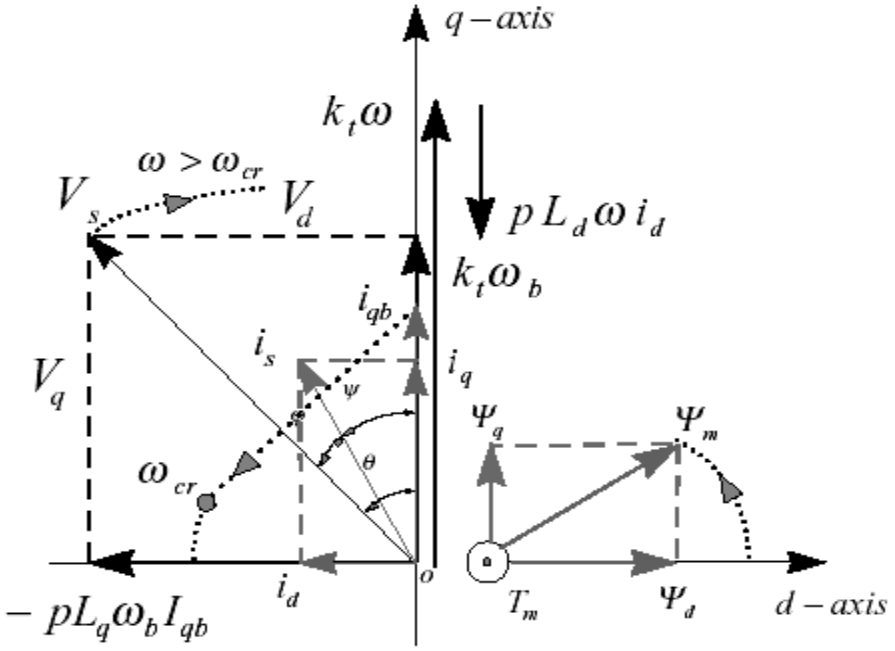

Figure 5.5 PMSM voltage d-q vector diagram for CVCP flux-weakening control

Another, usually neglected, fact is that the active power is not constant. In order to get constant power, the following condition must be satisfied

$$R\,i_d^2 + R\,i_q^2 - R\,I_{qb}^2 \approx p\,(L_q - L_d)\omega i_q\,i_d \qquad (5.23)$$

Finally, the power factor, cos φ, can be calculated from:

$$\cos\varphi=\cos(\theta-\Psi)$$
$$\Psi=\tan^{-1}(-i_d/i_q),\quad \theta=\tan^{-1}(v_d/v_q) \tag{5.24}$$

where φ ,θ, and Ψ are vector phase shifts from Figure 5.4. Eq.s (5.24) can be used for determination of the speed when cos φ reaches its minimum tolerable value, determined by the inverter limitation.

II. Constant Current Constant Power (CCCP) Control

A characteristic of this method is that neither i_q, nor i_d current depends on the motor parameters. The i_q current has the same expression as in the previous strategy, due to keeping the power constant. That implies that v_d voltage is also constant, Figure 5.6. However, the phase voltage *q-axis* component, v_q , depends on both, motor parameters and the current *q-axis* component base value.

The references for this control method are:

$$i_s = I_{qb} = const.$$
$$P_m = T_m\omega = \frac{3}{2}(v_d i_d + v_q i_q) = const. \tag{5.25}$$

From Eq.s (5.25), reference i_d and i_q currents for the current control loops are:

$$i_q = I_{qb}\frac{\Omega_b}{\omega}$$
$$i_d = -\sqrt{I_{qb}^2 - i_q^2} \tag{5.26}$$

The d-q voltage equations in steady-state, extracted from Eq.s (5.25) are:

$$v_d = -pL_q\omega i_q = const.$$
$$v_q = -pL_d\omega i_d + k_t\omega \tag{5.27}$$

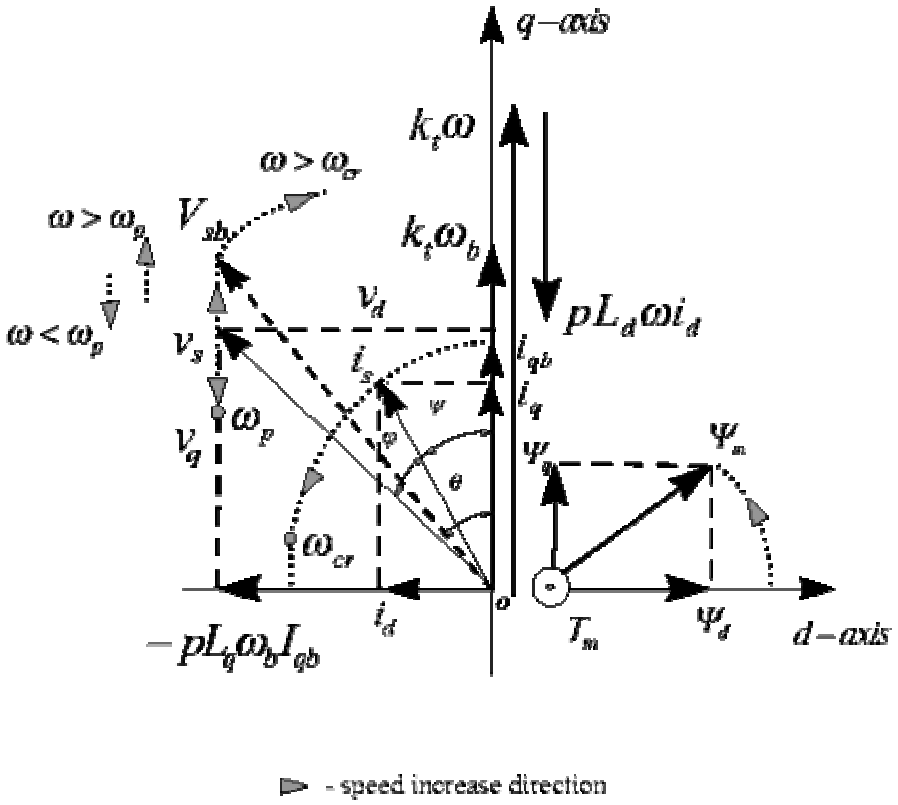

Figure 5.6 PMSM voltage d-q vector diagram for CCCP flux weakening control

By applying this strategy, the phase current vector i_s rotates around its origin, and phase voltage vector v_s, vertex moves along the v_d line, Figure 5.6.The ***prevailing speed***, ω_p, where voltage v_q passes its minimum is

$$\omega_p = \frac{\Omega_b}{\sqrt{1-\left(-\frac{V_d'}{V_{qb}}\right)^2}} \Rightarrow v_q = v_{q\,min} \tag{5.28}$$

where $V_d' = \frac{L_d}{L_q} V_d$ and $V_{qb} = k_t \Omega_b$.

A critical speed when voltage v_S reaches its maximum value is the same as in the previous example, but now the phase current i_s reaches its limit:

$$\omega_{cr} = \frac{I_p^2 + I_{qb}^2}{I_p^2 - I_{qb}^2}\Omega_b = \frac{V_{qb} + V_d^{'}}{V_{qb} + V_d^{'}}\Omega_b \qquad (5.29)$$

When $\omega=\omega_{cr}$,the phase voltage reaches its limit and stays constant under higher speed.
It causes a rapid decrease of current i_q , what implies the decrease of the motor torque, T_m.
Because transient elements di_q/dt and di_d/dt from the d-q voltage equations from Eq.s (2.42) cancel each other in Eq.s (5.25), active power P_m remains constant during the flux-weakening period until the critical speed is reached.

It is characteristic for both constant power control methods that the *d-axis* steady-state voltage component remains constant as long as both voltage and current don't reach their limits. In comparison with the constant voltage strategy, this strategy is more complex because of the reference i_d/i_q non-linearity. Its advantages are constant phase current and constant power in flux-weakening region between Ω_b and ω_{cr} . Different torque slopes, obtained after $\omega=\omega_{cr}$, are consequences of applied strategies, as well as of applied voltage limitation methods.

The same method doesn't produce the same effect on both strategies. How strong the effect is, how big the difference is, and what profiles the motor torque obtains after $\omega= \omega_{cr}$, also depends on motor characteristics and current and speed base values, as well as the load torque profile.

III. Optimum Current Vector (OCV) Control

Unlike the constant power flux-weakening control strategies, where phase voltage or current were reduced in order to keep constant active power, in this method the active power is allowed to change with a change of the power factor, ***cos φ***, while the magnitudes of phase current and phase voltage vectors are set to their maximum values:

$$i_S = I_{qb} = I_{s\,max} = const. \tag{5.30}$$
$$v_S = V_{qb} = V_{S\,max} = const\,.$$

In other words, by this control strategy the maximum allowable apparent power is used, although the active power is not constant. Hence, both vector trajectories are along their limiting circles, Figure 5.2 and Figure 5.3. The superimposed current, voltage and flux vector diagrams are shown in Figure 5.7. The expressions for the abovementioned conditions are:

$$v_S^2 = v_d^2 + v_q^2 = V_{S\max}^2 \tag{5.31}$$
$$i_S^2 = i_d^2 + i_q^2 = I_{S\max}^2 = I_{qb}^2 \tag{5.32}$$

The consequent expressions for reference currents i_d and i_q, are:

$$i_d = -I_{qb} K_1 \left(1 - \frac{\Omega_b^2}{\omega^2}\right) \tag{5.33}$$

$$i_q = I_{qb} \sqrt{1 - \left[K_1 \left(1 - \frac{\Omega_b^2}{\omega^2}\right)\right]^2} \tag{5.34}$$

where $$K_1 = \frac{I_{qb}}{2I_p} + \frac{I_p}{2I_{qb}} \tag{5.35}$$

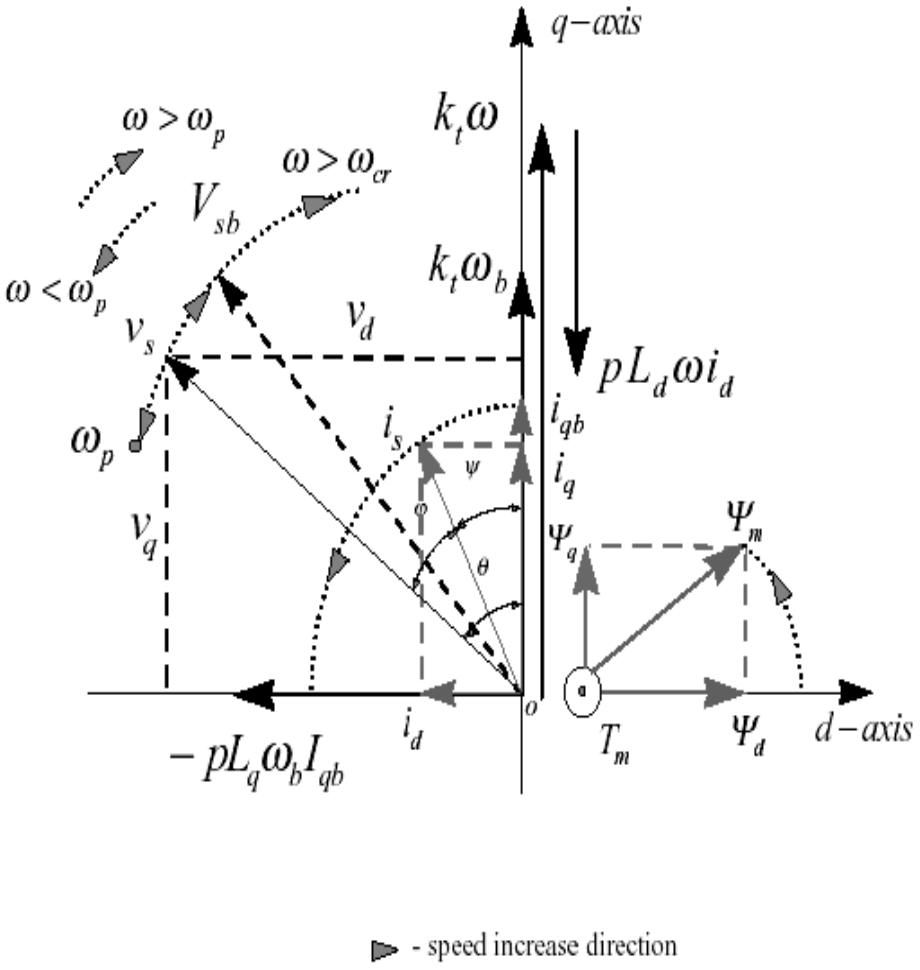

Figure 5.7 PMSM voltage d-q vector diagram for OCV flux-weakening control

for non-salient PMSM, where $L_d = L_q = L$, and

$$i_d = I_p^{'}\left[1 - \sqrt{1 + K_2\left(1 - \frac{\Omega_b^2}{\omega^2}\right)}\right] \tag{5.36}$$

$$i_q = I_{qb}\sqrt{1-\left(\frac{I_p^{'}}{I_{qb}}\right)^2\left[1-\sqrt{1+K_2\left(1-\frac{\Omega_b^2}{\omega^2}\right)}\right]^2} \tag{5.37}$$

for a salient pole machine, where

$$K_2 = \frac{L_{eq}}{L_d}\left(\frac{I_{qb}^2}{I_p^{'2}}\frac{L_q^2}{L_{eq}^2}+1\right) \tag{5.38}$$

$$L_{eq} = \frac{L_q^2 - L_d^2}{L_d} \tag{5.39}$$

and

$$I_p^{'} = \frac{k_t}{pL_{eq}} \tag{5.40}$$

Steady-state voltage equations of the salient PMSM when this strategy is applied are:

$$v_d \approx -pL_q i_q \omega = -pL_q I_{qb}\sqrt{\omega^2 - \left(\frac{I_p^{'}}{I_{qb}}\right)^2\left[\omega-\sqrt{\omega^2+K_2(\omega^2-\Omega_b^2)}\right]^2} \tag{5.41}$$

$$v_q \approx pL_d i_d \omega + k_t\omega = pL_d I_p^{'}\left[\omega-\sqrt{\omega^2+K_2\left(\omega^2-\Omega_b^2\right)}\right]+k_t\omega \tag{5.42}$$

The minimum v_q voltage is reached at a prevailing speed ω_p:

$$\omega_p = \Omega_b\sqrt{\frac{\frac{K_2}{(1+K_2)}}{1-(1+K_2)\left(\frac{L_d^2}{L_q^2}\right)}} \quad \Rightarrow v_q = v_{q\,min} \tag{5.43}$$

It should be noted from Figure 5.7 that when $\Omega_b \leq \omega \leq \omega_p$,normalized -i_d current (relative to I_{qb}) increase is higher than the normalized speed increase ω_b , which is, on the other side, higher than the normalized i_q current decrease. Consequently, the phase voltage vector v_s rotates toward the negative d-semi axis. At higher speed these relations are inverse, so that v_s rotates in the opposite direction, i.e. toward the positive q-semi axis. This observation is useful for the determination of the phase voltage limitation method, discussed earlier. Although its algorithm is more complicated than those of the constant power flux weakening control strategies, the advantages regarding the maximum torque profile, maximum exploited power, maximum extended speed for the same amount of energy and keeping constant voltage and constant current amplitudes during the whole period of flux-weakening, without any critical speed point, strongly recommend this strategy against the former ones, whenever the constant active power is not a strong prerequisite.

5.3.3 High-speed Closed Loop Control

In contrast to open loop operation, rotor position information is typically required to achieve high-performance motion control with the sinusoidal EMF PMAC machine. The rotor position feedback needed to continuously perform the self synchronization function is essentially the same as an induction motor. However, cogging torque (torque pulsations) due to interaction of the magnets with the stator slot harmonics places a heavier burden on the encoder to smooth out these effects. As result, an absolute encoder or resolver requiring a high resolution is frequently needed. In addition, in contrast to the induction machine, special provision is frequently needed to provide smooth, controlled starting performance since inappropriate energization at start can produce a brief negative rather than positive rotation.

One baseline approach for implementing this type of high-performance torque control for sinusoidal PMAC machines is shown in Figure 5.8. According to this approach, the incoming torque command (asterisk designates command) is mapped into commands for *d–q* axis current components and which are extracted from torque equation. These current

commands in the rotor *d–q* reference frame (essentially DC quantities) are then transformed into the instantaneous sinusoidal current commands for the individual stator phases (i_a^*, i_b^*, and i_c^*) using the rotor angle feedback θ_r, and the inverse vector rotation equations included in Figure 5.8.

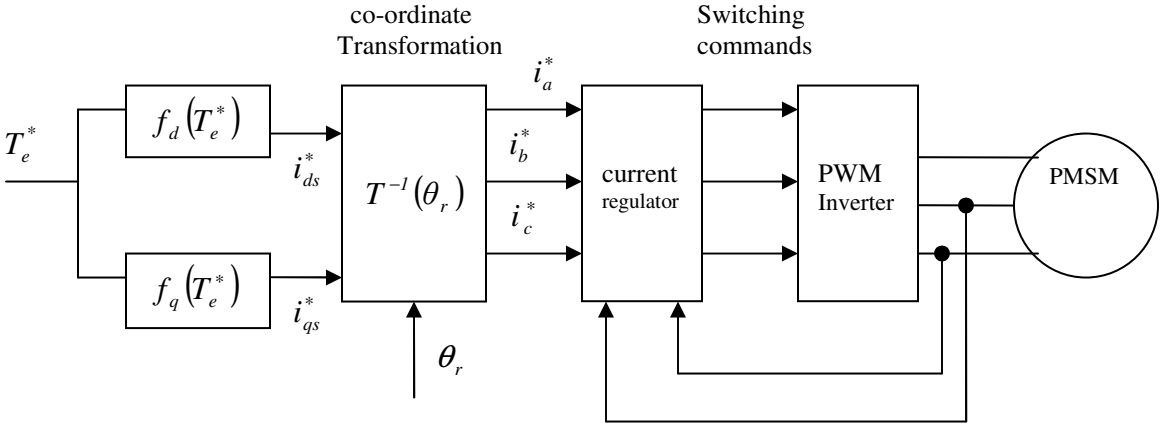

Figure 5.8 Torque control scheme for sinusoidal PMSM

The most common means of defining *d–q* current component commands i_{ds}^* and i_{qs}^* as a function of the torque command T_e^* into is to set a constraint of maximum torque-per-ampere operation which is nearly equivalent to maximizing operating efficiency. Trajectories of the stator current vectors i_{qds} the rotor *d–q* reference frame which obey this maximum torque-per-amp constraint are plotted in Figure 5.9 for a typical salient type of PMAC machine. The trajectories are plotted over a range of torque amplitudes ranging from negative (generating/braking) to positive (motoring) values.

It can be noted that the maximum torque-per-amp trajectory initially moves along the *q–* axis for low values of torque before swinging symmetrically into the second and third quadrant towards 45° asymptotes. For motoring operation, this behavior means that maximum torque for a given amount of stator current is developed by advancing the phase angle of the stator phase currents so that they lead their respective back–EMF waveforms by angles between zero and 45° (electrical).

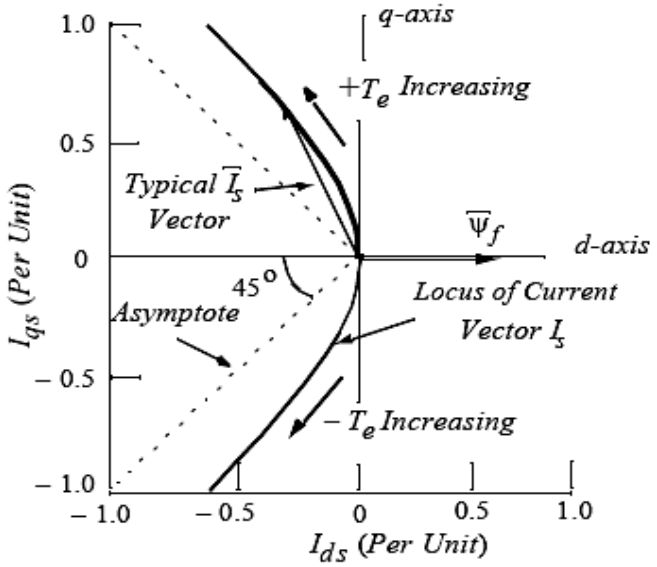

Figure 5.9 Trajectories of stator current vector I_S in the synchronous reference frame

The maximum torque-per-amp trajectory reflects the hybrid nature of the PM machine having the capability of producing reluctance torque as well as magnet torque. The corresponding currents I_{ds} and I_{qs} which define the maximum torque per-amp trajectory for the salient pole PMAC machine are plotted in Fig.(5.10). The figure shows that the maximum torque-per-amp trajectories are mirror images in the second and third quadrants. Stated in a different way, the I_{qs} function plotted in Figure 5.10 is sensitive to the polarity of the torque command, while the I_{ds} function depends only on its absolute value.

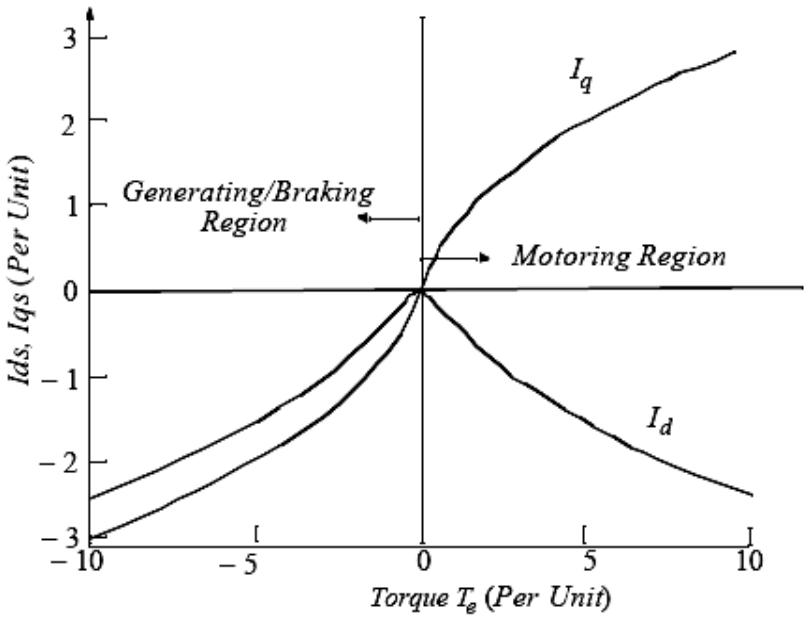

Figure 5.10 Direct and quadrature axis stator currents required to produce maximum torque per ampere for a salient pole permanent magnet machine(IPM)

5.3.4 Locus of current vector in the constant power region

The load torque limits in the speed range from zero to rated speed is set by the maximum current that can be supplied from the inverter, that is

$$\sqrt{I_{qs}^2 + I_{ds}^2} \le I_{max} \tag{5.44}$$

The limiting value of Eq.s (5.44) can be visualized as a circle in the i_{ds}–i_{qs} plane centered at the origin with radius $I_{max\,(I_S)}$. Beyond rated speed another constraint is imposed since the inverter pulse width modulator saturates and the output voltage becomes a constant. In this case, clearly

$$\sqrt{V_{qs}^2 + V_{ds}^2} \le V_{max} = \frac{2}{3} V_{dc} \tag{5.45}$$

using Eq.s (2.30) and Eq.s (2.31) of section (2.2.1) and rearranging the result, Eq.s (5.45) can be expressed as

$$\frac{2}{3}\frac{V_{dc}}{\omega_e} = i_{qs}^2 + \left(\frac{L_{ds}}{L_{qs}}\right)^2 \left(i_{ds} + \frac{\lambda_m}{L_{ds}}\right)^2 \tag{5.46}$$

Eq.s (5.46) can be visualized as an ellipse in the i_{ds}- i_{qs} plane with a focal point at $i_{qs} = 0$ and $i_{ds} = -\lambda_m/L_{ds}$. The size of the ellipse continues to decrease as the speed ω_e increases. Control of the *d-q* currents in the field weakening range must be such that the current remains in the circle of Eq.s (5.46) and tracks along the shrinking elliptical boundary as shown in Figure 5.11. It can be noted that the *d*–axis current is driven negative implying a stator mmf component acting to reduce the magnet flux (demagnetize the magnet). When I_{ds} becomes equal to λ_m/L_{ds} , the flux in the magnet has been driven to zero. Further negative increases in I_{ds} , must now be prevented. As a result the torque producing component I_{qs} now begins to decrease rapidly and constant horsepower operation can no longer be maintained. The field weakening region in Figure 5.11 corresponds to the segment from point A to point B.

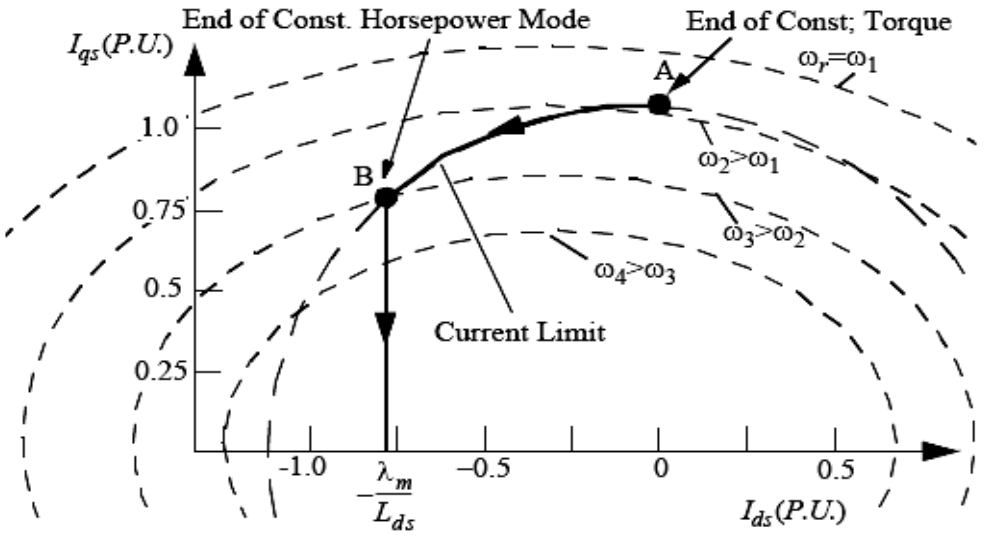

Figure 5.11 Locus of current vector in the d–q plane during operation above rated speed (constant power region is A–B)

5.3.5 Description of the FW control design

The designing of PM-machines has not matured yet to a degree which e.g. the designing of induction machines has. During recent years there has been a considerable increase of interest in using PM machines in applications where previously asynchronous machines have been used. The suitability of permanent magnet motor to a particular application is, however, dependent on the motor design. If for example large field –weakening range is needed, the motor has to have a large enough direct axis inductance.

As a review and to clarify the notation used henceforward, the IPMSM machine equations in the synchronous reference frame, are, given in matrix form below (see section 2.3).

$$\begin{bmatrix} V_d \\ V_q \end{bmatrix} = \begin{bmatrix} R_s & -\omega L_q \\ \omega L_d & R_s \end{bmatrix} \begin{bmatrix} i_d \\ i_q \end{bmatrix} + \begin{bmatrix} 0 \\ \omega_e \psi_{mf} \end{bmatrix}$$

$$T_m = T_L + J\frac{d\omega}{dt} + B\omega \quad , \qquad T_{fr} = B\omega \tag{5.47}$$

$$T_e = \frac{3p}{2}\left[\psi_{mf} i_q + (L_d - L_q) i_d i_q\right] = \frac{3p}{2}\left[\psi_d i_q - \psi_q i_d\right]$$

A precise current control of an IPMSM (IPM) drive becomes a complex issue owing to nonlinear coupling among its winding currents and the rotor speed as well as the nonlinearity present in the torque equation. The system nonlinearity become severe if the IPM drive operates in the field weakening region where the direct axis current $i_d \neq 0$.This results in the appearance of a nonlinear term, which would have vanished under the existing vector control scheme with $i_d = 0$.

Drive Structure Design

The IPM motor drive designed for this work featured a wide flux-weakening region. As a counterpart, the presence of both reluctance and PM torque requires involved control strategies, to guarantee effective drive operations at all conditions. The block schematic of the complete drive structure is reported in Fig 5.12.

The throttle knob position (tkp^*) is here considered as a speed reference, and it is compared with the actual mechanical speed ω_m, as shown in Fig.5.12. A light proportional and integral control PI then delivers the stator current reference space vector i_S^*.The main issues for an efficient control are proper current settings delivery and the avoidance of any inverter voltage saturation.

A. constant Torque controller

The magnitude of the output of the speed controller i_s can be expressed as (see Fig 5.13)

$$|i_s| = \sqrt{i_q^2 + i_d^2} = I_{S\,max} \tag{5.48}$$

and $$i_d = i_S \sin\gamma$$

$$i_q = i_S \cos\gamma$$

From Eq.s (5.47) , the d-q axis components of the current vector for the maximum torque per-ampere are derived as follows:

$$i_q = sign(i_s).\sqrt{i_s^2 - i_d^2}$$

$$if \quad i_s \geq 0, sign(i_s) = 1$$

$$i_s < 0, sign(i_s) = 1 \tag{5.49}$$

where

$$i_d = \frac{\psi_m - \sqrt{\psi_m^2 + 8(L_q - L_d)^2 i_s^2}}{4(L_q - L_d)}$$

Figure5.12 IPM motor drive block schematic

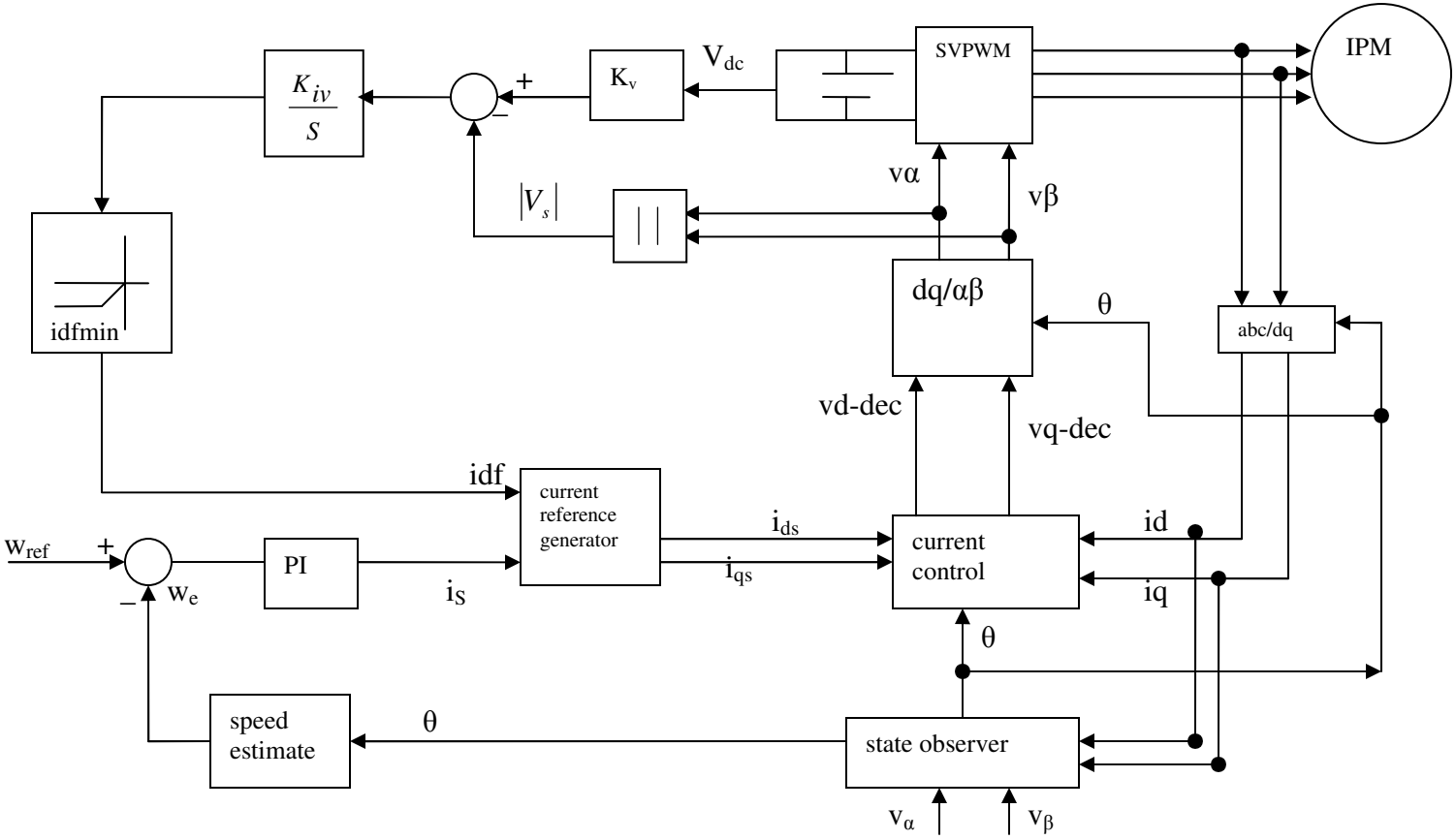

One can also obtain the optimal angle γ as

$$\gamma_{max} = \sin^{-1}\left(\frac{-\psi_m + \sqrt{\psi_m^2 + 8.(L_q - L_d)^2.i_S^2}}{4.(L_q - L_d).i_S}\right) \tag{5.50}$$

and this angle (Fig 5.13) is actively controlled with the specific saliency ratio ξ (L_q/L_d) as the reluctance torque is utilized for a maximum possible torque production. In the case of SPM motors, γ is 90^0 as saliency ratio is approximately equal to unity and only i_q is applied to produce the torque.

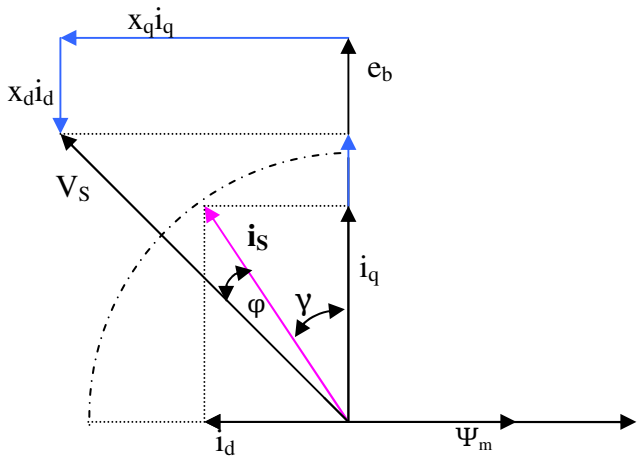

Figure 5.13 Phasor diagram of the PMSM.

B. Operating limit in the flux weakening region

The maximum voltage that the inverter can supply to the machine is limited by the dc link voltage and the PWM strategy. A PWM strategy based on voltage space vector is used and V_{smax} is $V_{dc}/\sqrt{3}$. Also the maximum current $I_{s\ max}$ is determined by the inverter current rating and machine thermal rating. Therefore, the voltage and current of the motor have the following limits

$$v_S^2 = v_d^2 + v_q^2 \le V_{S\,mac}^2 \qquad (5.51)$$
$$i_S^2 = i_d^2 + i_q^2 \le I_{S\,\boldsymbol{max}}^2$$

where $V_{S\,max} = 1/\sqrt{3}\, V_{dc}$ ... with SVM, and $V_{S\,max} = 1/2\, V_{dc}$ ... with Sinusoidal-PWM

C. Current reference generator

The amplitude of stator current i_s is directly linked to the torque production. Nevertheless, there are infinite couples i_d, i_q that give the same vector i_s, each producing a different torque value. In the constant-torque operating range, various profiles in the i_d, i_q plane can be selected, depending on the optimization objective of the specific application. In the drive schematic of Fig (5.12), the output of the proportional-integral (PI) speed regulator is the (signed) amplitude of the stator current space vector i_S^*.

If the direct current reference i_d^* is expressed as a function of i_q^* that maximizes the torque by imposing

$$\frac{\partial T}{\partial i_q^*} = 0 \qquad (5.52)$$

that gives, in turn,

$$i_q^* = sign(T)\sqrt{\frac{(2i_s^*)^2 - i_{da}^2 + \sqrt{i_{da}^4 + 8(i_{da} i_s^*)^2}}{8}} \qquad (5.53)$$

where $$i_{da} = \frac{\psi_m}{(L_d - L_q)} \quad . \qquad (5.54)$$

A common way to derive the adequate current references for FW is based on the calculation of the intersection between the actual current circle and the voltage limit ellipse in the i_d-i_q plane. For a given current i_s^* and rated amplitude $V_{\lim}$ (V_b) of voltage vector, the

i_d^*, i_q^* couple can be derived from Eq.s (5.51) and the steady state voltage balance equation (from Eq.s 4.12)

$$L_q^2 i_q^2 + (L_d i_d + \psi_m)^2 = \frac{V_{lim}^2}{\omega_e^2} \tag{5.55}$$

in which ω_e is the electrical speed ($p\omega$) and the stator resistive drops have been neglected. It is, then,

$$i_d^* = \frac{L_d \psi_f - \sqrt{\psi_m^2 L_q^2 - (L_q^2 - L_d^2)(\frac{V_{lim}^2}{\omega_e^2} - (L_q i_s^2)^2)}}{\left(L_q^2 - L_d^2\right)} \tag{5.56}$$

It is worth noticing that the theoretical value Eq.s (5.56) is a function of either current and voltage vector amplitude and of the motor speed as well. The use Eq.s (5.56) as a current reference generator requires the knowledge of the electrical speed ω_e in which the FW has to triggered, given by

$$\omega_e = \pm \sqrt{\frac{V_{lim}^2}{L_q^2 i_q^2 + (L_d i_d + \psi_m)^2}} \tag{5.57}$$

NOTE: As previously mentioned in the above discussion, a maximum toque T_{max} can be achieved by utilizing the reluctance torque with an optimized current angle gamma; the speed increases with this possible maximum torque until the inverter reaches the limitations, i.e., the rated condition of the drive. The torque is decreased when the speed further increases above the rated speed; this operation is known as constant power operation.

In the field-weakening region, the controller uses the feedback i_d and reference i_{dref} corresponding to the reference speed calculated according to Eq.s (5.57).The switching

between the constant torque and the field weakening controller is implemented by comparing the feed back speed and the known rated speed of the drive.

Theoretically a maximum speed ω_{max} with zero torque is reached when i_d is set to be the rated current. Without a proper flux weakening operation, the current regulator would be saturated and lose its controllability at higher speed. A smooth transition from the constant torque to the flux –weakening region is guaranteed by an external voltage close –loop regulation, as depicted in Figure 5.12, which delivers a FW component i_{df} that is added to the actual i_d when the space-vector-modulated (SVM) inverter voltage limit is approached. The quadratue current reference i_q is now limited by

$$i_{q,lim} = sign(i_S)\sqrt{i_S^2 - (i_d + i_{df})^2} \tag{5.58}$$

The design now focuses on the choice of K_{iv} and K_V which fixed the reference voltage limit of the loop. The choice of the voltage limit K_V has to be harmonized with that of the integral gain K_{iV} , which in turn must preserve the overall system stability. It is worth noting that the greater K_V , the closer the voltage limit to the inverter saturation. If this is the case, a prompt flux-weakening action is required. Of course, this calls for higher value of K_{iv} , whose upper limit is yet imposed by system stability. In this paper, a value of K_v=0.54 has been used.

Another crucial parameter is the maximum negative current $i_{df,\min}$,which limits the output of the integrator(Fig.5.12).It is worth performing an adaptive limitation, according to the actual working point, by setting

$$i_{df,min} = I_N - i_{d,n} \tag{5.59}$$

where I_N is the rated stator current and $i_{d,n}$ is the direct current that the current reference generator would give in the absence of voltage limitation. Several experimental tests have highlighted that if a fixed limitation is chosen instead, instability may arise at load detaching during operation far above the base speed.

D) Current regulators (controllers)

In every modern ac drive, the current control plays a crucial rule and can be fully considered a distinguished feature of the drive itself. Actually, a proper current control can be achieved in the synchronous d-q coordinates system by conventional proportional plus integral (PI) controllers, as shown in Figure 5.14.In the synchronous frame, the motor model presents coupling terms between d and q axes. These terms can be considered as disturbances that complicate the design of PI controllers and reduce the overall dynamic performances. A decoupling and feedforward algorithm has been implemented in the drive, as sketched in Figure 5.14. A decoupling and feedforward algorithm (blocks DC_1 and DC_2) reduces the cross-coupling effects between the two axes and simplifies the PI regulators design. An exact decoupling action could be obtained by including inductance saturations.

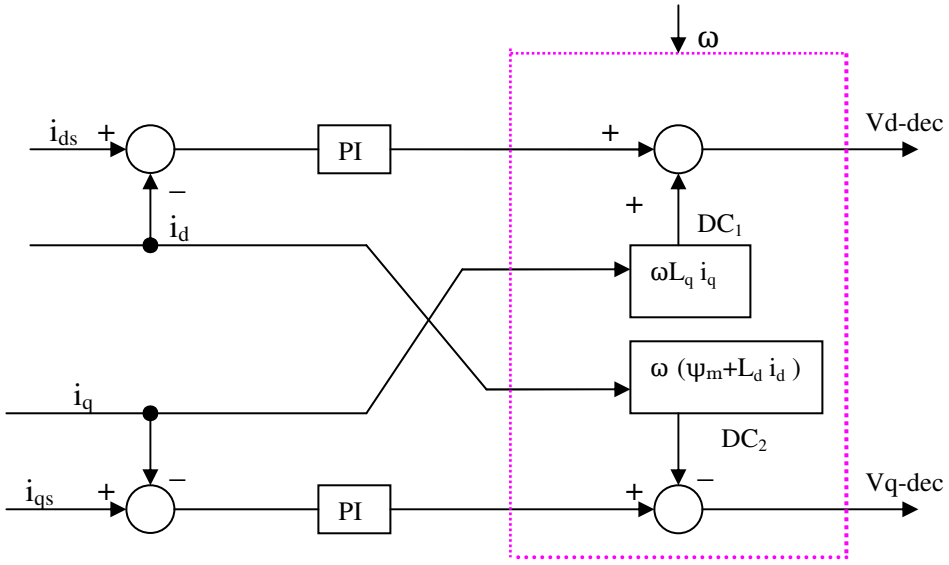

Figure 5.14 Decoupling scheme in current control

Chapter 6

Simulated Result, Discussion and Conclusion

In order to validate the mathematical analysis and, hence, to establish the effectiveness of the proposed field weakening control scheme, the performance of IPM drive based on the proposed control scheme is investigated both theoretically and by simulation at different operating conditions. Therefore this section of the thesis is concerned with formulating a software (matlab) code that will be used to develop the closed loop control of the system under field weakening.

The software design is the point of convergence for this thesis project. This is because it is the point where all theories and practices presented through the course of this report come to together to form an appropriate software design. A matlab code is prepared to realize control of PMSM with field weakening .The constructed software design can be done also in a C-code. Developing the model using matlab/simulink provides portability and maintainability. This allows for the design to be prototyped relatively quickly (relative to programming with c++) and the model can be optimized to this particular design architecture.

In this section general software flowchart will be explained. Furthermore, simulation outputs of the relevant parameters are analyzed and monitored to show that the proposed scheme run properly. The software implementation is done based on the system shown in Figure 5.12.

6.1 Software Organization

Overall algorithm of simulation may be divided into two: initialization and running the program .The initialization step defines and initializes the software variables and constants while the second step is running the program .Discrete simulation have been carried out for the implementation of the drive using Matlab. The IPM drive system shown in Figure 5.12 is considered here again with software analysis of field weakening.

The following flow chart is followed to investigate the control of PMSM over a high speed.

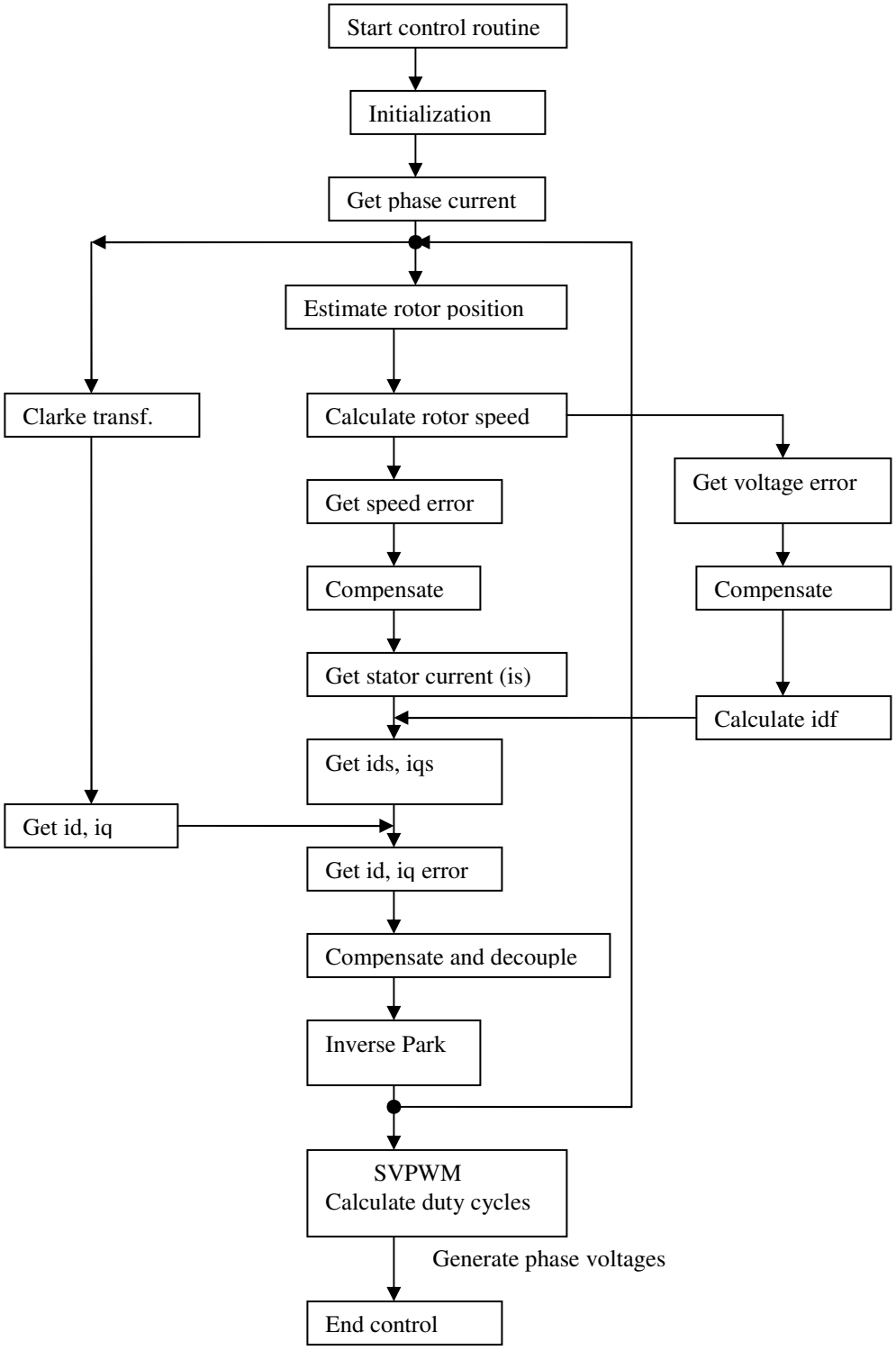

Figure 6.1 Flow chart of the closed loop drive

The discrete forms of PI controllers are used for digital simulation. The sliding mode observer simulation is done in α-β reference frame with constant gain –matrix as derived in section 3.3.A discrete–time version of relevant equations suitable for implementation on a matlab program can be derived using a Z-transform .For transformation from continuous system to discrete we use backward transformation, i.e., $S = \frac{z-1}{Tz}$,where T (t=kT) is the sampling time of the system and k is the sample number. A carrier signal of variable frequency is used, with switching frequency in the inverter of 1KHZ, which is also equal to the sampling frequency. The control algorithm including the proposed flux weakening scheme is implemented with this software.

The proposed model for flux weakening control of IPM drive block shown in Fig.5.12 is implemented using Matlab and the simulation voltage and phase currents are shown in the next section. Parameters of the Interior Permanent Magnet Synchronous machine used in simulation is presented in Table.4.

TABLE4 The PMSM (IPM) control design data (Motor specification)

dc link voltage	220V
Inertia	0.0015Kg.m^2
magnetic flux linkage	0.272Wb
pole pairs	2
rated power	960W
speed(nominal)	128rad/s
stator resistance	0.8ohm
q-axis inductance	67mH
d-axis inductance	27mH
friction coefficient	0.001Nm/rad/s
sampling time	0.001sec

The field –oriented controller is based on a current controlled voltage source inverter (VSI) structure. The control loops are arranged in two –phase *synchronously rotating reference frame dq* aligned with the rotor flux, while the sliding mode observer operates in two –phase *stationary reference frame αβ.* The value of V_{Smax} is set according to the dc link voltage. The nominal value of V_{Smax} is about 120V.

A reference speed of ramp and constant value is considered. In practice, a ramp speed command is preferred to a step speed change to avoid controller saturation, which leads to the development of maximum torque almost instantaneously. A sliding mode closed loop observer is analyzed which exhibits stable speed control and hence provides the rotor position (needed for the field orientation).The observer can successfully replace sensors. There exist three PI regulators in the FOC structure. Saturation techniques for current regulators are a major issue in determining the performance of motor that can be expected when working close to the inverter voltage limit.

6.2 Simulation results and discussion

Next, simulation results obtained for the drive being investigated are presented for the sake of comparison. The software represents all the switches as ideal switches.

The simulation has been performed for the verification of the proposed strategy in the drive system of section 5.

The phase voltages are compared with high- frequency carrier signal to generate the pulse width –modulated (PWM) signals, which act as firing pulses for the six transistors of the inverter. The sector number generated by comparing the triangle with the sinusoidal reference voltage is plotted in Fig.6.2. And in Fig.6.3 the reference voltage together with reference speed and the six sectors which used for duty cycle determination are shown. As we can see the reference speed in this case is considered to be a constant ,20rad/sec.Later in this section we considered different speed reference values ,which includes a ramp having a certain slope for the sake of comparison.

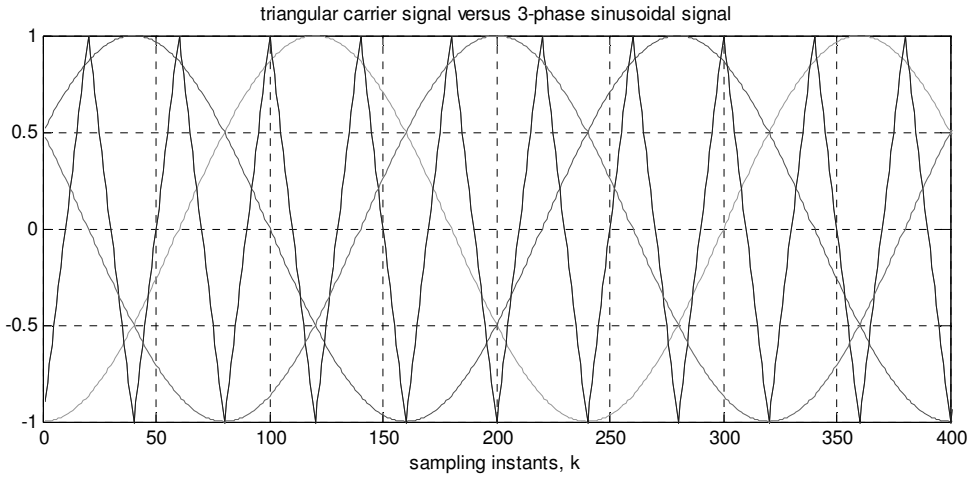

(a)

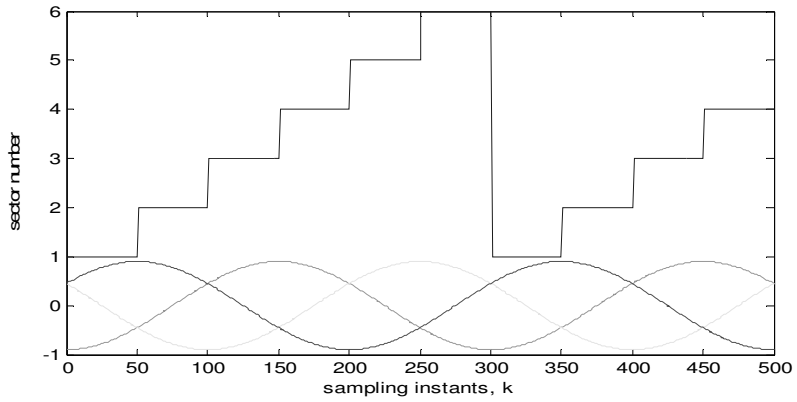

(b)

Figure 6.2 Simulation results with voltage references (a) determination of sectors (b) sector numbers of voltage vectors.

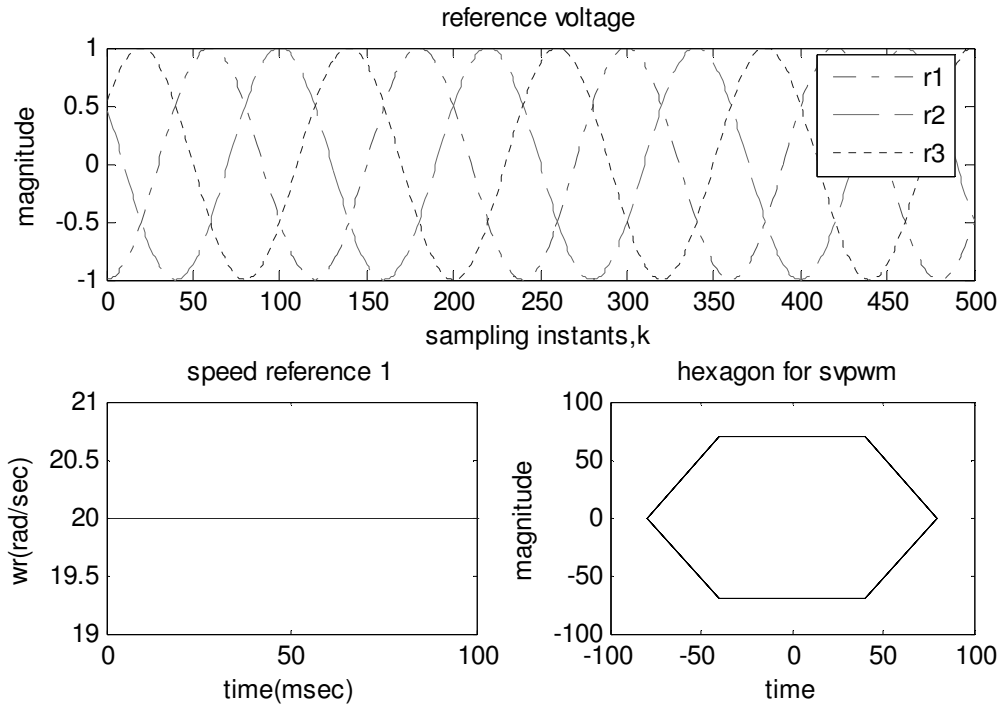

Figure 6.3 Reference voltages, reference speed, and generated six side polygon (sectors)

Fig 6.4 shows the pole voltages waveforms of the drive, i.e. VA0, VB0 and VC0.These continuous output voltage waveform pattern is obtained after the carrier has been taken out. Based on switching sawtooth functions ,the inverter voltage parameters ,such as va0,vb0,vc0,vn0,line to line voltages (vab, vbc, vca),and phase voltages (van, vbn, vcn),are presented in Fig.6.5 and Fig.6.6.The voltage vn0 represents the equivalent common mode zero sequence voltage source of the system.

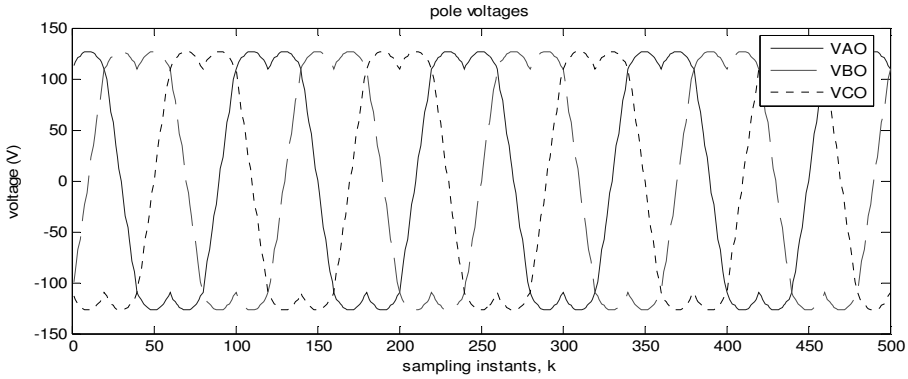

Figure 6.4 The wave form of space vector PWM outputs (pole voltage)

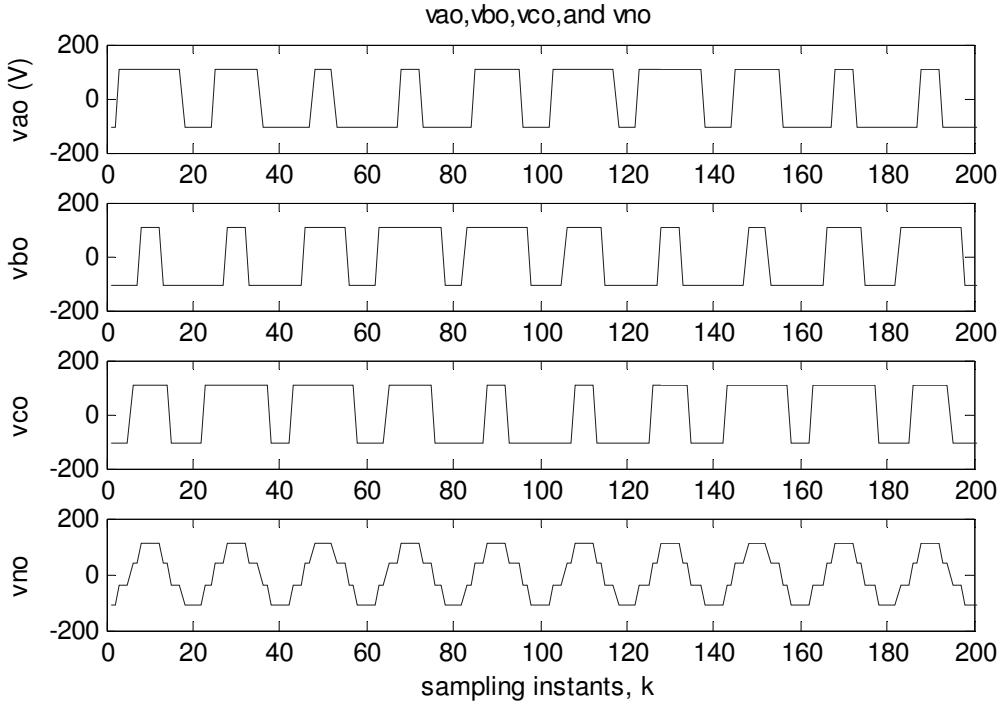

Figure 6.5 Voltage waveforms vao, vbo, vco and vno.

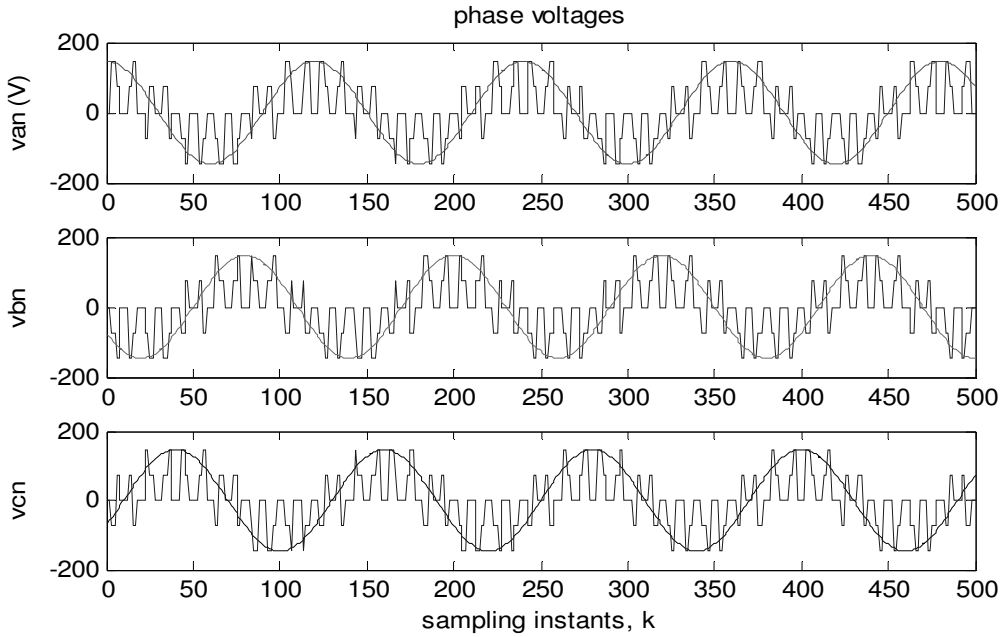

Figure 6.6 Discrete and continuous phase voltage waveform

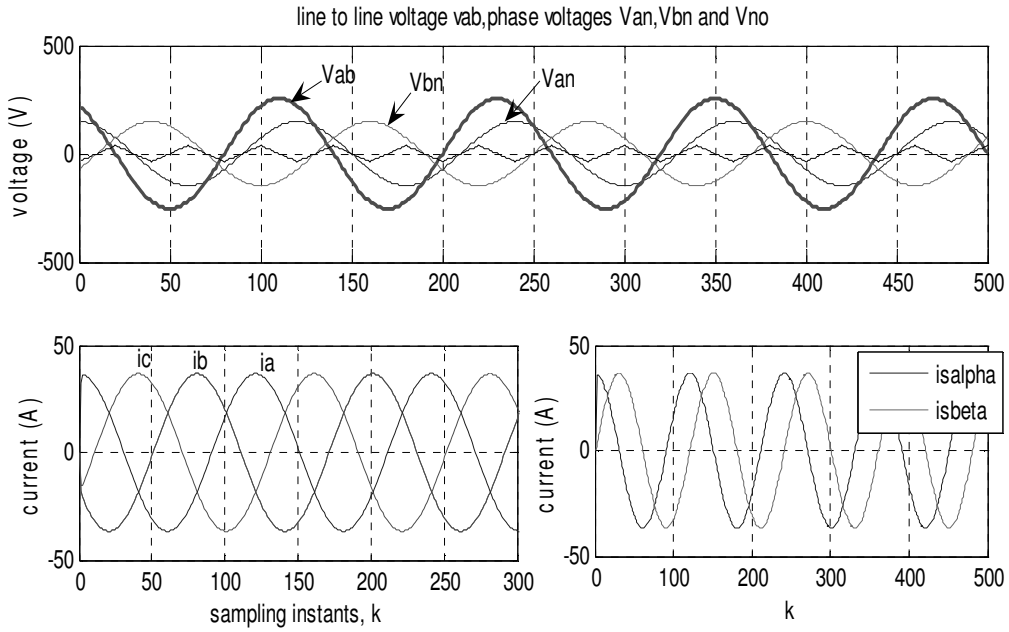

Figure 6.7 Phase Voltage and current waveforms

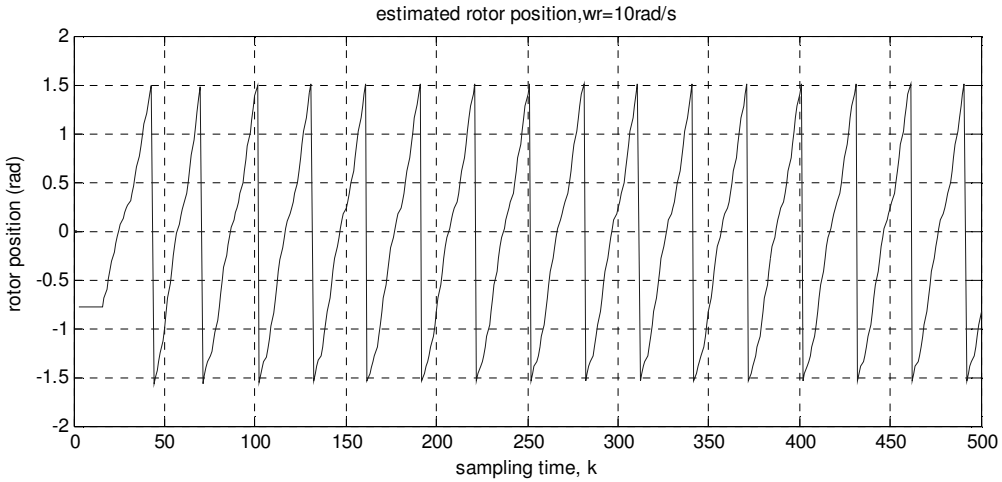

Figure 6.8 Estimated rotor position by application of sliding mode observer for w_r=10rad/s

Fig.6.7 shows matlab simulation results of the proposed SVPWM. The input inverter balanced load/phase currents and output line to line are shown. Also, the stationary alpha and beta axis phase currents are shown. From Fig.6.7, it can be noted that the phase currents of the rectifier are modulated during each cycle. Their values comprised of the three phase output currents. On the other hand, the output voltages are also modulated, and are composed of portions of the three phase input voltages. From Fig.6.7, it can be observed that the waveforms of three phase output currents are essentially sinusoidal. This result, in turn, demonstrates that there are no low order harmonics in the output voltage.

Fig.6.8 shows the estimated rotor position waveform obtained based on sliding–mode observer for reference speed of 10rad/s. For the drive system, the pertinent control objective of sliding mode observer is to estimate rotor position and to track the rotor angular speed. Fig .6.9 shows the simulated response of the motor speed and corresponding filtered and unfiltered speed errors. The motor current is practically sinusoidal and the estimated rotor speed nearly follows the reference speed but obviously with some ripple in the speed error. This error variable can be stabilized by proper selection of control input and also using a low pass filter. A low pass filter is used to get rid of the high –frequency ripples caused by differentiation and noise in the current and voltage signals generated. In Fig.6.9b it can be observed that the speed error smoothes out after about 0.03sec.The time constant in the first case (Fig.6.9a) is τ=RC=0.08sec and in the time constant in the second case (Fig.6.9b) is τ=0.01 seconds.

An increase in the reference speed from 10rad/sec to 50rad/sec is well handled by the sliding mode observer. Fig .6.10 shows the simulated response of the motor rotor position and speed for constant reference speed of 50rad/s .The estimated speed (w_{fb} ,feed back speed) does converge after an elapse of time while unmodeled space harmonics appear as ripple in the speed estimate. The error between w_{ref} and w_{fb} feeds the current regulating loop. The estimated speed w_{fb} in Fig .(6.10b) is a low pass filtered output of the reference speed, w_{ref} =50rad/sec.The observer behaves well in this incremented speed reference. The error between w_{ref} and w_{fb} feeds the current regulating loop. The speed drops, but recovers to the commanded value in the steady state.

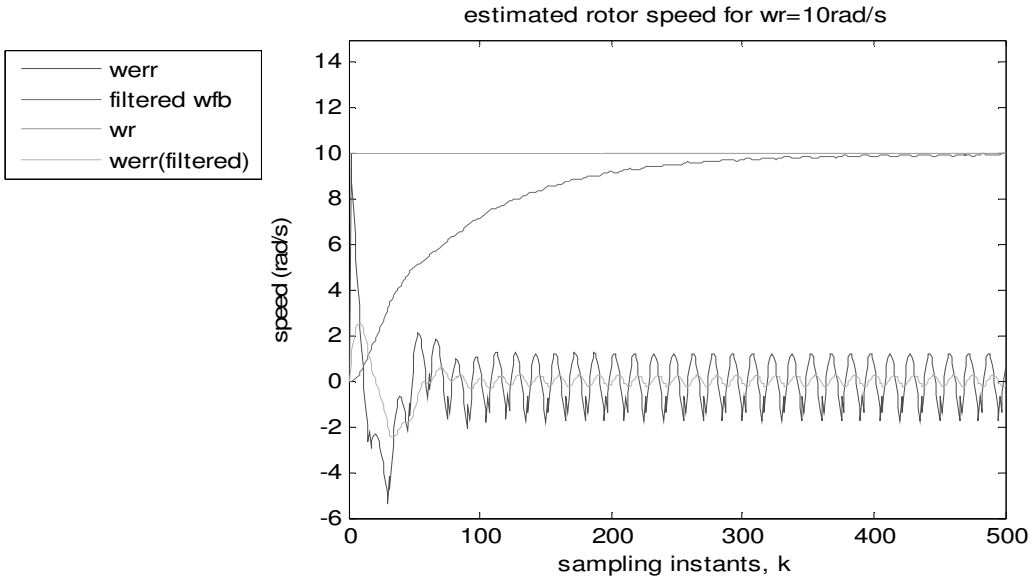

(a)

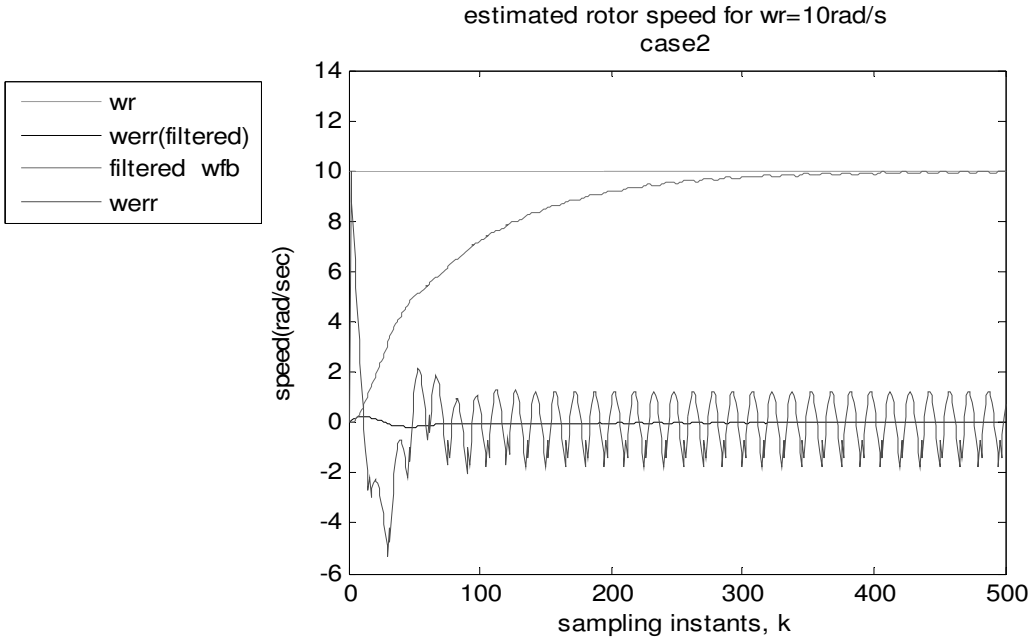

(b)

Figure 6.9 Simulated responses of estimated speed and corresponding error at different time constant a) τ=0.08sec (b) τ =0.01sec

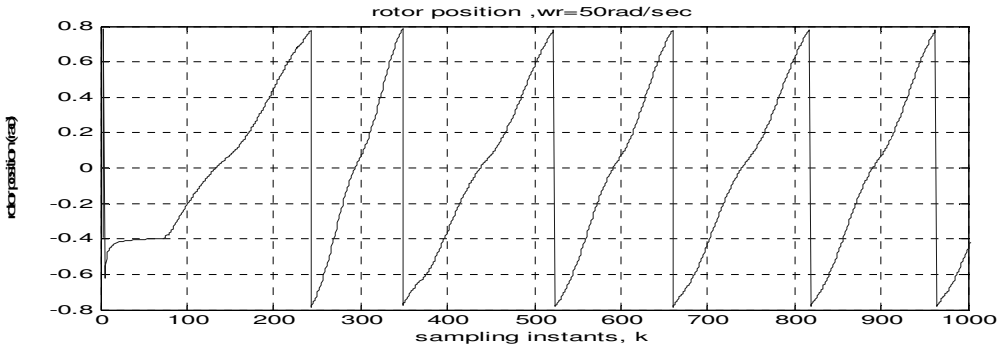

(a)

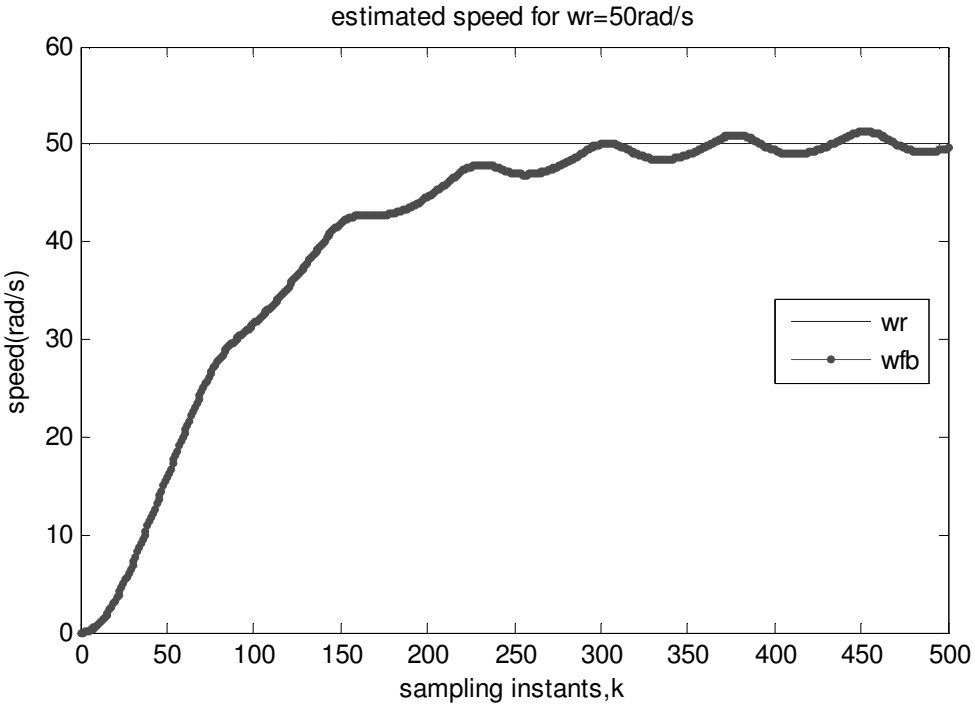

(b)

Figure 6.10 Simulated drive response for an increase in speed, w_r =50rad/sec (a) rotor position and (b) the estimated speed

A reference ramp speed profile is applied to the drive. The desired motor speed varies from 0 to 15rad/s. Fig.6.11 shows the results corresponding to a ramp reference speed. The steady- state error between the estimated and reference speed is almost negligible.

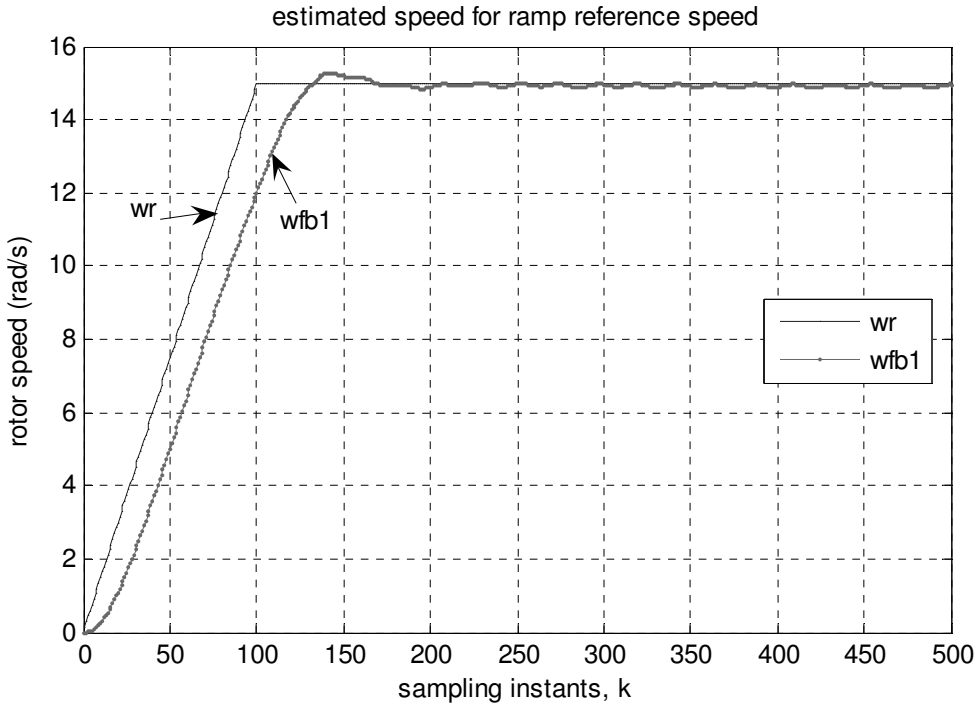

Figure 6.11 Simulated drive response for a ramp speed profile.

Fig.6.12 show the simulated current response and waveform of the stator current, d-axis and q-axis currents for the ramp speed command under the fixed DC link voltage of 220V.A certain delay in i_q response can be observed.

The simulation waveforms in Fig.6.13 illustrate the i_d versus i_q trajectory in the d-q plane. When rated speed is reached, the dynamic field weakening algorithm is activated and the reference vector is modified and generates the appropriate currents.

This phenomenon is illustrated in Fig.6.14.

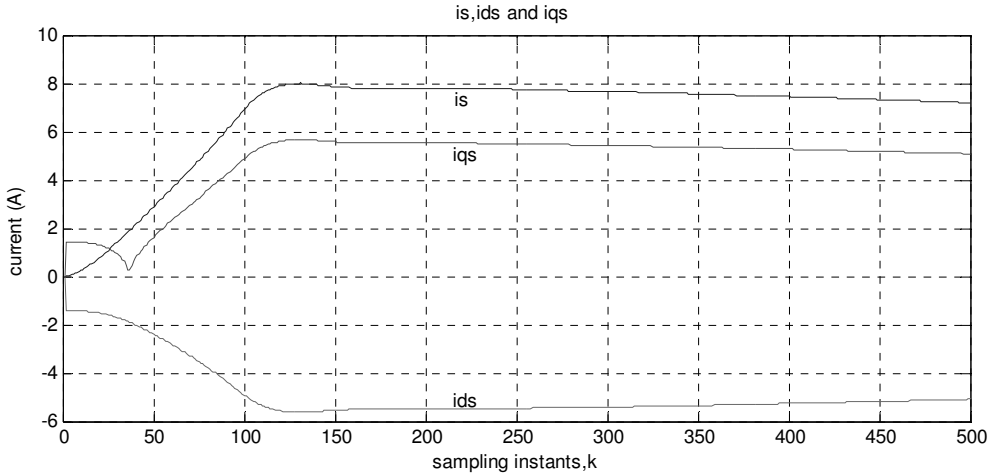

Figure 6.12 Reference current generation

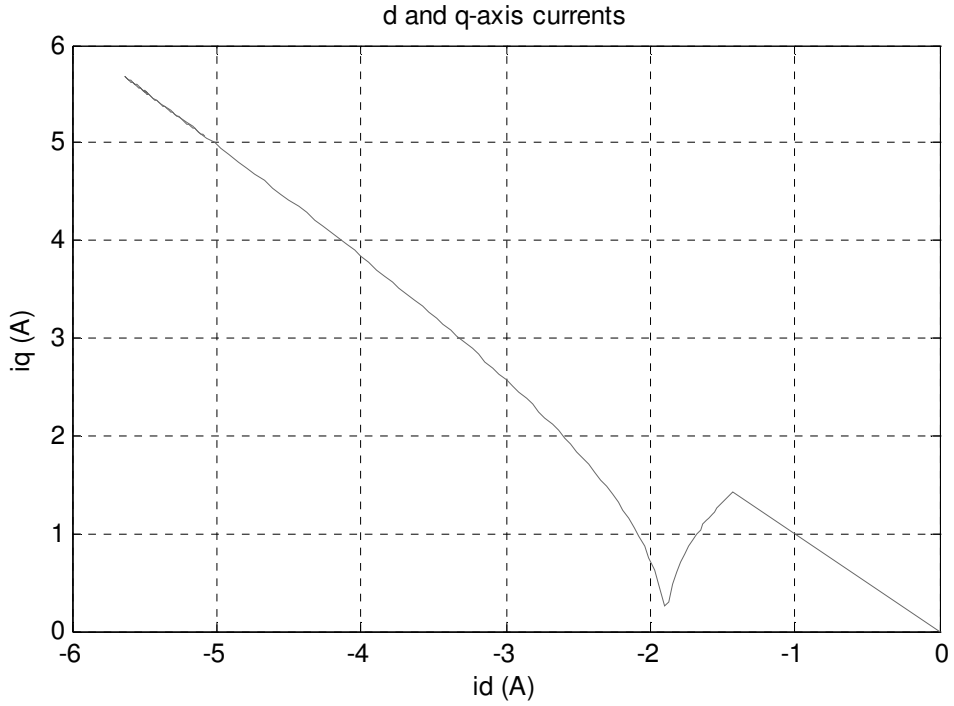

Figure 6.13 Maximum torque per ampere trajectory (i_d versus i_q trajectory)

Fig.6.15 also shows the speed-torque curve of IPM drive in FW actions. Particular care has been paid for the management of current regulators output and integral limitation. Actually, a proper current control can be achieved in the synchronous d-q coordinates system by conventional proportional plus integral (PI) controllers.

The transition into constant power is illustrated in Fig.6.16 .when V_{qd} reaches V_{smax} , the flux weakening operation begins at this speed. The error between V_{qd} and V_{smax} feeds the voltage regulating loop to generate i_{dfmin} .The beginning of field weakening at the rated speed bring about a decrease in torque component i_q and an increase in i_d current toward the negative direction to keep the current regulator from saturation as shown in Fig.6.15.

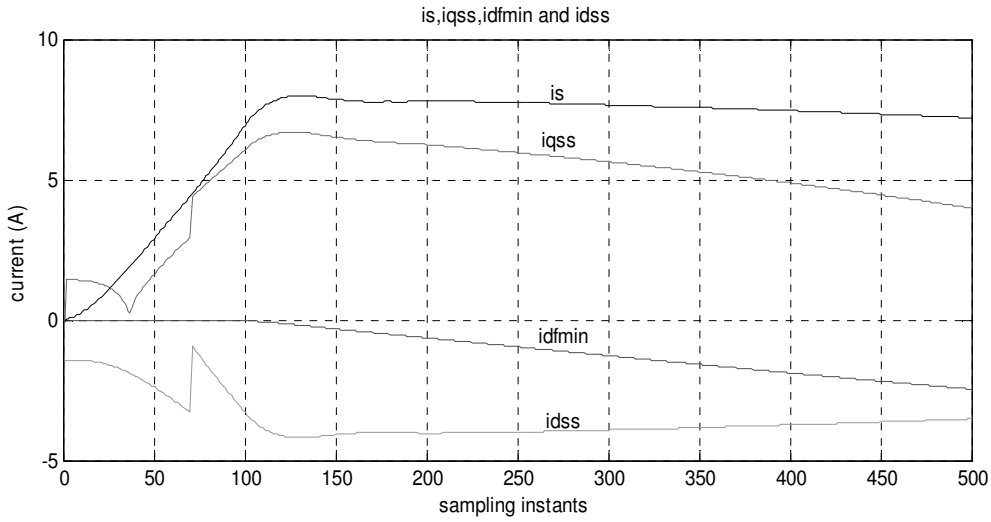

Figure 6.14 Currents in the FW action

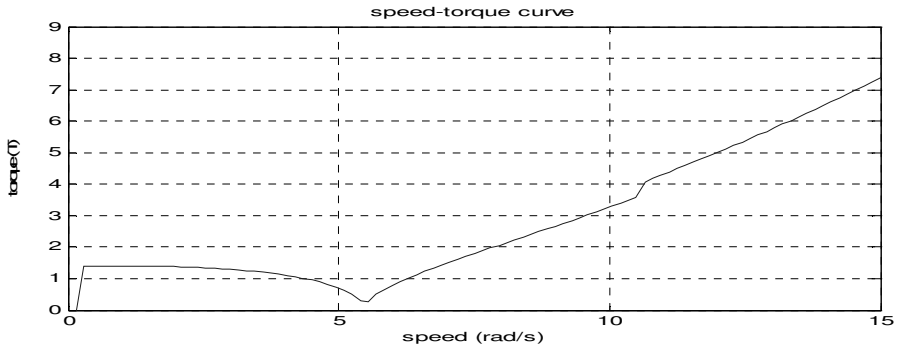

Figure 6.15 IPM drive speed –torque curve.

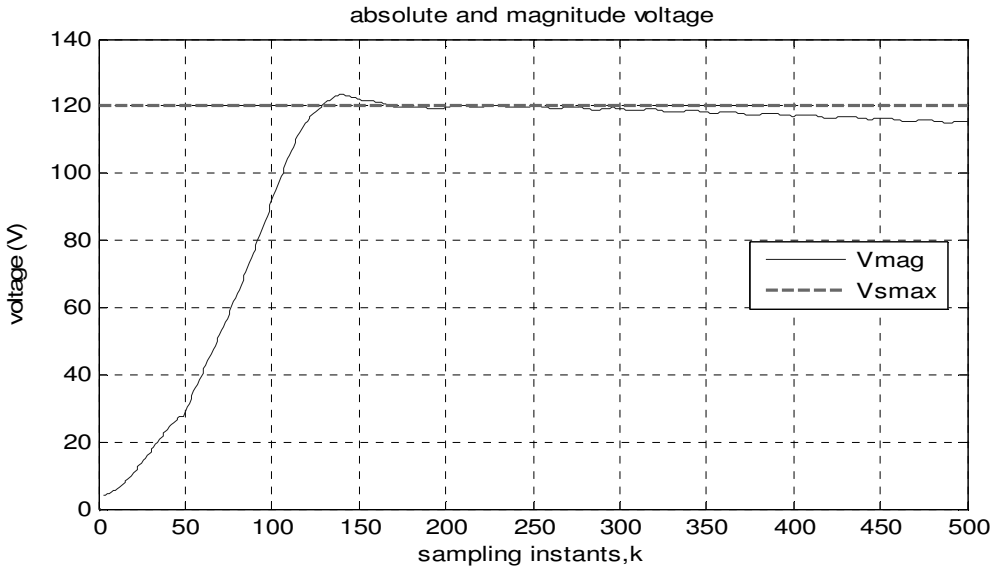

Figure 6.16 Magnitude of output voltage in stationary frame (alpha-beta coordinate)

6.3 Conclusion and future work

6.3.1 Conclusions

The objective of this work is to explain and analyze field weakening control of a voltage source inverter (VSI) fed PMSM drive system for Electric vehicle (EV).The dynamic performance of flux/field weakening control of PMSM motors has been studied. The demagnetizing effect of the negative direct current to weaken the air gap flux was presented in detail.

In this master thesis various types of PM –synchronous motors internal configuration is discussed and their main differences is also reported. Among which an IPM drive are gaining widespread interest for their inherent flux-weakening capability. The control of an IPM motor is more involved, since it features both PM and reluctance torque. The detailed derivation of the motor model has been provided. The work implied an extensive theoretical approach which incorporates many mathematical derivations.

First, generalized dynamic mathematical model of the PM-Synchronous motor was studied and developed in both stationary and rotating frame. A detailed description of comparative analysis of flux-weakening control methods and modeling of the motor drives are the main accomplishments of this work. This includes modeling of PI regulators, Space Vector Pulse Width Modulators (SVPWM), and estimation of the rotor angle is discussed in chapter 3. But its biggest contribution is having them all together on one place - in a single master's thesis project so that a concise, but complete motor drive design for this specific application is available to a reader.

The estimation of initial angle of the rotor is a vital part of both an open loop and a closed loop vector controlled PMSM drive. The presence of state observer for rotor position estimation has made the calculation very complex. Researches are still working to obtain better performance of Field Weakening control of sensorless PMSM drive.

The motor drive system simulation model was developed and assessed using matlab code. For a fully digital implementation, the system model has been discretized by rectangular transformation (back transformation).In addition, SVPWM algorithm used in this paper is simulated and the results are reported. In addition to the implemented SVPWM algorithm of Chapter3, over-modulation techniques may also be implemented in order to utilize

entire dc link voltage. With the analysis and implementation of FW control of PMSM machines presented in this thesis, a good performance can be obtained.

Future research in the areas of the adaptive and robust control systems in real time application, and flux-weakening control methods, is a natural continuation of this work.

The author's hope is that the above-mentioned accomplishments can serve as a small contribution to future research in this wider and more interesting than expected, but less explored than expected area .

6.3.2 Future Work

The theoretical and simulation works show the great promise of the studied methods in this thesis. However, due to equipment limitations these methods are not tested practically. The presented analysis of the machine parameters gives guidelines for further studies. Further research should be performed to combine the analysis and selection of the parameters of the PMSM with the actual magnetic design of a machine. The d-q axes inductances of IPM synchronous motors are susceptible to saturation due to high current excitation, and should be modeled by making L_d and L_q as function of the d-q axes currents, i_d and i_q. Further, the magnet flux density changes with temperature. Temperature can affect the flux density of the magnet so also the field-weakening performances. Thus, saturation effect of d-q axis inductances and temperature dependence of the magnet should be included in future research to complete the prediction of the losses (iron losses, stray losses, etc...).

.

References

[1] Werner Leonard "*Control of Electrical Drives*", 2nd revised edition, 1993

[2] G.K. Dubey, "*Fundamental of Electrical drives*," Narosa, Kanpur, 4th edition, 1997.

[3] A.E. Fitzgerald, J.C. Kingsly, and S.D. Umans, "*Electric Machinery*" Tata-McGraw- Hill Edition, Delhi, sixth-edition, 2003.

[4] Girma Mullisa, "*Introduction to Control Engineering*", Addis Ababa University text book series, Addis Ababa,1997.

[5] Y.K. Chin and J.Soulard, "*Modeling of iron losses in PMSM with Field-Weakening Capability for Electric Vehicles*", abstract from the internet

[6] Texas Instruments, "*SVPWM with TMS320C2XX*", Literature number: SPRA 524, 2001

[7] Analog Devices, "*Implementing Space Vector Modulation with the ADMC300*", Literature number: AN300-17

[8] M.A. Rahman, M.Vilathgamuwa, and N. Uddin, " *Nonlinear Control of Interior Permanent-Magnet Synchronous Motor*", *IEEE Ind. Applications*, vol39, No.2. pp.17-33, Mar/Apr.2003

[9] Texas Instruments Inc., "*Field Orientated Control of 3-Phase AC-Motors"*, www.ti.com, Texas Instruments Literature number BPRA073, Europe, 1998

[10] Texas Instruments Inc., "*Clarke and Park Transforms on the TMS320C2xx",* www.ti.com, Texas Instruments Literature number BPRA048, Europe, 1998

[11] Texas Instruments Inc., "*Implementation of a Speed Field Oriented Control of 3-phase PMSM Motor using TMS320F240* " , www.ti.com, Texas Instruments Literature number SPRA588, Europe, 1999

[12] B.H. Bae , S.K. Sul, J.H. Kwon, and J.S. Byeon "*Implementation of Sensorless Vector Control for Super-High-Speed PMSM of Turbo-Compressor"*, *IEEE Trans. Ind Applicat.*, vol. 39, pp. 811–817, May/June. 2003.

[13] S.H. Kim and S.K. Sul, "*Maximum Torque Control of an Induction Machine in the Field- Weakening region*," *IEEE Trans. Ind. Applicat.*, vol.31, pp. 787–794, July/Aug. 1995.

[14] H. Grotstollen and J.Wiesling, "*Torque Capability and Control of a Saturated Induction Motor over a Wide range of Flux Weakening,*" *IEEE Trans. Ind. Electron.* vol. 42, pp. 374–381, Aug. 1995.

[15] S.H. Kim and S.K. Sul, "*Voltage Control Strategy for Maximum Torque Operation of an Induction Machine in the Field Weakening Region*," *IEEE Trans. Ind.Electron.* vol. 44, pp. 512–518, Aug. 1997.

[16] B. J. Seibel, T. M. Rowan, and R. J. Kerkman, "*Field-Oriented Control of an Induction Machine in the field-weakening region with dc-link and load disturbance rejection,*" *IEEE Trans. Ind. Applicat.*, vol. 33, pp. 1578–1584, Nov./Dec. 1997.

[17] J. Solsona, M .I.Valla, and C. Muravchik, "*A Nonlinear Reduced Order Observer for Permanent Magnet Synchronous Motors*", *IEEE Trans.Ind. electr*, vol.43,No 4, Aug 1996, pp. 492–497.

[18] S.-H. Kim and S.K. Sul, "*Speed Control of Interior Permanent Magnet Synchronous Motor Drive for the Field Weakening Operation*", *IEEE Trans. Ind. Applicat.* vol. 33, pp. 43–48, Jan./Feb. 1997.

[19] G. Zhu, A. Kaddouri, and L. A. Dessaint, "*A Nonlinear State Observer for the Sensorless Control of Permanent Magnet AC Machine*", *IEEE Trans.Ind.Electron,* vol.48, No.6, pp. 1098–1107.2001.

[20] D. S. Maric, S. Hiti, C. C. Stancu, J. M. Nagashima, and D. B. Rutledge, "*Two Flux Weakening Schemes for Surface-Mounted Permanent Magnet Synchronous Drives- Design and Transient Response Considerations*," in *Proc. ISIE'99*, vol. 2, 1999, pp. 673–678.

[21] T. M. Jahns, "*Flux-Weakening Regime Operation of an Interior Permanent-Magnet Synchronous Motor Drive*", *IEEE Trans. Indust .Applicat.* vol.23, pp. 681-689, July/Aug. 1987.

[22] J.W. Park, D.H. Koo, and J.M .Kim, "*Improvement of Control Characteristics of Interior Permanent Magnet Synchronous Motor for Electric vehicle*," *IEEE Transactions on Industry Applications*, Vol. 37, No. 6,., pp.1754-1761, Nov/Dec.2001

[23] F. Boriz, A. Diez, M.W.Dagner, and R. D. Lorenz, "*Current and Flux Regulation in Field –Weakening Operation*", *IEEE Trans. Indust .Applicat*, vol 37, No 1, pp 42-49, Jan/Feb 2001

[24] N. Bianchi and S.Bolognani, " *Innovative design and optimization of electrical Machines*", *IEE Proc. Electr. Power Applications* Vol.140, 2001.

[25] R.F.Schifferl and T.A.Lipo, "*Power capability of salient pole permanent magnet synchronous motor in variable speed drive applications*", *IEEE Trans.Ind. Applicat*, vol.34,No 2, 1990.

[26] Morimoto, S., Takeda, Y., Hirasa, T. and Taniguchi. K, *"Expansion of operating limits for permanent magnet motor by current vector control considering inverter capacity", IEEE Trans*. IAS-26, pp. 886 - 871, 1990.

[27] W.L. Soong, and T.J.E. Miller, "*Field-Weakening Performance of Brushless Synchronous AC Motor Drives*", *IEE Proc.- Electr. Power Appl .,* vol. 141, no. 6, pp. 331-339, 1994.

[28] A.K. Adnanes, "*Torque Analysis of Permanent Magnet Synchronous Motors*," *Proc. IEEE Power Elec. Specialists Conf.,* pp. 695-701, 1991.